1995-03

# Comparative resistance calculations for SLICE/SWATH hulls

Al-jowder, Jassim Abdulla

Monterey, California. Naval Postgraduate School

# NAVAL POSTGRADUATE SCHOOL
# MONTEREY, CALIFORNIA






# THESIS

**COMPARATIVE RESISTANCE CALCULATIONS FOR SLICE/SWATH HULLS**
**by**

**Jassim Abdulla Al-jowder**

**March 1995**

**Thesis Advisor:** **Fotis A. Papoulias**

**Approved for public release; distribution is unlimited.**

# REPORT DOCUMENTATION PAGE

Form Approved
OMB No. 0704-0188



| 1. AGENCY USE ONLY (Leave blank) | 2. REPORT DATE | 3. REPORT TYPE AND DATES COVERED |
|---|---|---|
| | March 1995 | Master's Thesis |

**4. TITLE AND SUBTITLE**
COMPARATIVE RESISTANCE CALCULATIONS FOR SLICE/SWATH HULLS

**5. FUNDING NUMBERS**

**6. AUTHOR(S)**
Jassim Abdulla Al-jowder

**7. PERFORMING ORGANIZATION NAME(S) AND ADDRESS(ES)**
Naval Postgraduate School
Monterey, CA 93943-5000

**8. PERFORMING ORGANIZATION REPORT NUMBER**

**9. SPONSORING / MONITORING AGENCY NAME(S) AND ADDRESS(ES)**

**10. SPONSORING / MONITORING AGENCY REPORT NUMBER**

**11. SUPPLEMENTARY NOTES**
The views expressed in this thesis are those of the author and do not reflect the official policy or position of the Department of Defense or the United States Government.

**12a. DISTRIBUTION / AVAILABILITY STATEMENT**
Approved for public release; distribution unlimited.

**12b. DISTRIBUTION CODE**

**13. ABSTRACT** *(Maximum 200 words)*

Comparative resistance calculations are performed for SLICE and SWATH hulls. For the purposes of this study, the primary difference between these two hull types is in the underwater pods. It is assumed that both ship types have identical surface piercing struts, speed, and displacement. The underwater pods are continuous for the SWATH design and discontinuous for the SLICE. Resistance calculations are based on I.T.T.C. skin friction, empirical regression of existing experimental data for form drag, and surface singularities distribution for wavemaking. Results are presented for two cases, length limited where the overall length between the two hull types remains constant, and diameter limited where the pod diameter remains constant. Parametric studies in terms of pod geometry, separation distance, ship speed, displacement length ratio, and draft indicate that a SLICE hull may offer decreased resistance compared to a similar SWATH, depending on the range of the above design parameters.

| 14. SUBJECT TERMS | 15. NUMBER OF PAGES |
|---|---|
| pod geometry, viscous drag, wavemaking resistance, potential flow | 122 |
| | 16. PRICE CODE |

| 17. SECURITY CLASSIFICATION OF REPORT | 18. SECURITY CLASSIFICATION OF THIS PAGE | 19. SECURITY CLASSIFICATION OF ABSTRACT | 20. LIMITATION OF ABSTRACT |
|---|---|---|---|
| UNCLASSIFIED | UNCLASSIFIED | UNCLASSIFIED | UL |

Approved for public release; distribution is unlimited

# COMPARATIVE RESISTANCE CALCULATIONS FOR SLICE/SWATH HULLS

by

Jassim Abdulla Al-jowder
Major, Bahrain Navy
B.S.M.E. Ned University of Engineering and Technology, 1980

Submitted in partial fulfillment of the
requirements for the degree of

**MASTER OF SCIENCE IN MECHANICAL ENGINEERING**

from the

**NAVAL POSTGRADUATE SCHOOL**

March 1995

Author: [redacted]
Jassim Abdulla Al-jowder

Approved by: [redacted]
Fotis A. Papoulias, Thesis Advisor

[redacted]
Matthew D. Kelleher, Chairman
Department of Mechanical Engineering

# ABSTRACT

Comparative resistance calculations are performed for SLICE and SWATH hulls. For the purposes of this study, the primary difference between these two hull types is in the underwater pods. It is assumed that both ship types have identical surface piercing struts, speed, and displacement. The underwater pods are continuous for the SWATH design and discontinuous for the SLICE. Resistance calculations are based on I.T.T.C. skin friction, empirical regression of existing experimental data for form drag, and surface singularities distribution for wavemaking. Results are presented for two cases, length limited where the overall length between the two hull types remains constant, and diameter limited where the pod diameter remains constant. Parametric studies in terms of pod geometry, separation distance, ship speed, displacement length ratio, and draft indicate that a SLICE hull may offer decreased resistance compared to a similar SWATH, depending on the range of the above design parameters.

# TABLE OF CONTENTS

# LIST OF TABLES

# LIST OF FIGURES

# I. INTRODUCTION

## A. BACKGROUND

The main idea of SLICE hull follows the successful design of SWATH; i.e., small waterplane area twin hull. The SWATH geometry consists of an approximately rectangular structure or deck box joined to submerged slender cylindrical hulls by streamlined struts or columns which can be one or two per hull. The submerged pods are the primary buoyancy providing modules, while the struts provide necessary structural rigidity (Rodriguez, 1995). Due to its small waterplane area, a SWATH experiences small exciting forces from waves and has excellent seakeeping properties. In the SLICE concept there are four submerged hulls, each having its own streamlined struts or columns. This configuration is suggested in order to reduce resistance while maintaining seakeeping characteristics at least as good as for a SWATH.

For a given speed, the resistance of a body moving in a fluid is the force of the fluid acting on the body to oppose its motion. The resistance is equal to the component of the fluid forces acting parallel to the axis of motion of the body. The term resistance is the preferred term in ship hydrodynamics, while the term drag is generally used in aerodynamics and for submerged bodies. In this study we use both terms since we study the resistance of the submerged pods as explained in the next section.

## B. OBJECTIVE

Resistance could be the main reason in selecting a SLICE hull form or SWATH. Therefore, comparative resistance calculations must be performed for both hulls including both the viscous drag (skin friction as well as form drag) along with wave-making drag. Since the presence of discontinuous struts could be a common feature

for both SWATH and SLICE, in this work we concentrate on the submerged pods (Figure 1.1). The main question is whether two disconnected pods can offer reduced resistance compared to a single pod. It is assumed that in both cases the volume is the same (so that ship displacement does not vary) while either the overall length or diameter remains the same. We refer to the first case as the length limited or inactive diameter constraint, and to the second case as the diameter limited or inactive length constraint.

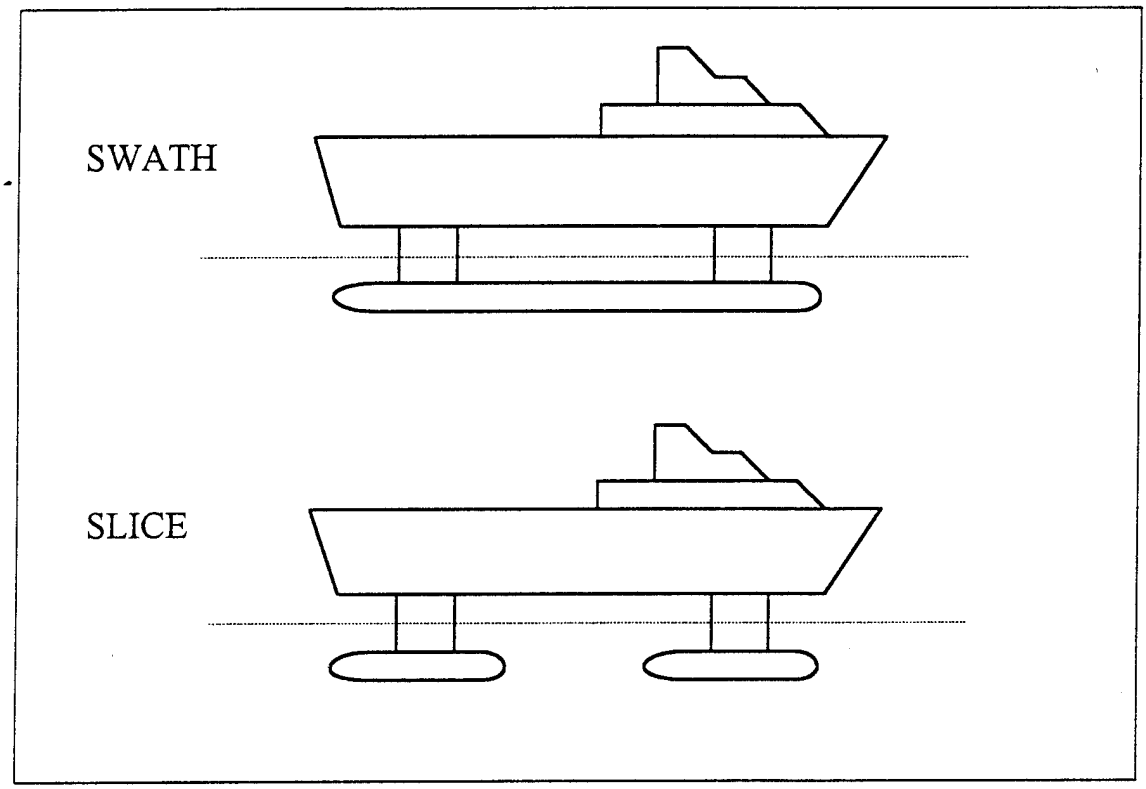


**Figure 1.1: SWATH and SLICE hull forms.**

In this study, the comparative resistance calculations are presented in Chapter II, starting with the definition of the pod geometry. The different parameters and all the coefficients are explained and formulated. A typical pod hull consists of three

sections, the entrance (bow) the shape of a parabolic body of revolution, the parallel middle body of a cylindrical shape, and the run (stern) the shape of an ellipsoid of revolution (Jackson, 1992). Proper assumptions are very important in performing meaningful calculations. These assumptions are with regards to the two hull forms, in order to reduce the size of the problem and ensure better and fair comparisons. Also in this chapter viscous resistance calculations are presented in the form of frictional resistance, and form drag. The investigation in this case leads to a better understanding to the frictional resistance, and the effects of changing the different parameters defining the pod geometry on the results. The background theory of the wavemaking resistance, is discussed in this chapter. Formulation for calculating the wavemaking drag and brief explanation of the numerical solution techniques followed in this study are also presented. After exploring the above resistance types the total resistance is calculated, for which the final comparison is based on for the two hull forms. Chapter III presents these results. After determining the total resistance, for the two cases, limited length, and limited diameter, the results are focused on three effects. First the body shape effects dealing with the length to diameter ratio, the displacement to length ratio, and finally the prismatic shape factor are discussed in detail. Second the speed effects, and third the draft effects are presented. For easy presentation to all of these effects, the results are also tabulated. Conclusions from this work and recommendations for further studies are summarized in Chapter IV.

# II. CALCULATIONS

## A. POD GEOMETRY

The geometry for the underwater pod is typically similar to the geometry of most modern submarines. A generic body of revolution is considered, which is composed of three main sections. First is the entrance at the forward section of the pod, second is the parallel middle body, and third is the run at the after end of the pod. The following variables define the shape of the body, which is schematically shown in Figure 2.1:

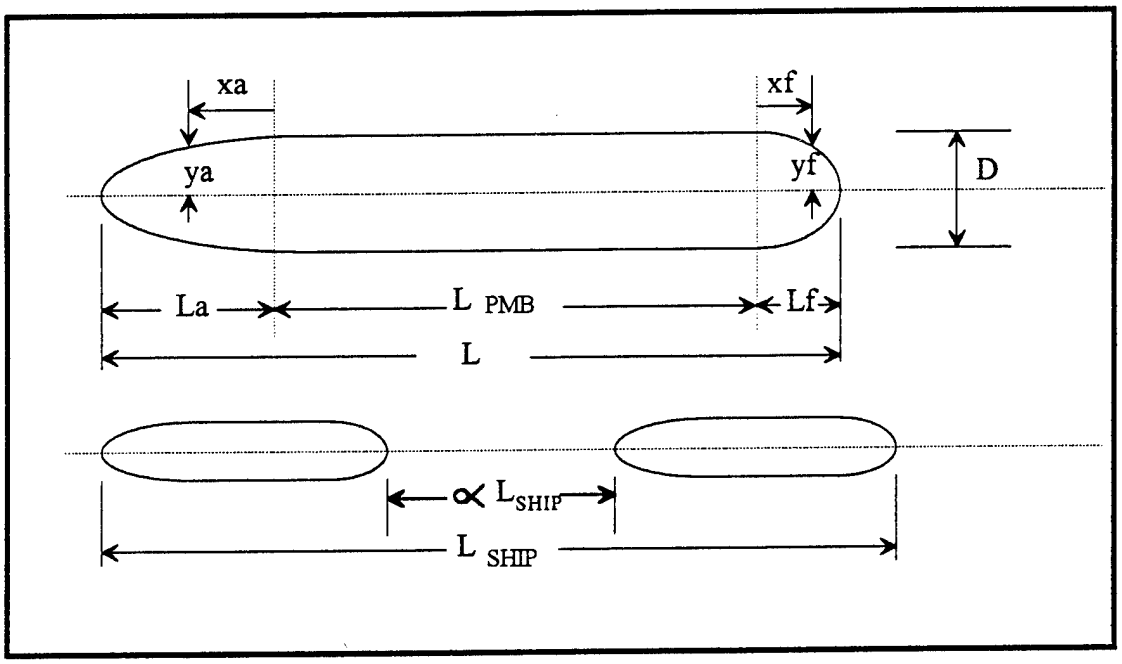


**Figure 2.1: Basic geometry definitions.**

$D$ = pod diameter

$\ell$ = pod length in the absence of parallel mid body

$L$ = pod length

$L_f$ = forward or entrance length

$L_a$ = aft or run length

$L_{\text{SHIP}}$ = overall length from entrance bow to run stern pod

$\alpha$ = dimensionless pod separation for SLICE hull

$n_f$ = forward shape factor

$n_a$ = aft shape factor

PMB = parallel middle body

From an article on submarine design concept (Jackson, 1992), the entrance is defined as a parabola body of revolution having a length, $L_f$, equal to 2.4 times the diameter. The run is defined as a ellipsoid body of revolution having a length, $L_a$ equal to 3.6 times the diameter. Values of $L_f$ and $L_a$ are evaluated with, or without the parallel middle body. The parallel middle body has a cylindrical shape, where the difference of $L - \ell$ is the length of the parallel middle body PMB, or the algebraic sum of the lengths, $L_f$, $L_a$, and $L_{\text{PMB}}$ is the overall length of the pod.

The body coordinates which define the pod forward shape, as well as its aft shape without the parallel middle body are:

$$y_f = \frac{D}{2}\left[1 - \left(\frac{x_f}{L_f}\right)^{n_f}\right]^{1/n_f} \tag{2.1}$$

$$y_a = \frac{D}{2}\left[1 - \left(\frac{x_a}{L_a}\right)^{n_a}\right] \tag{2.2}$$

while the fore/aft lengths are given by,

$$L_f = 0.4\ell\,, \tag{2.3}$$

$$L_a = 0.6\ell\,. \tag{2.4}$$

The shape factor coefficients $n_f$ and $n_a$ control the shape of the fore and aft bodies, respectively. Higher values of those coefficients correspond to full hull shapes, and lower values to finer shapes. The values of $x_f$ and $x_a$ are the offsets from the maximum pod diameter, and $y_f$ and $y_a$ are the pod radii at the respective offset points. Typical forms for different $n_f$, $n_a$ are shown in Figure 2.2.

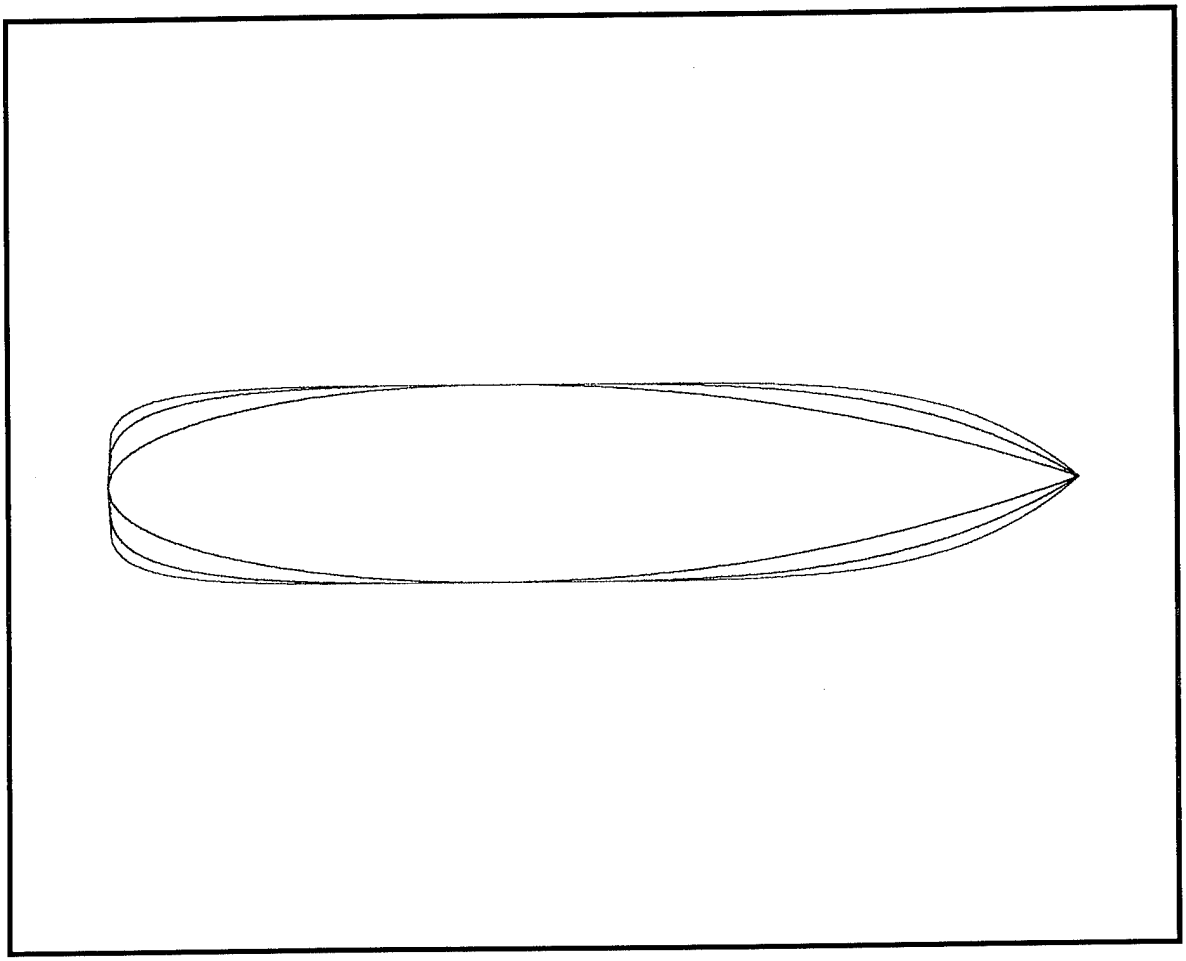

**Figure 2.2: The effect of changing the shape factor coefficients on the pod shape.**

Using the above expressions, the pod volume, $V$, and the wetted surface area, $S$, can be easily calculated as follows,

$$V = \frac{\pi D^2}{4}(L - \ell + L_f C_{pf} + L_a C_{pa}), \tag{2.5}$$

$$S = \pi D(L - \ell + L_f C_{wsf} + L_a C_{wsf}, \tag{2.6}$$

where the different coefficients are defined as,

$$C_{pf} = \text{fore prismatic coefficient}$$

$$C_{pa} = \text{aft prismatic coefficient}$$

$$C_{wsf} = \text{fore wetted surface coefficient}$$

$$C_{wsa} = \text{aft wetted surface coefficient}$$

and are computed by,

$$C_{pf} = \int_0^1 (1 - x^{n_f})^{2/n_f}\, dx, \tag{2.7}$$

$$C_{pa} = \int_0^1 (1 - x^{n_a})^2\, dx, \tag{2.8}$$

$$C_{wsf} = \int_0^1 (1 - x^{n_f})^{1/n_f}\, dx, \tag{2.9}$$

$$C_{wsa} = \int_0^1 (1 - x^{n_a})\, dx. \tag{2.10}$$

These integrals are numerically evaluated using the built-in "quad" function in Matlab, although analytic evaluation is also possible,

$$C_{pf} = \frac{\Gamma\left(1 - \frac{2}{n_f}\right)\Gamma\left(\frac{1}{n_f}\right)}{n_f \Gamma\left(1 + \frac{33}{n_f}\right)}, \tag{2.11}$$

$$C_{pa} = \frac{2n_a^2}{1 + 3n_a + 2n_a^2}, \tag{2.12}$$

$$C_{wsf} = \frac{\sqrt{\pi}\Gamma\left(\frac{1}{n_f}\right)}{(2)^{2/n_f} n_f \Gamma\left(\frac{1}{2}+\frac{1}{n_f}\right)}, \tag{2.13}$$

$$C_{wsa} = \frac{n_a}{1+n_a}, \tag{2.14}$$

where denoted the Gamma function defined in (Abramowitz and Stegun, 1970).

## B. ASSUMPTIONS

To proceed in performing the comparative resistance calculations between the SLICE and the SWATH hull forms, a number of assumptions have to be made, so that the results of these calculations ensure fairness between the two hull forms. These assumptions are with regards to the struts, the underwater configuration, the interaction between the pods, and finally the additional resistance. Each one of the assumptions is separately explained below.

### 1. Struts

As it was mentioned before the main difference between the SLICE and the SWATH is in the underwater pods, where it is continuous for the SWATH, and separated in forward and afterward pods for the SLICE. Therefore, in order to concentrate on the underwater hulls only, it was necessary to assume that the SWATH design should have a continuous pod and disconnected struts as shown in Figure 2.3. Therefore, we can say that both SLICE and SWATH strut designs are identical, and disregard them from the comparative resistance calculations.

### 2. Configuration Considerations

For the sake of comparative resistance calculations it is important to consider some of the pod design configuration parameters to be kept the same during the calculation process. The reason behind it is to ensure a fair comparison between the

SLICE and SWATH pod configuration. Therefore the following parameters are kept the same for both hull forms:

- Displacement, $V$
- Speed, $U$
- Baseline length to diameter ratio, $\ell/d$
- Body shape factor, $n_f$ and $n_a$

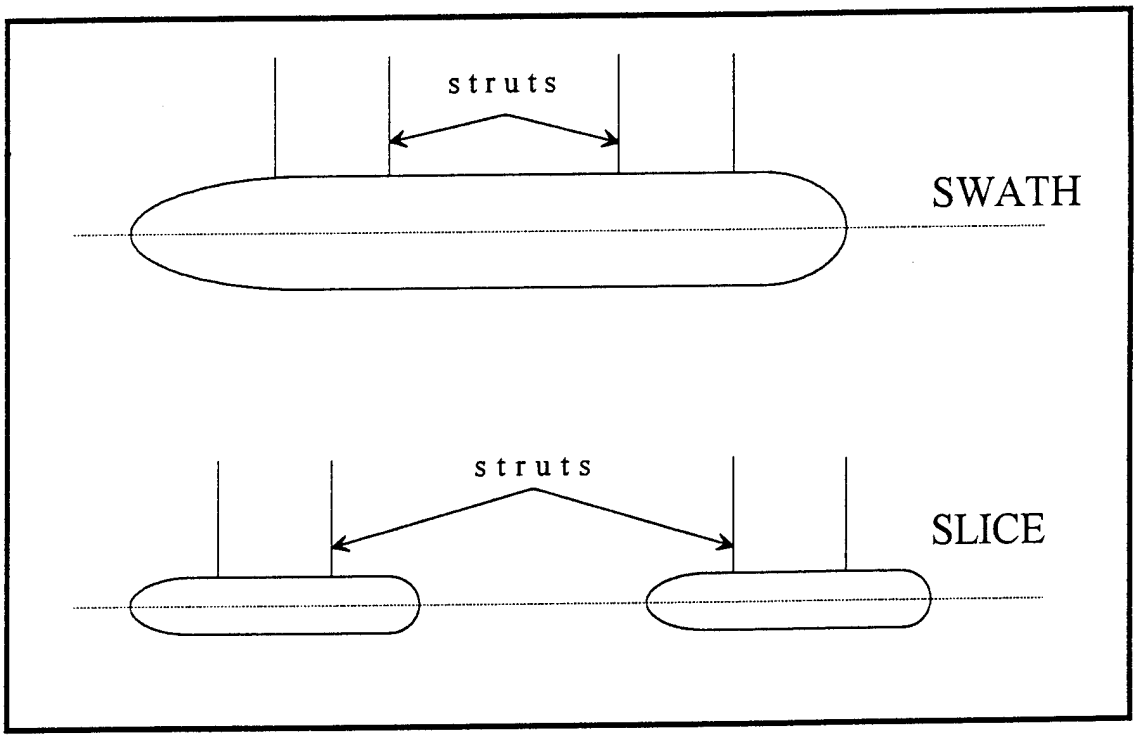


**Figure 2.3: Similarity of the strut designs for SWATH and SLICE.**

Two more parameters in addition to the above have to be considered. They are the length, $L_{\text{SHIP}}$, and the pod diameter, $D$. To keep both these parameters the same for both hull forms is impossible. The length, $L_{\text{SHIP}}$, is related to overall deck area, and to have the same deck areas for both designs, the beam must be assumed

the same for SLICE and SWATH. Therefore, since the volume, $V$, and $L_{\text{SHIP}}$ are kept the same this requires that the pod diameter, $D$, changes from SLICE to SWATH. We refer to this case as "length limited" or "inactive diameter constraint." Similarly, for the case where the diameter, $D$, is kept the same, this requires that the length $L_{\text{SHIP}}$ must change. We refer to this as the "diameter limited" or "inactive length constraint."

### 3. Pods Interaction

It is assumed that there is no viscous interaction between the SLICE pods, in other words the calculation will be performed for one pod, then multiplied by four to get the total resistance for all four pods. It should be emphasized that this is utilized for the viscous resistance only. The wavemaking part of the resistance depends heavily on the separation distance between the two pods. The lateral separation between the pods is neglected in computing the wavemaking drag. The justification for this assumption is that its effect is believed to be much smaller than the longitudinal separation. Furthermore, since both SLICE and SWATH designs have the same lateral pod separation, its effect on comparative resistance prediction will be minimal. Also the two pods on each side are in line and separated by a distance which is a function of the pod length, denoted by $\alpha$.

### 4. Additional Resistance

It is assumed that all remaining forms of resistance such as air resistance, appendage resistance, and steering resistance, are the same for both the SLICE and the SWATH. This is because it is basically the same design except for the underwater pods. Therefore we will disregard all additional resistance from our calculations and concentrate on the frictional resistance, the form resistance, and the wavemaking resistance which make the total resistance for our predictions.

## C. VISCOUS RESISTANCE $R_V$

For a fully submerged body in a fluid, the viscous resistance is the component of resistance associated with the energy expended due to viscosity of the fluid or viscous effect (Harvald, 1983). The viscous resistance is written as,

$$R_V = \frac{1}{2}\rho U^2 S C_V \ . \tag{2.15}$$

The viscous resistance coefficient, $C_V$, is defined as

$$C_V = C_F + C_A + C_r \tag{2.16}$$

where the different coefficients represent the following: $C_F$ is the frictional resistance coefficient, $C_A$ is the correlation allowance, and $C_r$ is the coefficient due to the form or parasitic drag.

### 1. Frictional Resistance $F_R$

The frictional resistance is the component of resistance obtained by integrating the tangential stresses over the wetted surface area of the pod in the direction of motion. This is a function of Reynolds number only, defined by

$$R_e = \frac{UL}{\nu} \ . \tag{2.17}$$

where the $U$ is the speed, $L$ is the pod length, $\nu$ is the kinematic viscosity of seawater.

#### a. Introduction

All fluids have viscosity, which causes friction. The importance of this friction in physical situations depends on the type of fluid and physical configuration or flow pattern. If the friction is negligible, the flow is called ideal. Viscosity is a measure of the fluid's resistance to shear when the fluid is in motion.

#### b. Boundary Layer

By boundary layer is meant the region of fluid close to a solid body where, owing to viscosity, the transverse gradients of velocity are larger compared

with the longitudinal variations, and the shear stresses significant. The boundary layer may be laminar, turbulent, or transition, and is sometimes called the frictional belt.

### c. Frictional Resistance Coefficient $C_F$

Calculation of the frictional resistance coefficient is based on the standard International Towing Tank Conference (ITTC) curve,

$$C_F = \frac{0.075}{(\log_{10} R_e - 2)^2}. \tag{2.18}$$

The correlation allowance is assumed constant (Arentzen and Mandel, 1960),

$$C_A = 0.0004. \tag{2.19}$$

## 2. Form Drag

It is hard to evaluate the form drag numerically because it is related to boundary layers and separated flows. Therefore for the third coefficient, $C_r$, we employ the following empirical calculation (Jackson, 1992) which is based on regression and curve-fitting of experimental data,

$$C_r = \frac{0.00789D}{L - \ell + L_f C_{wsf} + L_a C_{wsa}}. \tag{2.20}$$

# D. WAVEMAKING RESISTANCE

The wavemaking resistance is the component of resistance associated with the continuous energy dissipation which comes only from the pod motion through the water creating or generating gravity waves. These propagated waves are maintained by the movement of the pod through the water, and absorbed by the ocean. The wavemaking resistance can be divided into two parts: the wave pattern resistance and the wavebreaking resistance. In general, wave resistance means the wavemaking resistance neglecting the effect of wavebreaking resistance (Harvald, 1983). The

wavemaking resistance is a function of the Froude number, defined by

$$F_n = \frac{U}{\sqrt{gL}}. \tag{2.21}$$

### 1. Wave Pattern Resistance

This resistance can be experimentally evaluated from measurements of the elevations of the waves generated from the pod, where it is assumed that linearized theory can be used to relate the subsurface velocity field and, hence, the momentum transfer of the fluid to the wave pattern. This resistance does not include wavebreaking resistance.

### 2. Wavebreaking Resistance

The wavebreaking resistance is the resistance part related to the breakdown of the pod bow wave, and it is normally ignored.

### 3. Wavemaking Resistance Calculations

For the evaluation of the wavemaking resistance, it is important to start with defining a coordinate system for which the calculations can refer to. Therefore a right-hand $x$, $y$, $z$, coordinate system is selected, where the $x$-axis lies on the pod center line positive towards the bow in SWATH, and to the forward pod bow in SLICE. For the $y$-axis, positive is always to the port side regardless of the hull form. Finally the positive $z$-axis points upward. The origin of this coordinate system defers from SWATH to SLICE. For the SWATH hull form the origin is at the intersection of maximum diameter and the body horizontal centerline in absence of parallel middle body, and at the intersection of the middle of the parallel middle body and the horizontal centerline in the case of presence of PMB. On the other hand for SLICE the origin is normally at half the pod separation distance. The pod center line is at a depth H below the undisturbed waterline. Figure 2.4 illustrates the definition for the coordinate systems.

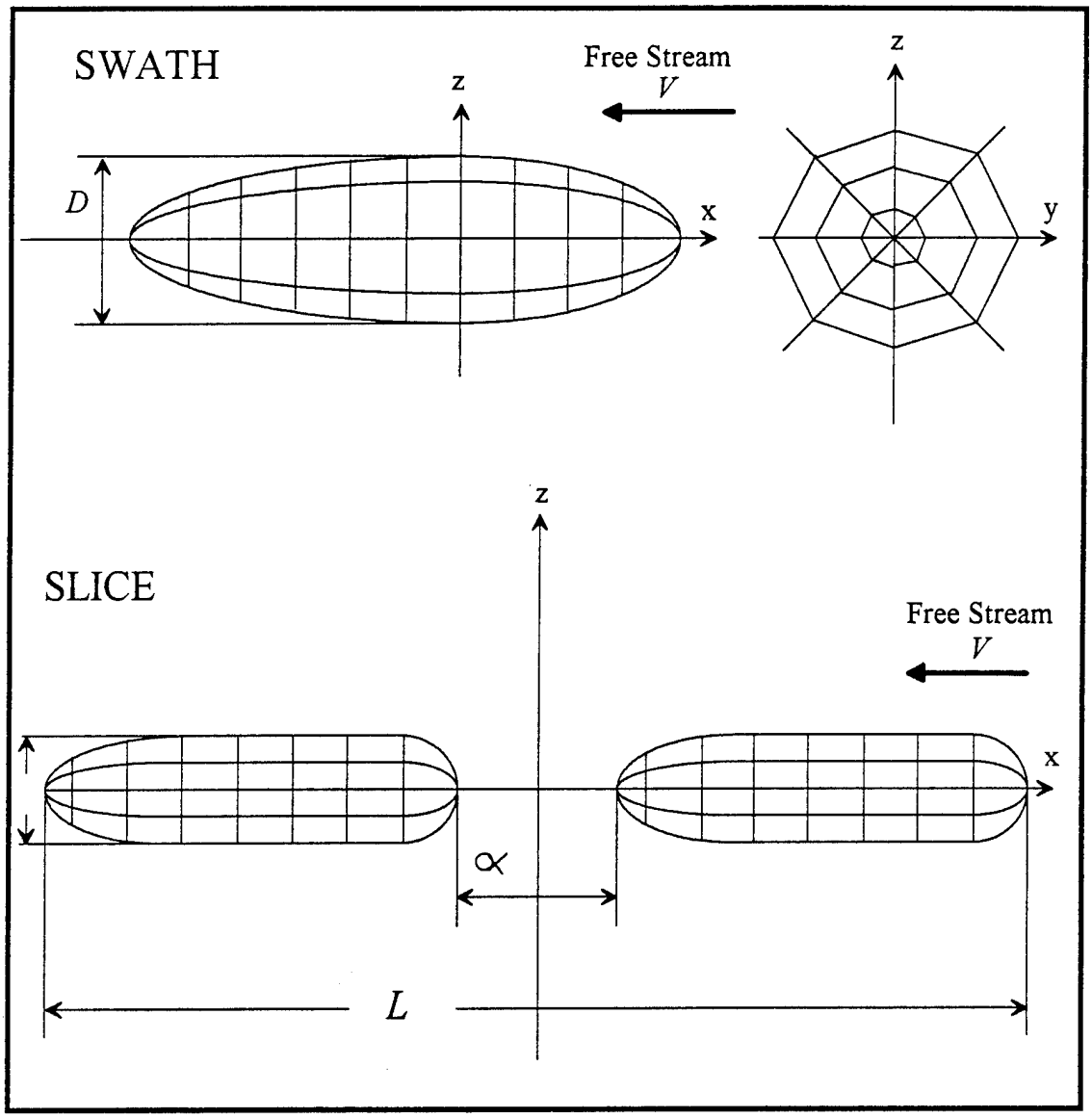


**Figure 2.4: Definition of the coordinate system for SWATH and SLICE.**

For a submerged body moving in a fluid with a constant advancing speed $U$, the potential and the fluid particle speed changes from point to point. According to Bernoulli's equation the pressure is changing from point to point. We denote by $\Phi$ the free stream potential, and $\phi$ the perturbation potential due to the body motion only. The flow around the body can be solved by distributing a number of sources and sinks along the body surface, where the total potential considering inviscid and incompressible fluid (Doctors and Beck, 1987, Papoulias, 1993, and Papoulias and Beck, 1988) is given by,

$$\Phi(x,y,z) = -Ux + \phi(x,y,z)\,, \tag{2.22}$$

This can also be written as,

$$\Phi(x,y,z) = -Ux + \int\int_{S_p} \sigma(\xi,\eta,\zeta) G(x,y,z,\xi,\eta,\zeta) dS\,, \tag{2.23}$$

where $(x,y,z,)$ is field or observation point, $\sigma(\xi,\eta,\zeta)$ is the source strength, $(\xi,\eta,\zeta)$ is the source point, and $G(x,y,z,\xi,\eta,\zeta)$ is called the Green's Function. Laplace's equation, the boundary value problem and the boundary conditions are written in terms of $\phi$. To do so, it is assumed that the value of $\phi$ is small compared to $Ux$ value, where Laplace's equation is written as,

$$\nabla^2\phi = 0\,. \tag{2.24}$$

Two free surface boundary conditions are involved in this problem, the dynamic and kinematics free surface boundary conditions. In the first condition the pressure on the free surface is constant and the wave elevation which is expressed as $\eta(x,y)$, is expanded using Taylor series about $z = 0$. Neglecting all higher order terms, we can reach at the following result,

$$g\eta + \frac{1}{2}\left\{(\Phi_x)^2 + (\Phi_y)^2 + (\Phi_z)^2\right\} = \frac{1}{2}U^2\,, \quad \text{on } z = \eta(x,y)\,, \tag{2.25}$$

where $g$ is the gravitational acceleration. The second boundary condition is the kinematic free surface boundary condition. For this condition it is necessary to have no flow through the free surface,

$$\Phi_x \eta_x + \Phi_y \eta_y - \Phi_z = 0\,, \quad \text{on } z = \eta(x,y)\,. \tag{2.26}$$

The dynamic, (2.25), and the kinematic, (2.26), free surface conditions can be rewritten as,

$$g\eta + \frac{1}{2}\left\{2U\phi_x + (\phi_x)^2 + (\phi_y)^2 + (\phi_z)^2\right\} = 0\,, \quad \text{on } z = 0\,, \tag{2.27}$$

and

$$U\eta_x + \phi_x \eta_x + \phi_y \eta_y - \phi_z = 0\,, \quad \text{on } z = 0\,, \tag{2.28}$$

In order to get the linearized free surface condition the following steps must be done:

- The quadratic terms in both equations, (2.27), and (2.28) are neglected.
- Differentiate the dynamic free surface condition with respect to $x$.
- Subtract the differentiation result from the kinematic free surface condition.

Once these steps are completed, the following linearized free surface condition is obtained:

$$\phi_{xx} + \left(\frac{g}{U^2}\right)\phi_z = 0 \quad \text{on } z = 0\,, \tag{2.29}$$

The body boundary condition requires that there be no flow through the surface of the body. In other words:

$$\frac{\partial \Phi}{\partial n} = 0\,, \quad \text{on the surface } f(x,y) - z = 0\,, \tag{2.30}$$

where the partial differential $(\partial/\partial n)$ indicates the directional derivation of the three dimensional normal vector pointing into the body $(\overline{n})$, and $f(x,y)$ represents the body

surface. Equation (2.30) can also be written as:

$$\frac{\partial \Phi}{\partial n} = \overline{U} \cdot \overline{n} = -U \frac{f_x}{\sqrt{1 + (f_x)^2 + (f_y)^2}}, \quad \text{on the same surface.} \tag{2.31}$$

A fundamental solution of the Laplace's equation, (2.24), and the free surface boundary condition equation, (2.29), is the Greens function, which is given by,

$$G(x, y, z, \xi, \eta, \zeta) = \frac{1}{r} - \frac{1}{r'} + \hat{G}(x, y, z, \xi, \eta, \zeta), \tag{2.32}$$

where $(x, y, z)$ is the field or observation point, $(\xi, \eta, \zeta)$ is a source point of a strength on the body equal to $-4\pi$. The term $r$ is defined as the distance between the field or observation point and the singularity point, where the term $r'$ is the distance between the field point and the singularity point image with respect to the free surface. The term $1/r$ in equation (2.32) represents a source and sink distribution typically found in potential flow problems. Both $r$ and $r'$ can be written as:

$$r, r' = \left[(x - \xi)^2 + (y - \eta)^2 + (z \mp \zeta)^2\right]^{1/2}. \tag{2.33}$$

Finally, the wave part of the Green's function $\hat{G}$ is defined by:

$$\begin{aligned} \hat{G}(x, y, z, \xi, \eta, \zeta) \;=\; & \frac{(g/U^2)}{\pi} \int_{-\pi}^{\pi} d\theta \\ & \lim_{\mu \to 0} \int_0^{\infty} \frac{\exp\{k[z + \zeta + i(x - \xi)\cos\theta + i(y - \eta)\sin\theta]\}}{(g/U^2) - k\cos^2\theta - i\mu\cos\theta} dk. \end{aligned} \tag{2.34}$$

The term $\mu$ in equation (2.34) is the Rayleigh virtual viscosity. The radiation condition is satisfied if the value is small and positive. The $\theta$ and $k$ are the wave direction and wave number respectively. The remaining terms in equation (2.34) represent a series of waves in which the linearized form of the free surface boundary condition, equation (2.29), is satisfied. Therefore, all conditions are satisfied except

the body boundary condition equation (2.31). For a large volume of fluid containing the body, the following result can be obtained for the perturbation potential in terms of the unknown source strength, $\sigma$:

$$\phi(x,y,z) = -\frac{1}{4\pi}\int\int_{S_p} G(x,y,z,\xi,\eta,\zeta)\sigma(\xi,\eta,\zeta)dS\,, \tag{2.35}$$

where $dS$ is the body wetted surface area. To solve for the source strength, first differentiate the perturbation potential, equation (2.35), with respect to the normal on the body. Then equate the result to the body boundary condition which requires that the normal velocity on the hull be zero. Therefore, we can write

$$Un_x = -\frac{1}{2}\sigma - \frac{1}{4\pi}\int\int_{S_p} G_n(x,y,z,\xi,\eta,\zeta)\sigma(\xi,\eta,\zeta)dS\,, \tag{2.36}$$

To solve the above equation, the Hess and Smith method (Hess and Smith, 1964) can be used, which divides the surface area of the body into plane quadrilateral panels as it is explained briefly in the next section. The approach is also known as the Neumann-Kelvin method.

## 4. Numerical Solution

In this work the Source Panel Method by Doctors and Beck is used to solve for the source strength by satisfying the body boundary condition. The body surface is represented as a finite number of elements having constant source strength. The integral then depends only on the geometry at the various panels. The detailed approach is described below.

We have the field or observation point $(x,y,z)$, and from the last section the velocity potential was derived in equation (2.35) as,

$$\phi(x,y,z) = -\frac{1}{4\pi}\int\int_{S_p} G(x,y,z,\xi,\eta,\zeta)\sigma(\xi,\eta,\zeta)dS\,, \tag{2.37}$$

The source strength $\sigma(\xi,\eta,\zeta)$ must be computed in order to satisfy the boundary condition on $S_p$. The source strength can be brought outside the integral if the surface

is represented by a finite number of elements each having constant source strength $\sigma(\xi, \eta, \zeta)$. With a finite number of unknowns the boundary conditions can be satisfied only at an equal number of discrete points. The pod surface is then divided into $N$ quadrilaterals, the elements or panels. Constant source strength $\sigma_j$ is assumed over each quadrilateral, where $j$ is the quadrilateral surface, $j = 1, 2, 3, \ldots, N$. Now it is possible to move the source strength $\sigma_j$ outside the integral before performing the integration, where the perturbation potential becomes,

$$\phi(x, y, z) = -\sum_{j=1}^{N} \left(-\frac{1}{4\pi}\right) \sigma_j \int\int_{S_{pj}} \frac{1}{\sqrt{(x-\xi_j)^2 + (y-\eta_j)^2 + (z-\zeta_j)^2}} dS_j \,, \quad (2.38)$$

the point $(\xi_j, \eta_j, \zeta_j)$ is the source point at the $j^{\text{th}}$ panel, and $dS_j$ is the $j^{th}$ panel surface area. With this the integration can be performed algebraically in terms of $x, y, z$ and the four corners $(\xi_\ell, \eta_\ell, \zeta_\ell)$, where $\ell = 1, 2, 3, 4$. By applying the body boundary condition at one point in each quadrilateral, and then solving the $N$ linear equations for $N$ unknowns, the source strength $\sigma_j$ can be determined. After determining the source strengths, it is possible to compute the control point velocities using the following formula,

$$U_i = -\hat{i}U + \sum_{j=1}^{N} \nabla G_{ij} \sigma_j \,, \quad (2.39)$$

where the term $\nabla G_{ij}$ is the gradient of the total Green function. Ignoring the hydrostatic pressure, the dynamic pressure is computed by using the Bernoulli Equation

$$p_i = \frac{1}{2}\rho \left(U^2 - U_i^2\right) . \quad (2.40)$$

The Hess and Smith program uses two steps to perform this process in practice. The first step is the quadrilateral generation, where a number of points defining the body surface are inputted into the program. Then the program generates quadrilaterals as flat surfaces, computing the normal to these surfaces along with the null points, which can be defined as the point where the source of its own panel

produces no tangential velocity. At the end of this step it provides an output for checking the points. The second step is the solution. The program satisfies the body boundary condition at the null point of each quadrilateral to form $N$ equations. Then the program proceeds to solve for the velocity and the pressure at each null point for unit inflow in $x$, $y$, and $z$. Moreover the velocity and the pressure of specified points off the body can also be obtained.

## E. RESULTS PRESENTATION FORM

The results of these computations are presented in terms of the following nondimensional parameters:

The volumetric coefficient,

$$v = \frac{V}{(0.1 L_{\text{SHIP}})^3}, \tag{2.41}$$

the baseline length to diameter ratio,

$$\frac{\ell}{D}, \tag{2.42}$$

the speed $U$ in knots, the shape factors $n_f$ and $n_a$, and the pod separation $\alpha$.

Resistance comparisons are presented in terms of normalized SLICE resistance,

$$\frac{(R)_{\text{SWATH}} - (R)_{\text{SLICE}}}{(R)_{\text{SWATH}}}[\%]. \tag{2.43}$$

Positive values of this ratio indicate a higher SWATH resistance and are, therefore, in favor of a SLICE design. Negative values suggest that the SWATH would offer reduced resistance. These calculations are performed for both length limited and diameter limited. The details of the corresponding volume and geometry calculations are included in the next chapter.

# III. RESULTS

## A. INTRODUCTION

In this study, the comparative resistance calculations are based on the pod total resistance. This total resistance consists of the viscous drag and wavemaking components. For the viscous drag, a Matlab program was used to perform the calculations for the skin friction and the form drag as outlined in the previous chapter. The program starts first by inputting the values for the following parameters,

- $v$, the displacement to length ratio.
- $\ell/d$, length to diameter ratio.
- $U$, the ship speed in knots.
- $n_f$ and $n_a$, the shape factors.

Then the program computes the fore and aft prismatic and wetted surface coefficients using the Matlab quad function. Once these coefficients are computed, it is possible to solve for the coefficients of the following cubic equation for the SWATH hull diameter,

$$C_1 D^3 + C_2 D^2 + C_3 D + C_4 = 0 \tag{3.1}$$

The coefficients of the cubic are given by,

$$C_1 = (L_f C_{pf}) + (L_a C_{pa}) - \ell/d\,, \tag{3.2}$$

$$C_2 = L\,, \tag{3.3}$$

$$C_3 = 0\,, \tag{3.4}$$

$$C_4 = (-2V)/\pi\,, \tag{3.5}$$

By solving the cubic equation, the value of the SWATH hull diameter is determined. From this point the program proceeds to compute the hull wetted surface area by,

$$WS = 2\pi D^2\{[(L/D) - (\ell/d)] + (L_f C_{wsf}) + (L_a C_{wsa})\}\,. \tag{3.6}$$

The viscous drag for the SWATH hull is calculated using equations (2.16), and (2.17). For the limited length case, the computations start by finding the maximum SLICE pod diameter, and its minimum/maximum lengths, which are given by,

$$d_{\max} = \{V/\pi[(L_f C_{pf}) + (L_a C_{pa})]\}^{1/3}\,, \tag{3.7}$$

$$\ell_{\min} = (\ell/d) d_{\max}\,, \tag{3.8}$$

$$\ell_{\max} = 0.5\ L\,. \tag{3.9}$$

Now according to the changes in the SLICE pod diameter, the pod separation distance denoted by $\alpha$, also changes. Therefore, the program monitors these changes and presents them in matrix form, where each change has its own wetted surface area and viscous drag.

For the limited diameter case, the computations start by equating the SWATH hull diameter to the SLICE pod diameter. This is followed by computing the SLICE pod length,

$$\ell = \frac{(V/\pi) - [(C_F C_{pf} + L_a C_{pa} - (\ell/d))D^3]}{D^2} \tag{3.10}$$

Once the SLICE pod length is calculated, the wetted surface is calculated along with the viscous drag. For both of the above cases the viscous resistance is calculated for both the SWATH twin hull, and for all four SLICE pods.

For the wavemaking resistance a FORTRAN program based on the Neumann-Kelvin method was used to calculate the hydrodynamic forces and moments acting on a moving body in a fluid with a constant speed. This program is based on (Doctors and Beck, 1987 and Papoulias and Beck, 1988), and it requires two data files.

The first file is IN.DAT, which includes the following parameters: RHO—water density, G—gravitational acceleration, AL—body length (for SWATH is the hull length, where for SLICE is the length from the entrance of the fore pod till the run of the aft pod), B—pod beam, C—pod draft, V—the body speed, NX—number of points longitudinally, NZ—number of points vertically, NH—number of points in $\theta$-integration. Some of these parameters must be changed from one run to another according to the calculation case to be performed. In all runs the water density, gravitational acceleration, number of points longitudinally, vertically, and in $\theta$-integration values never change. The second file is SUB.DAT, which contains a set of longitudinal points along the pod, with their corresponding radius ($R$). These data are the results of equations (2.1), and (2.2), and these data change for each run. From these data a subroutine computes the y and z points from the following relations,

$$y = R\sin(\pi(IZ - 1.0)/(NZ - 1.0)), \tag{3.11}$$

and

$$z = R\cos(\pi(IZ - 1.0)/(NZ - 1.0)) - H, \tag{3.12}$$

where $IZ$ is a successive vertical point and $H$ is the depth. With the above data, half of the pod surface is created. Another subroutine is used to create the second half of the pod surface, by reflecting the first half points about the pod centerline. Using this full shape, the program finds the solution to the hydrodynamic forces and moments by the Neumann-Kelvin method by discretizing into plane quadrilateral panels.

The output results from the program are stored in a separate file named RES.OUT, from which we can get the different values for the input data as well as results such as the Froude number, the wetted surface area, the wavemaking resistance, and the wavemaking resistance coefficient. These results are utilized in this study.

In the next sections we present the results of the comparative resistance calculations. Each section shows the different effects on the results for the two cases, limited length, and limited diameter. For the limited length case results, we present the percentage total resistance ratio vs. the pod separation distance $\alpha$. This distance is controlled by the diameter of the SLICE pod. Since the volume of the underwater pods is the same for the two hull forms, any change in the diameter leads to a change in pod length to maintain volume. Therefore, the distance $\alpha$ is directly related to the pod diameter, and in the calculation it is a function of the SWATH hull length. For the limited diameter case results, we present the percentage total resistance vs. $v$, $\ell/d$, $U$, $n_a$, and $n_f$. The pod separation distance $\alpha$ in this case was fed to the program as a function of the SLICE pod length. Matlab was used to plot all results, and a cubic spline was introduced to smooth these curves for better presentation. Positive percentage total resistance ratio means that the SLICE hull experiences less resistance than the SWATH hull, while for negative it is the opposite. Therefore positive is in favor of SLICE, and negative is in favor of SWATH. For both cases, unless otherwise mentioned, we take the draft to be equal to the pod diameter.

## B. BODY SHAPE EFFECTS

In this section we study the effects of the parameters defining the pod shape such as, $v$, $\ell/d$, $n_a$, and $n_f$. Considering the limited length case first, by varying the volume to length ratio, $v$, and keeping all other parameters constant we get the results shown in Figure 3.1. For small values of pod separation distance $\alpha$, the results are in favor of the SWATH. As the separation distance increases, a transition occurs at about $\alpha = 0.15$, where the results change in favor of the SLICE. This continues up

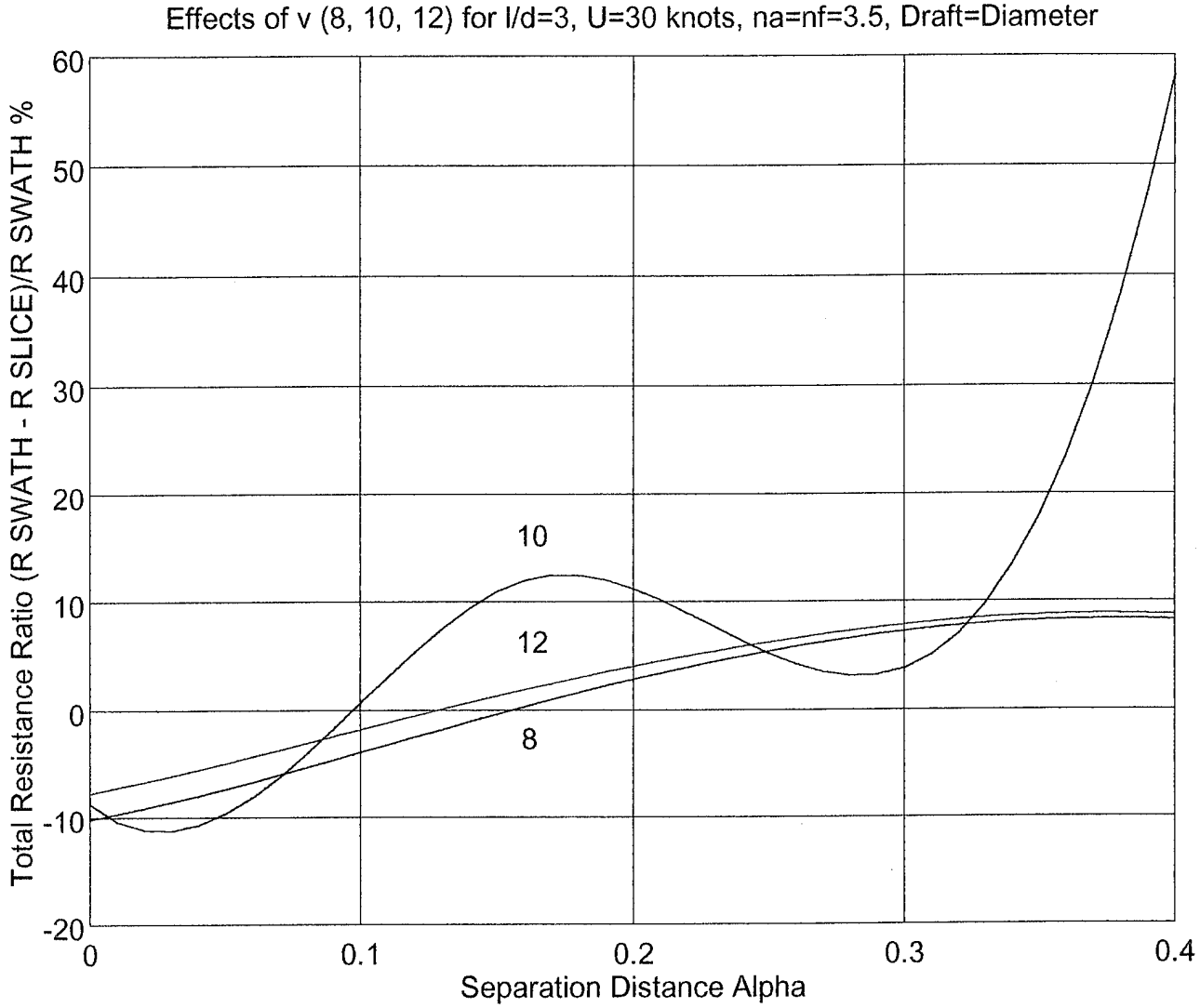


**Figure 3.1: Total resistance ratio vs. separation distance alpha for limited length case for different displacement to length ratios.**

to $\alpha = 0.4$, which is the maximum limit for $\alpha$. Another conclusion that can be drawn from Figure 3.1, is the oscillatory nature of the results for certain values of $v$. By varying the length to diameter ratio, $\ell/d$, and keeping the other parameters constant, Figure 3.2, we get similar results as for variations in the displacement to length ratio. At small $\alpha$ the resistance calculations are in favor of SWATH, while as the distance increases they change to be in favor of SLICE. Finally by varying the prismatic shape factor, which controls the fore and aft pod shapes, and keeping the other parameters constant we get Figure 3.3. For small $\alpha$ and for $n_a$ values of 3.5, and 5, both curves start in favor of SWATH and as $\alpha$ increases the values pass a turning point where the results change to be in favor of SLICE.

For the limited diameter case, varying the displacement/length ratio, keeping the other parameters constant, and plotting the results for different values of the pod separation distance $\alpha$ we get Figure 3.4. For all these runs SLICE produces less resistance than SWATH, and this difference can be improved even better by increasing $\alpha$. The increase in the percentage total resistance ratio is almost linear. By varying the length/diameter ratio, and keeping the rest constant we get Figure 3.5. It starts with results in favor of SLICE configuration, then as this value of $\ell/d$ increases the percentage drops almost linearly except for $\alpha = 0.3$. This shows that as the pod gets longer for the same diameter, it increases the total resistance for the SLICE. Also the higher the value of $\alpha$, the better the SLICE advantage over the SWATH. Finally varying the $n_a$ value while keeping the others parameters constant we get Figure 3.6. These results show that the SLICE hull configuration offers reduced total resistance than the SWATH hull. Although it drops at higher values of $n_a$ it continues to maintain reduction in the total resistance.

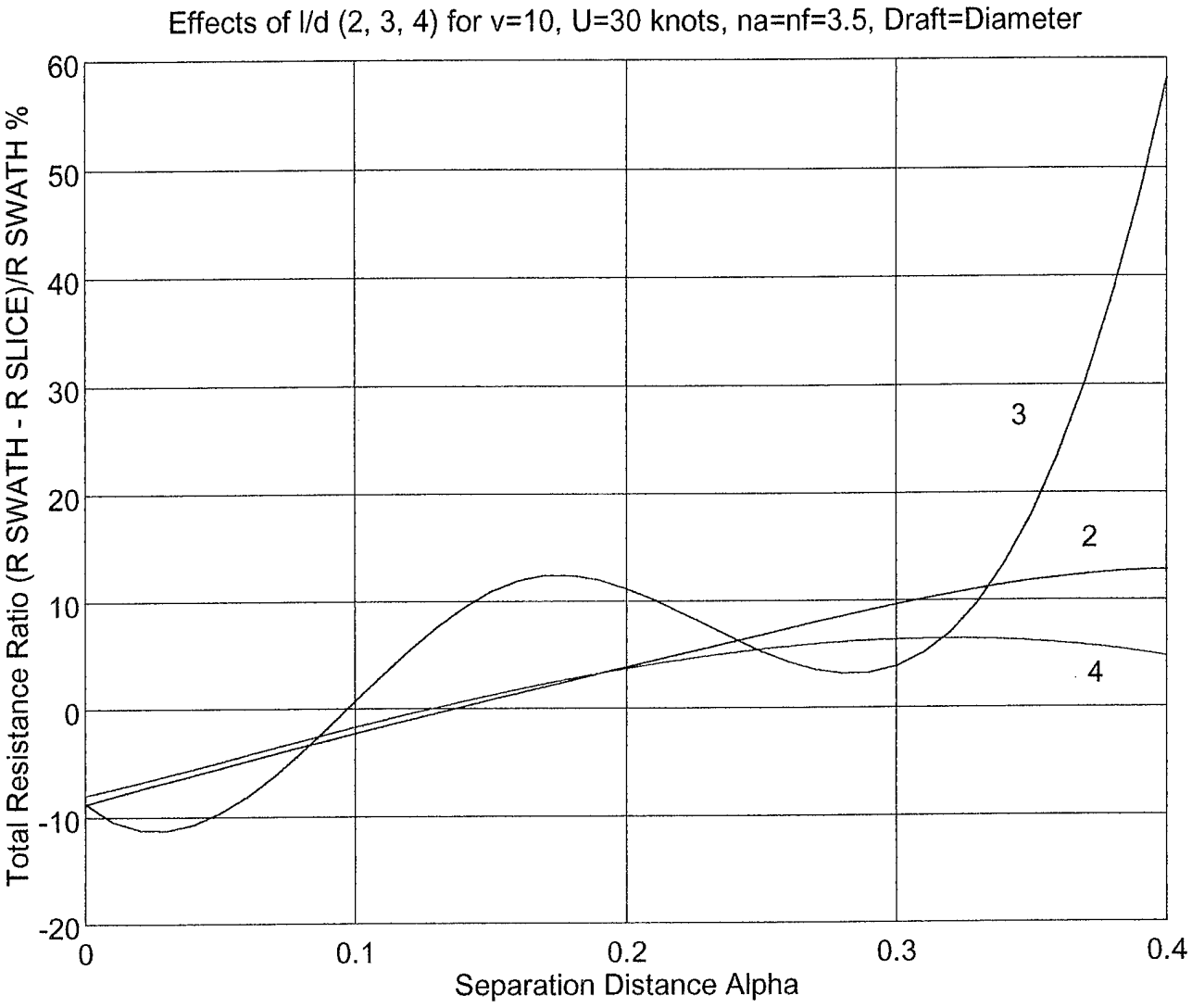


**Figure 3.2: Total resistance ratio vs. separation distance alpha for limited length case for different length to diameter ratios.**

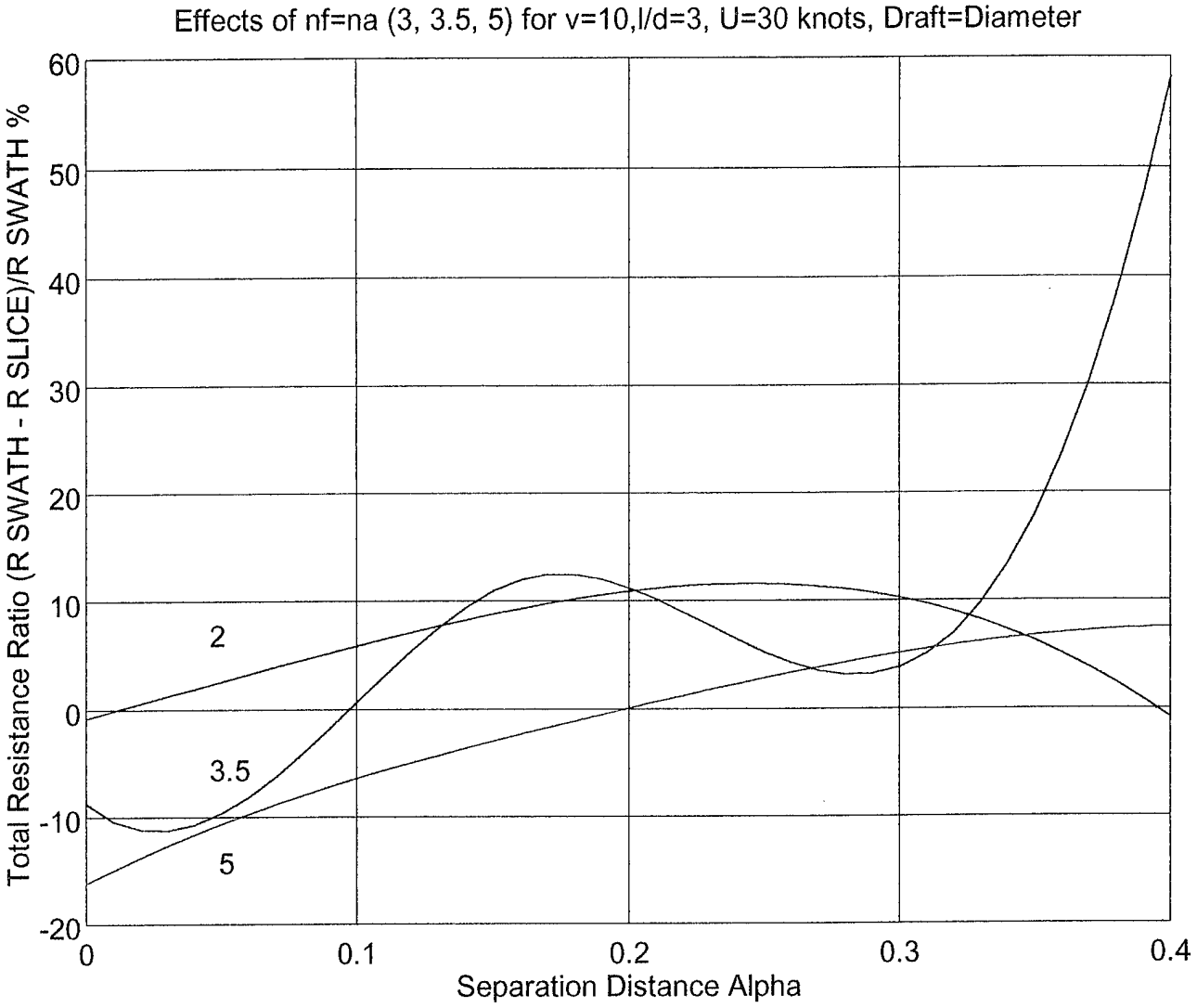


**Figure 3.3: Total resistance ratio vs. separation distance alpha for limited length case for different shape factors.**

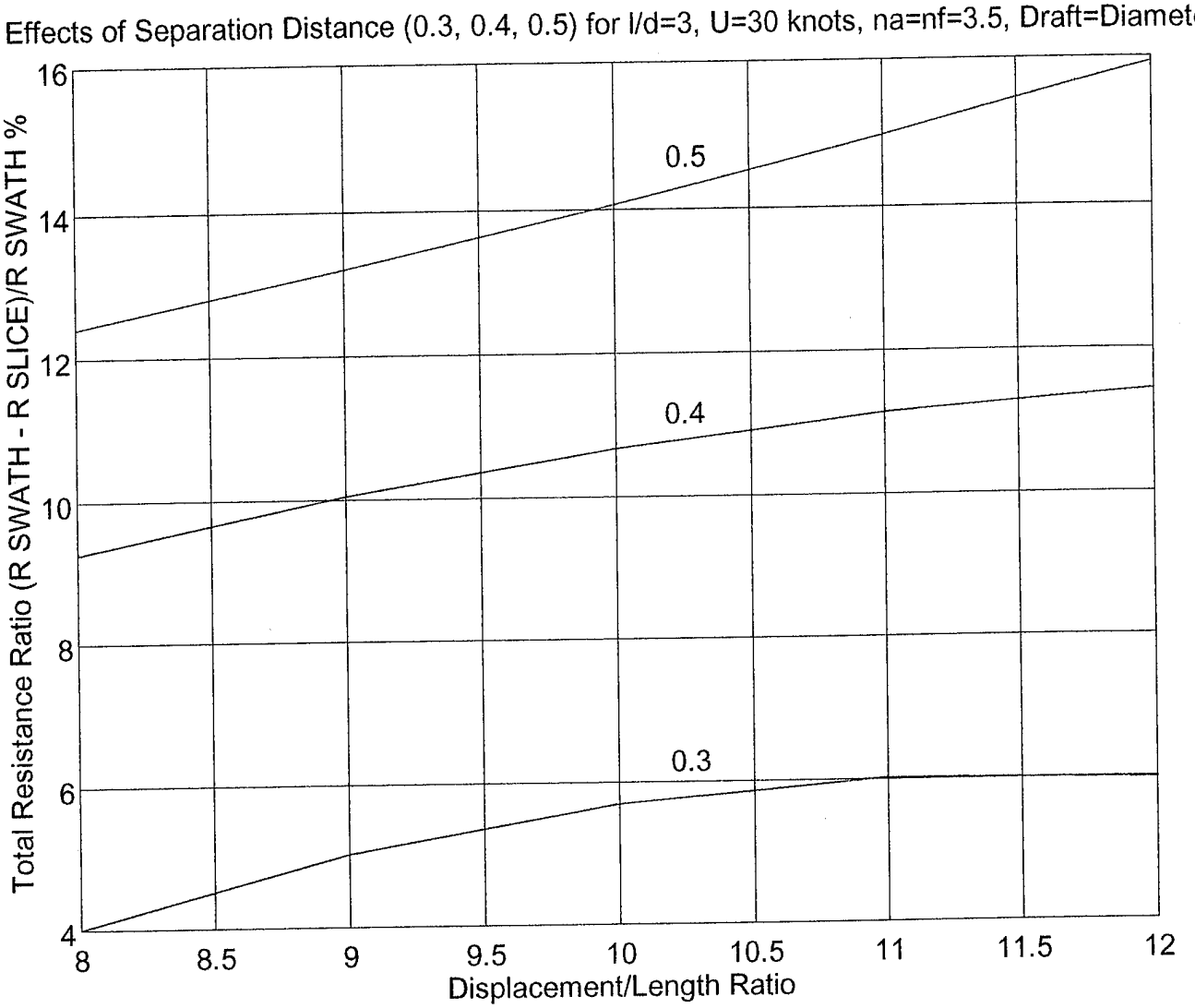


**Figure 3.4: Total resistance ratio vs. displacement to length ratio for limited diameter case for different separation distance alpha.**

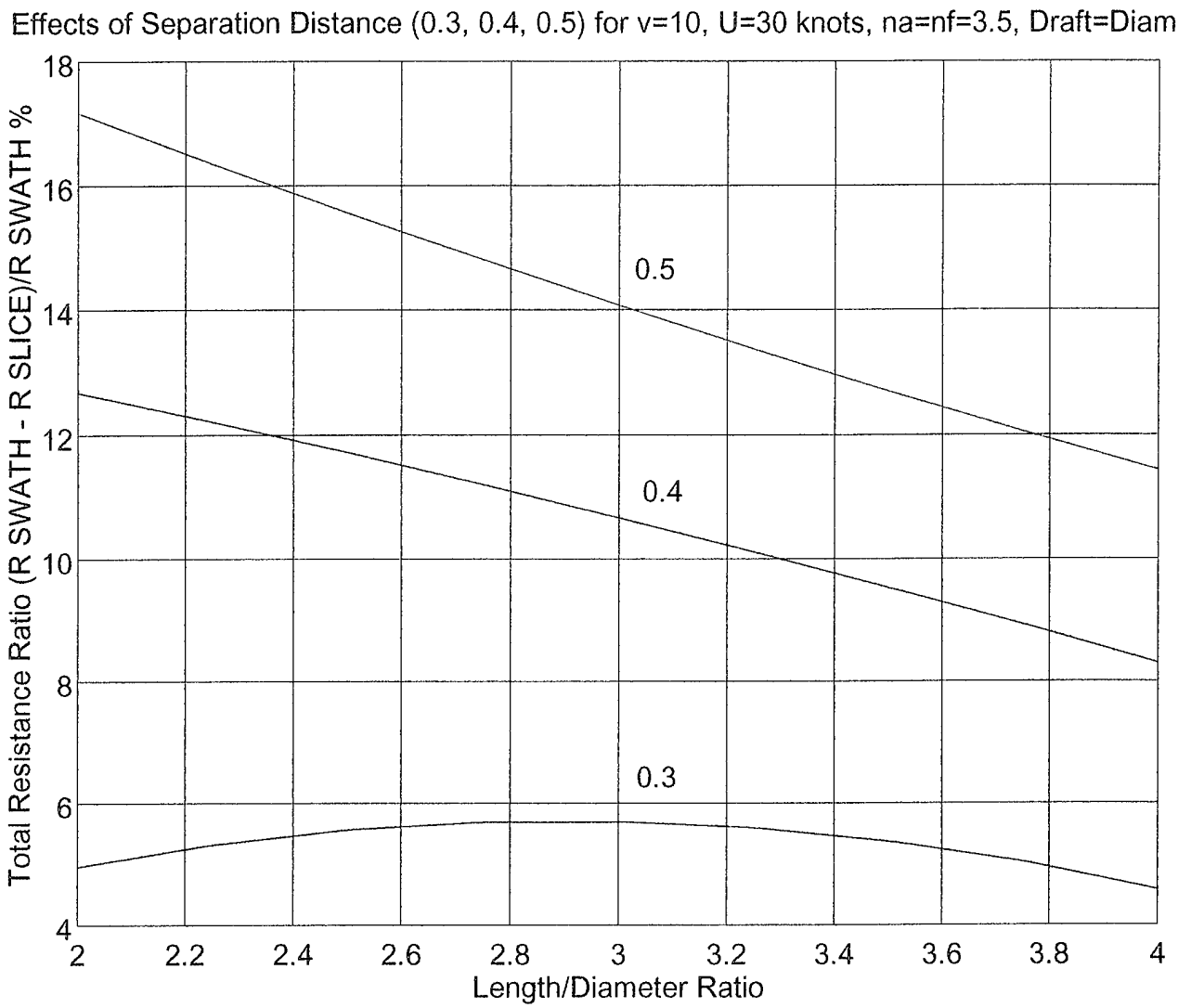


**Figure 3.5: Total resistance ratio vs. length to diameter ratio for limited diameter case for different separation distance alpha.**

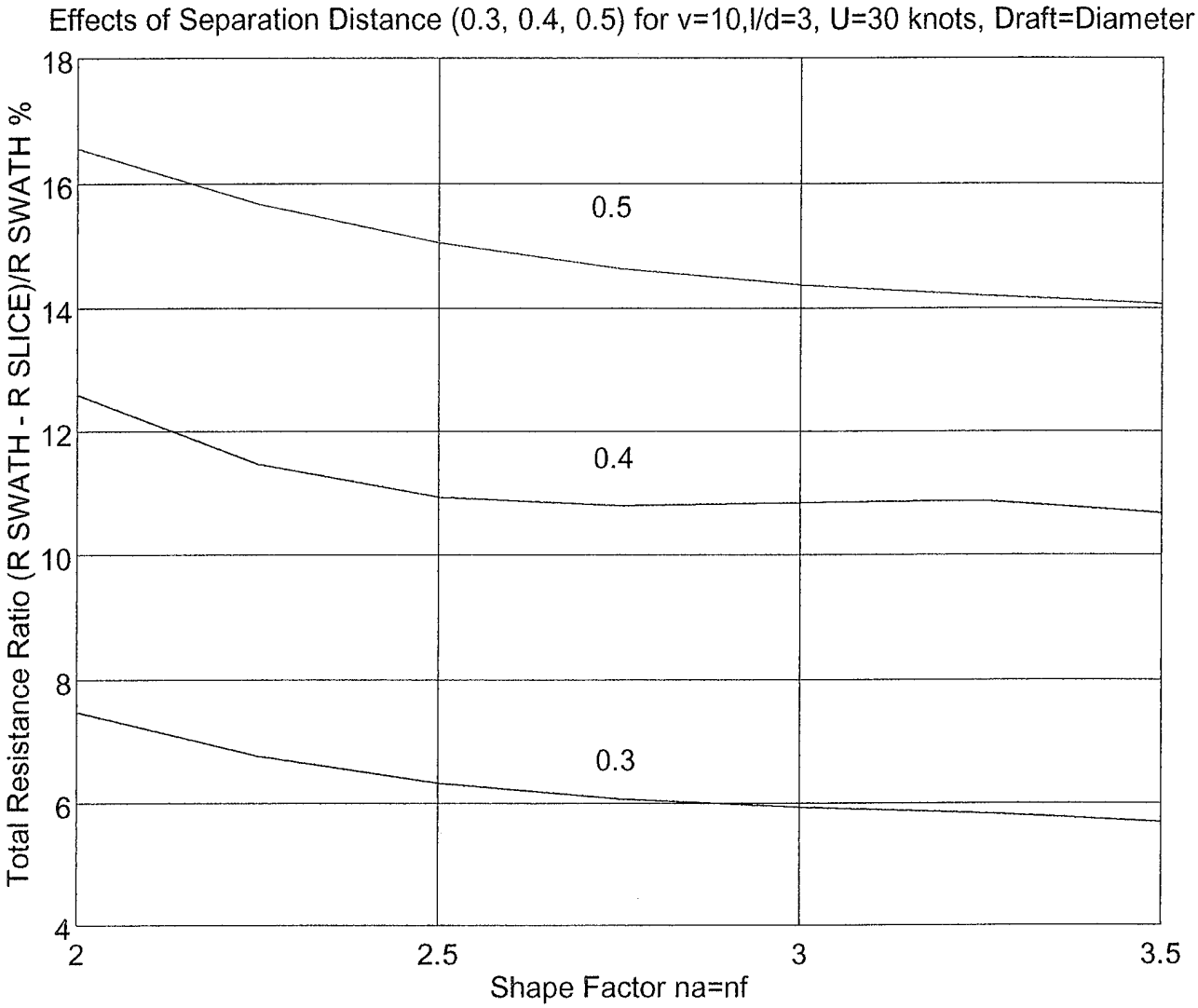


**Figure 3.6: Total resistance ratio vs. shape factor for limited diameter case for different separation distance alpha.**

## C. SPEED EFFECTS

First we start with the limited length case, where the total resistance ratio percentage is plotted vs. the pod separation distance for different speeds, 20, 30, and 40 knots. The results are shown in Figure 3.7. We can see that the speed has a general oscillatory behavior, and the total resistance ratio becomes more positive as the pod separation distance $\alpha$ increases. The 20, and 30 knots speeds start in favor of the SWATH until $\alpha = 0.1$, then in favor of SLICE until the maximum value of $\alpha$. The 40 knots speed remains in favor of SWATH for the entire range of $\alpha$, except at the maximum separation value. For the limited diameter case, the total resistance ratio plotted vs. ship speed is shown in Figure 3.8. The results were calculated for three different values of the pod separation distance, 0.3, 0.4, and 0.5. The results show that the resistance ratio has also an oscillatory behavior, where it starts with a high wave amplitude and a large period.

## D. DRAFT EFFECTS

In order to assess the effects of pod draft, all previous calculations were performed for a draft of two times the diameter. The results are presented in Figures 3.9 through 3.16, and there is a one-to-one correspondence with the previous results of Figures 3.1 through 3.8 for draft equal to the diameter. Comparing Figures 3.1 and 3.9 we can observe the same qualitative features in the results, although the actual numbers are more negative; i.e., lower draft favor SLICE vice SWATH. The same conclusion is reached by comparing Figure 3.2 with 3.10, 3.3 with 3.11, 3.4 with 3.12, 3.5 with 3.13, and 3.6 with 3.14. The difference between the two drafts were not as pronounced for the separation distance variations, as illustrated by Figures 3.7 and 3.15. Finally, the speed variation of Figure 3.16 showed similar effects as

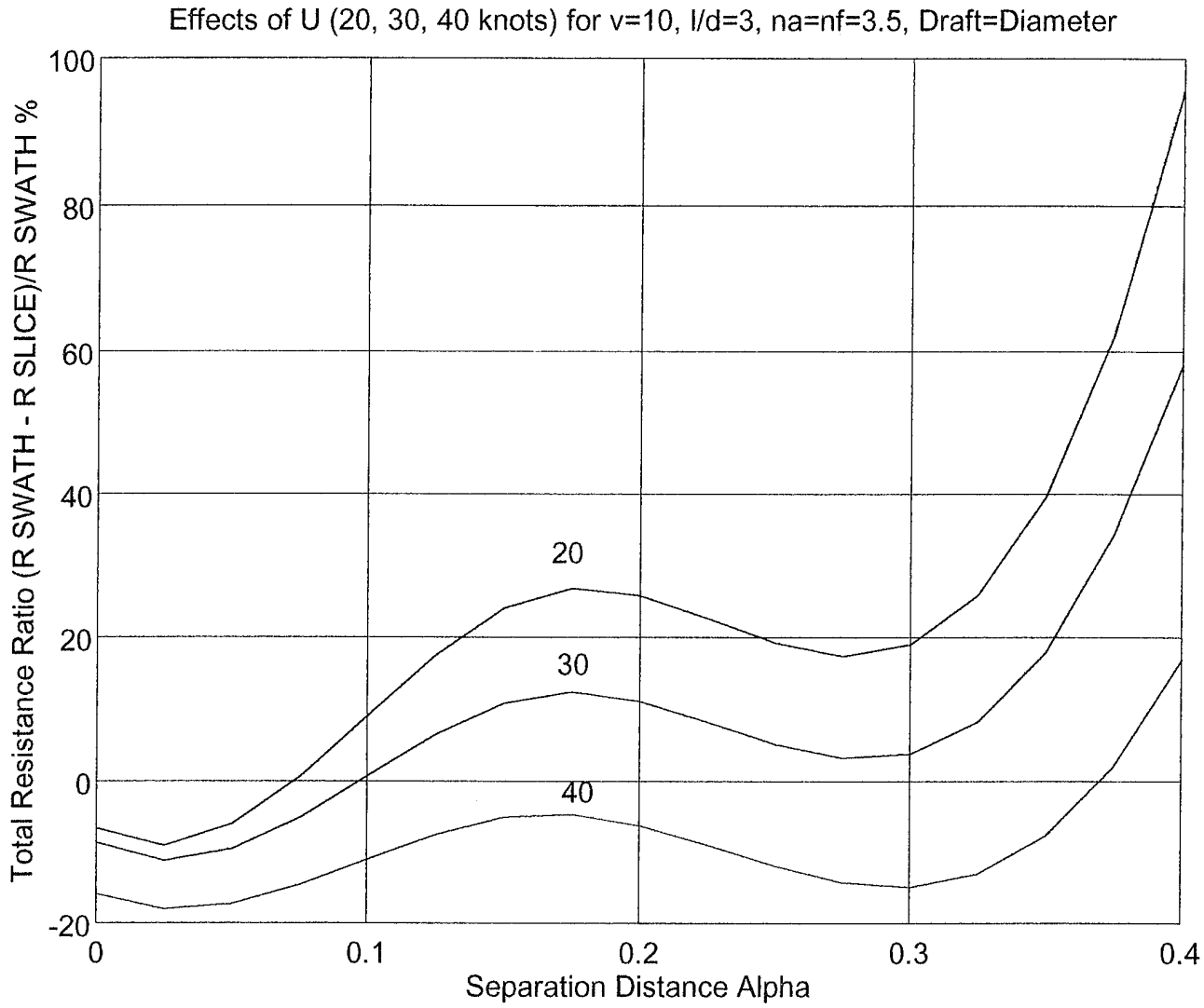


**Figure 3.7: Total resistance ratio vs. separation distance alpha for limited length case for different speeds.**

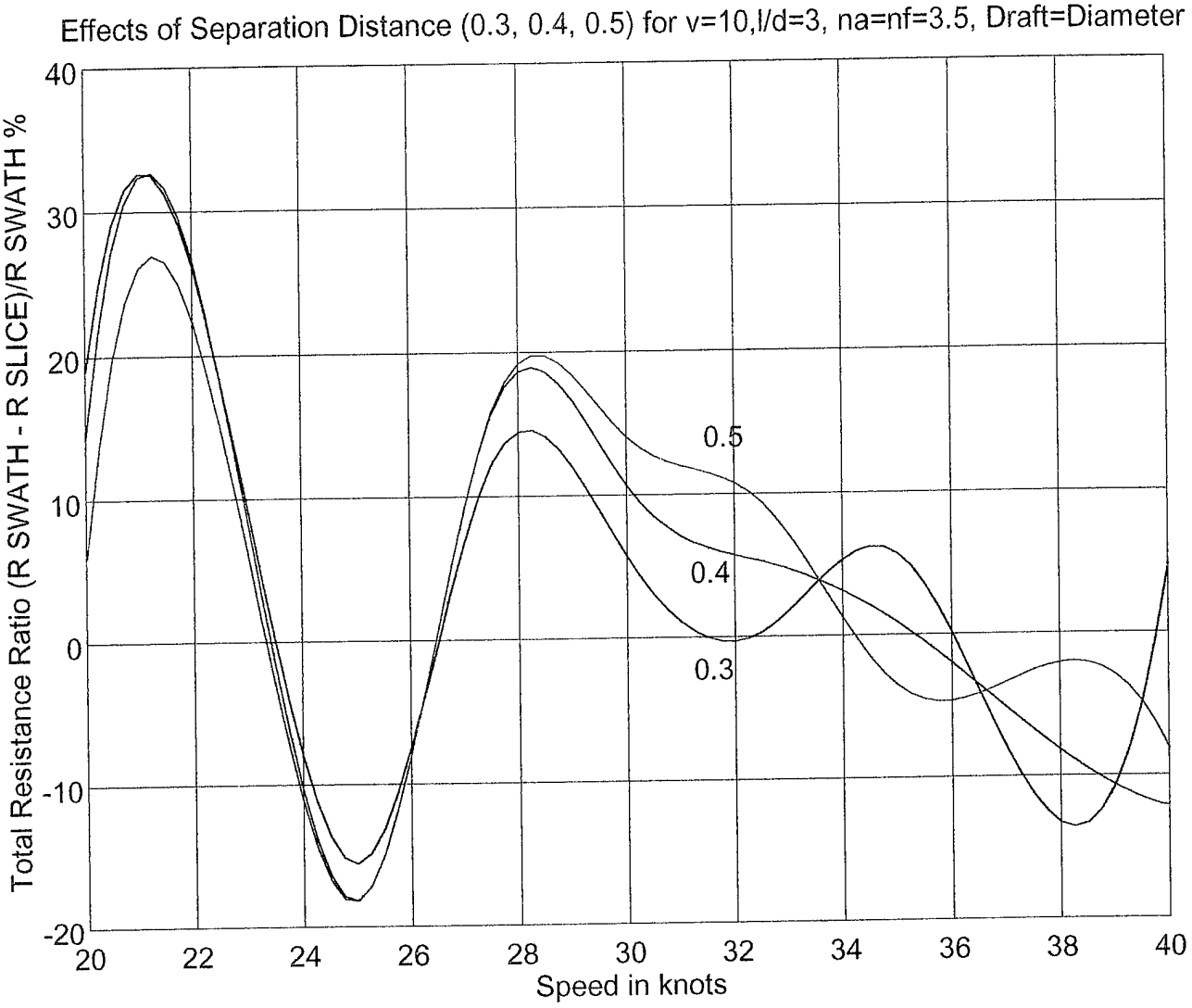


**Figure 3.8: Total resistance ratio vs. speed for limited diameter case for different separation distance alpha.**

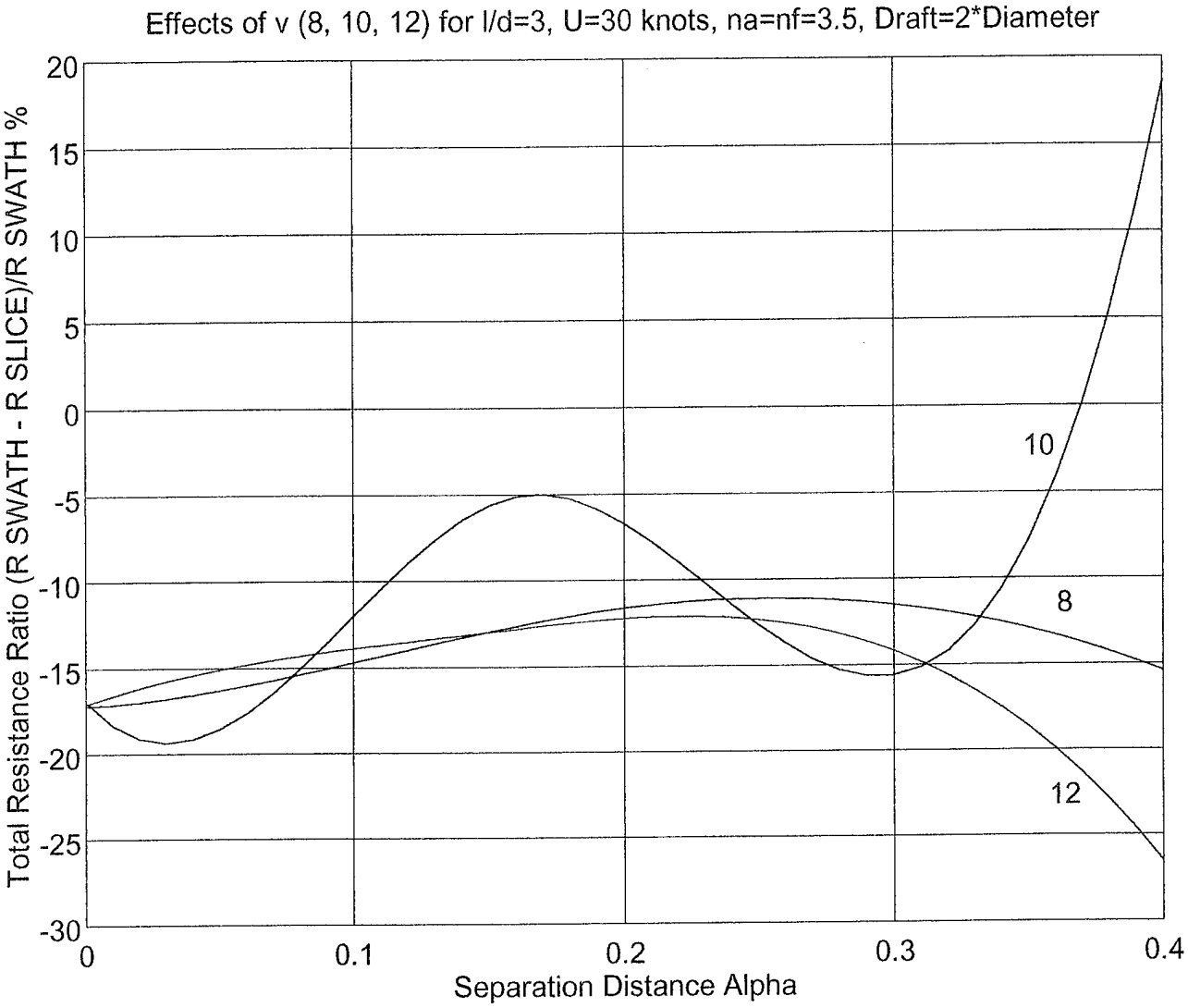


**Figure 3.9: Total resistance ratio vs. separation distance alpha for limited length case for different displacement to length ratios.**

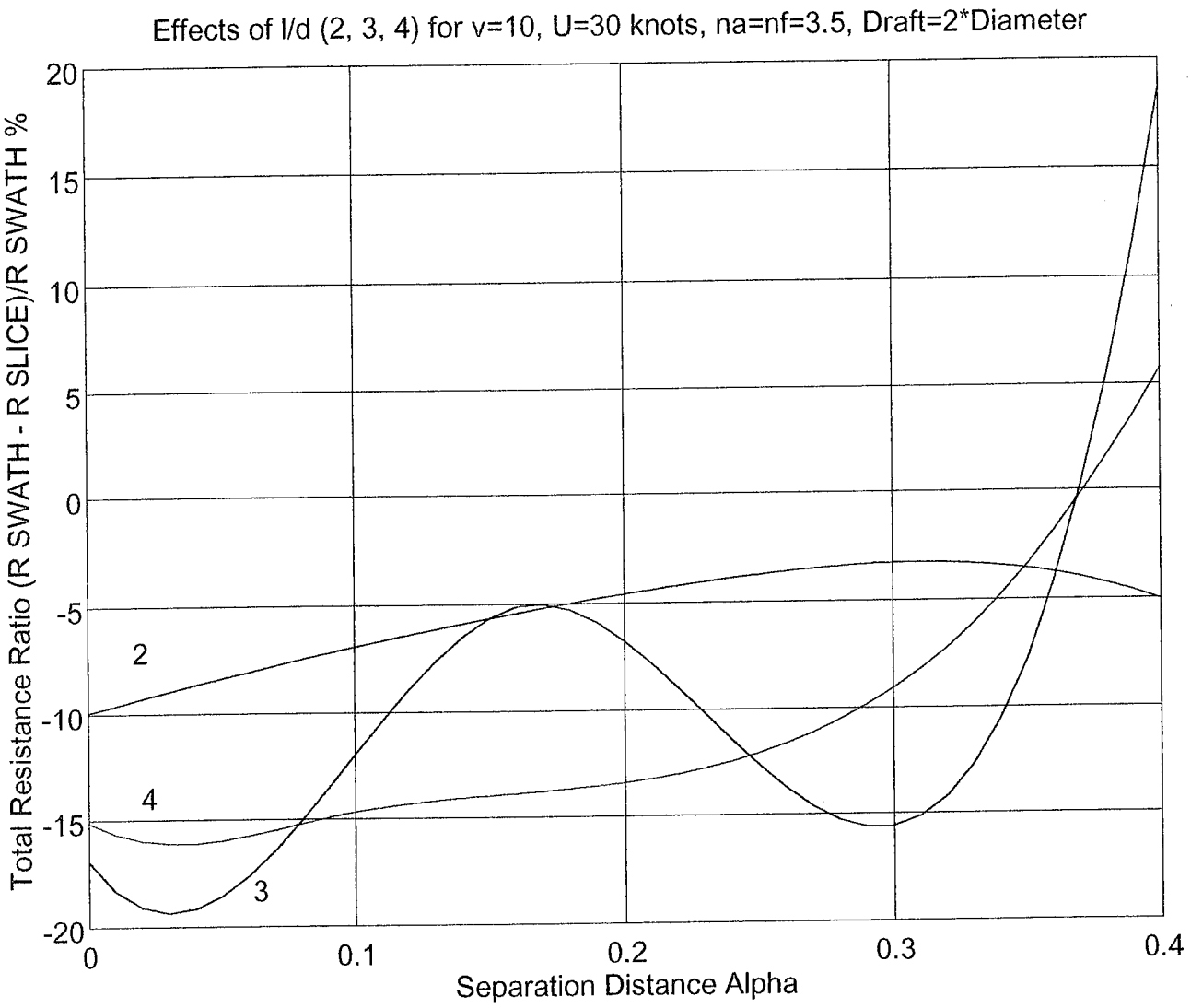


**Figure 3.10: Total resistance ratio vs. separation distance alpha for limited length case for different length to diameter ratios.**

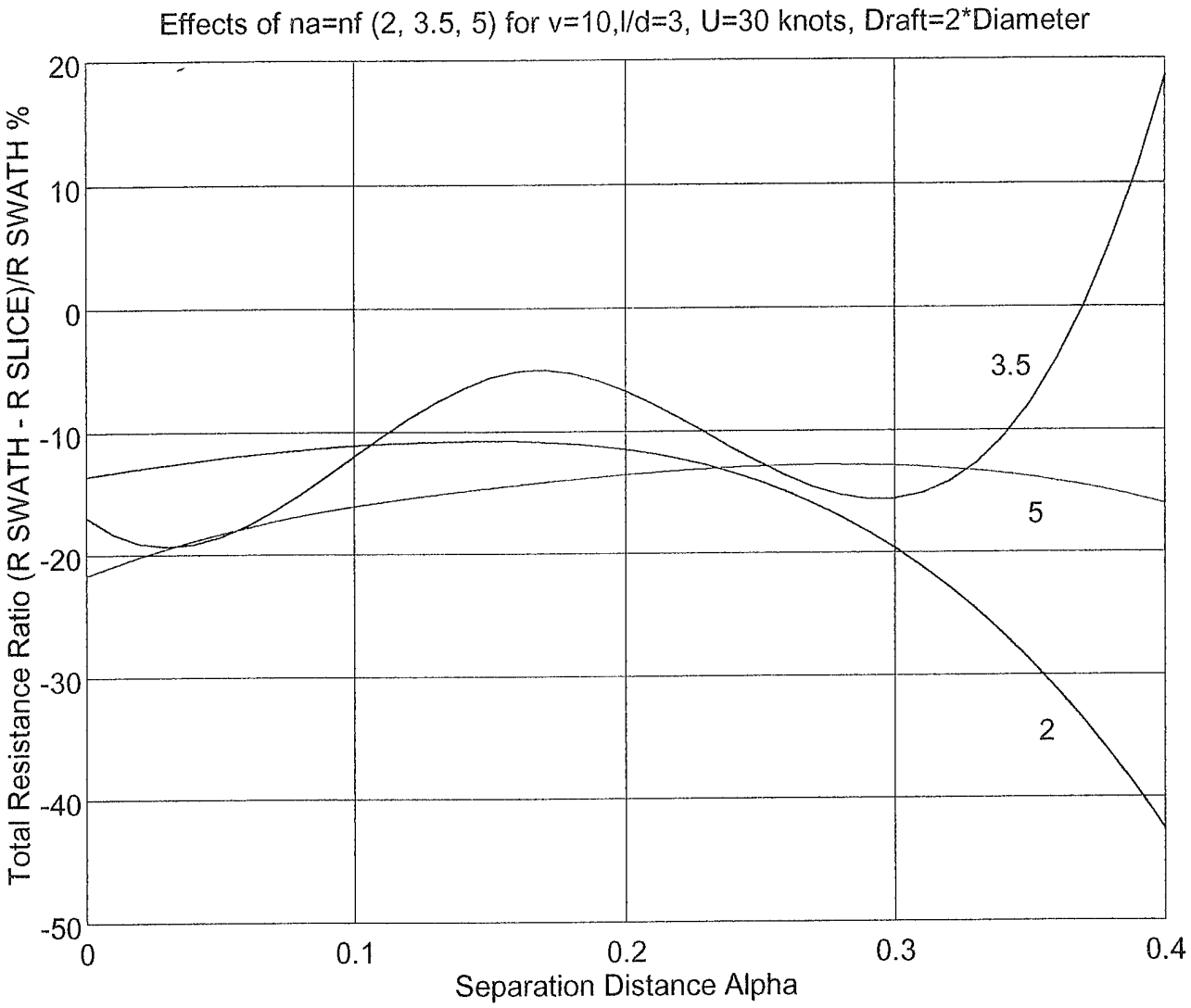


**Figure 3.11: Total resistance ratio vs. separation distance alpha for limited length case for different shape factors.**

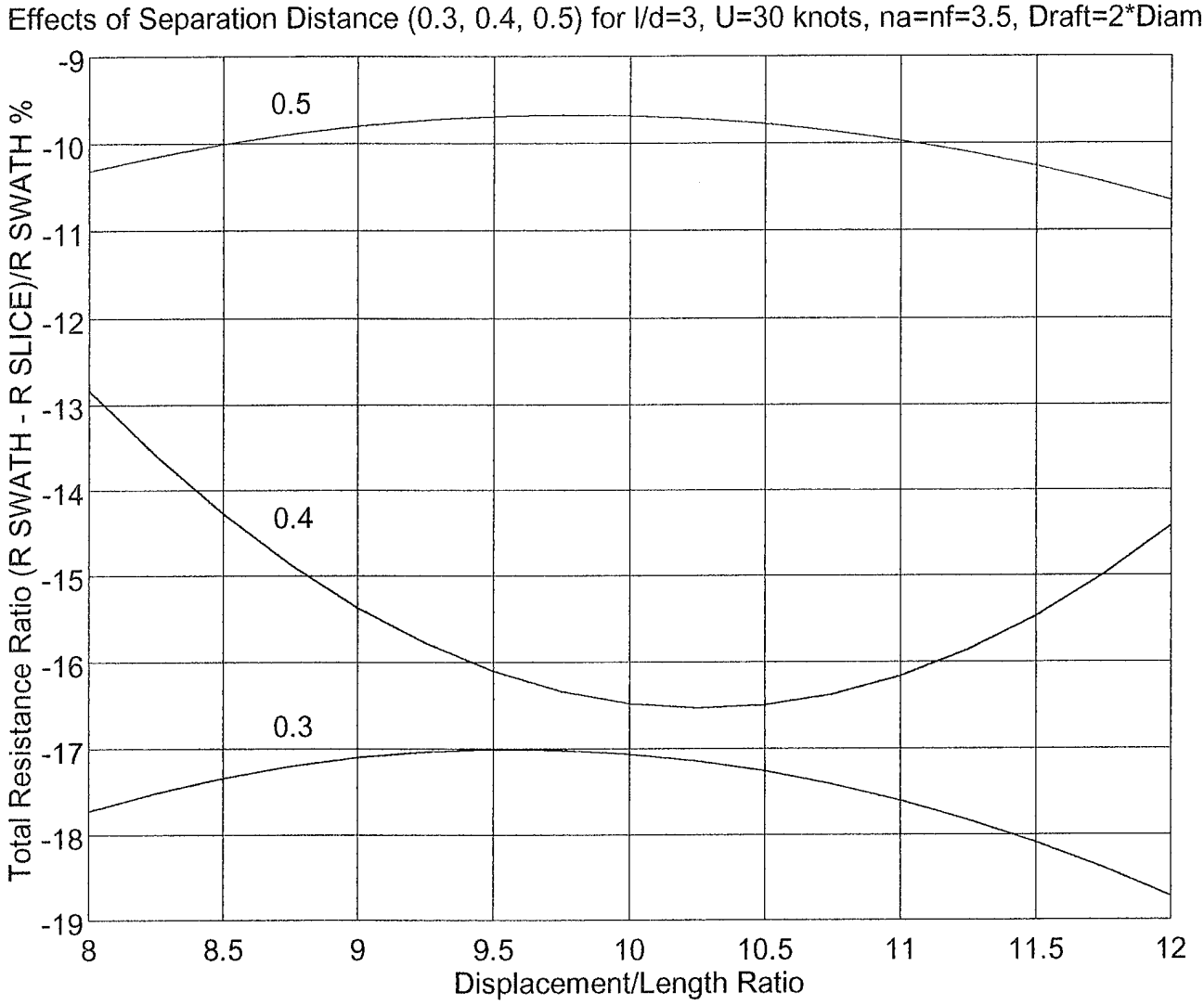


**Figure 3.12: Total resistance ratio vs. displacement to length ratio for limited diameter case for different separation distance alpha.**

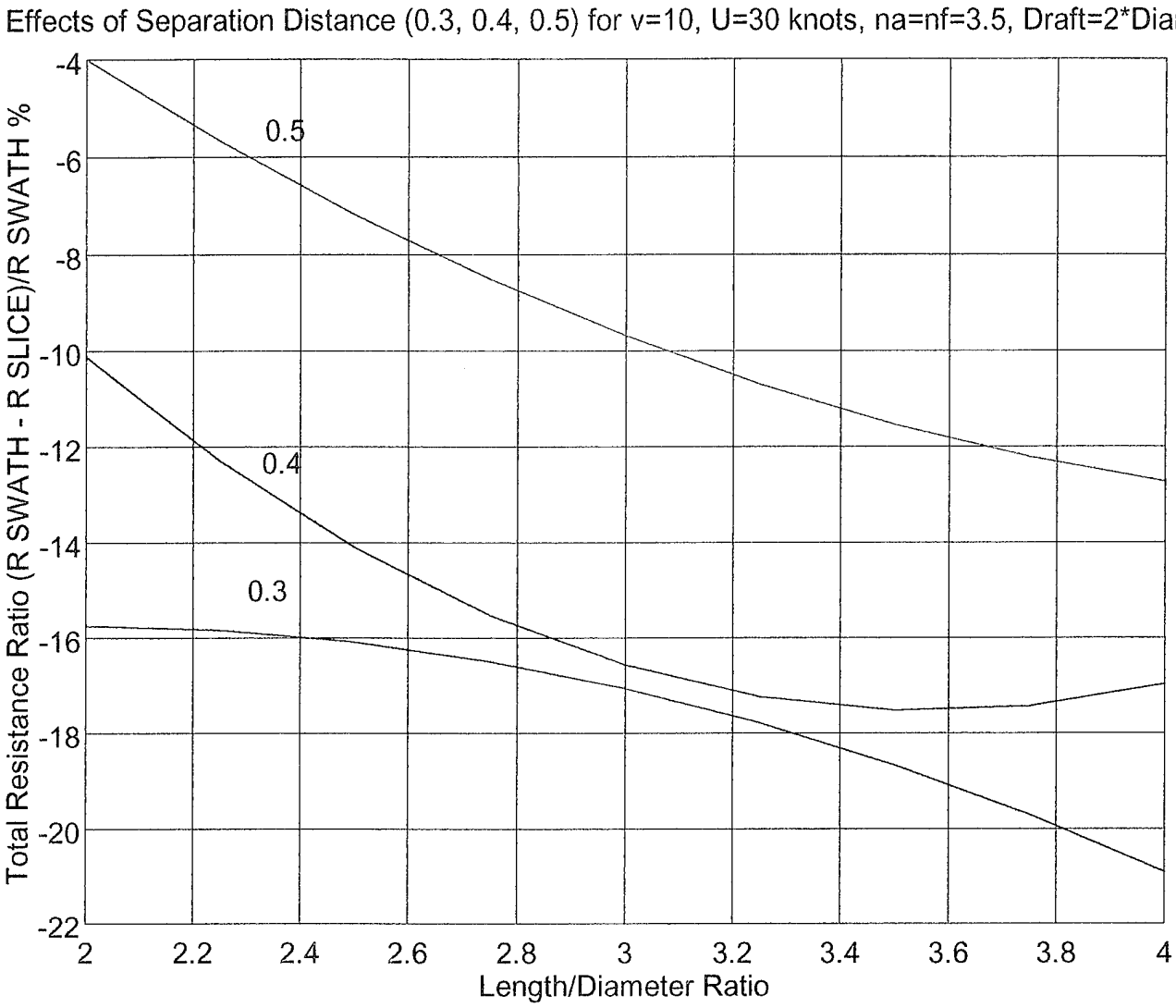


**Figure 3.13: Total resistance ratio vs. length to diameter ratio for limited diameter case for different separation distance alpha.**

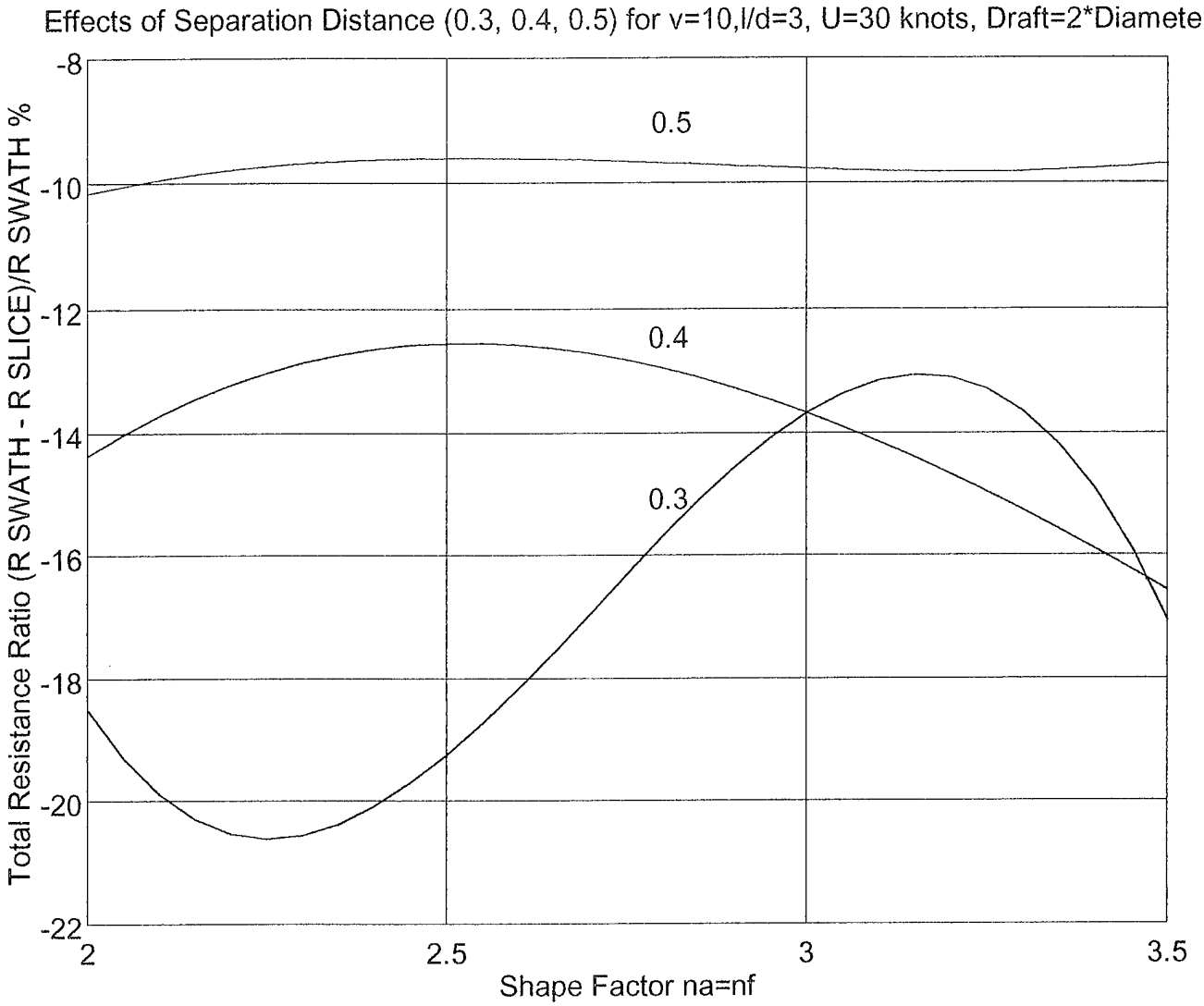


**Figure 3.14: Total resistance ratio vs. shape factor for limited diameter case for different separation distance alpha.**

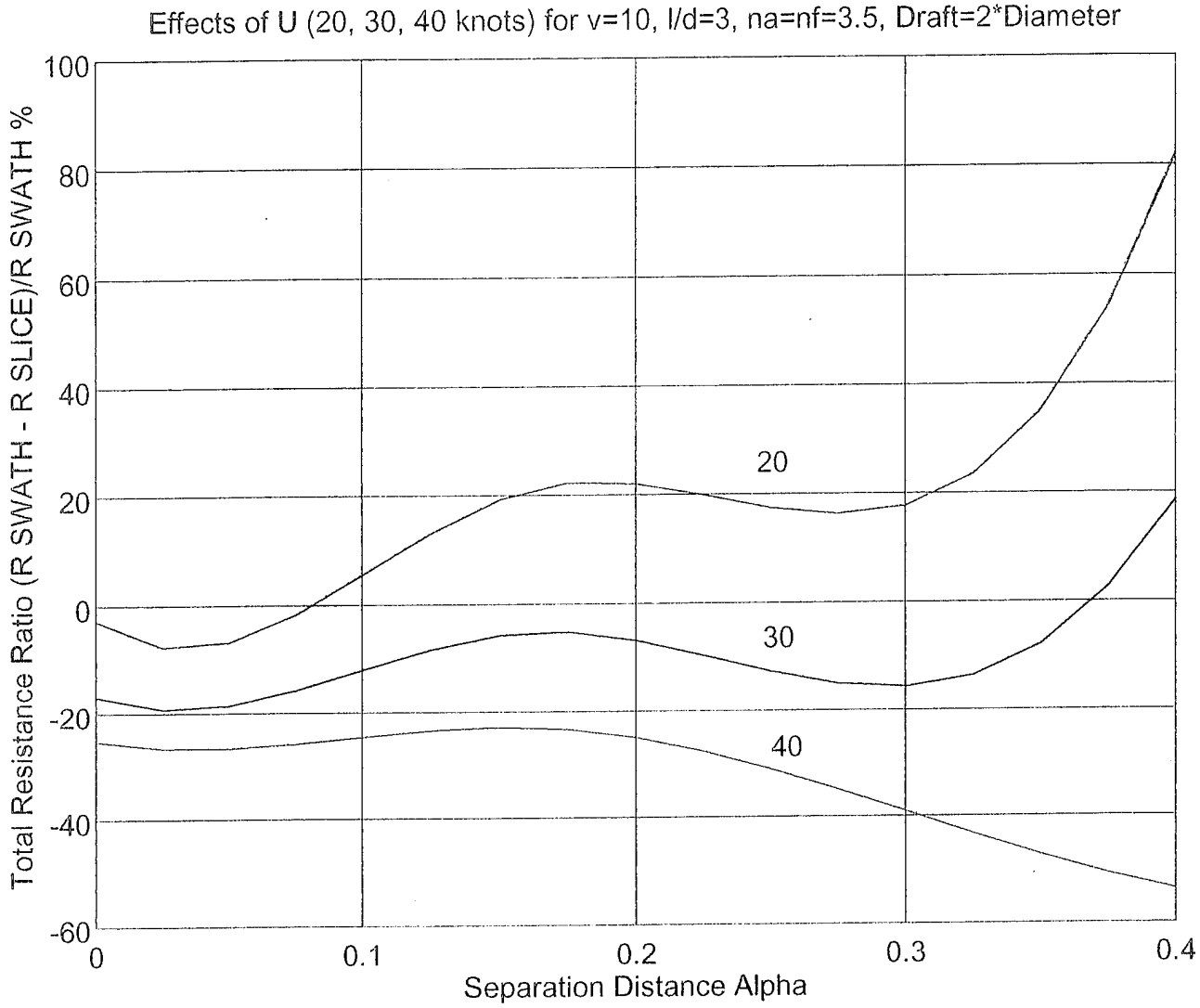


**Figure 3.15: Total resistance ratio vs. separation distance alpha for limited length case for different speeds.**

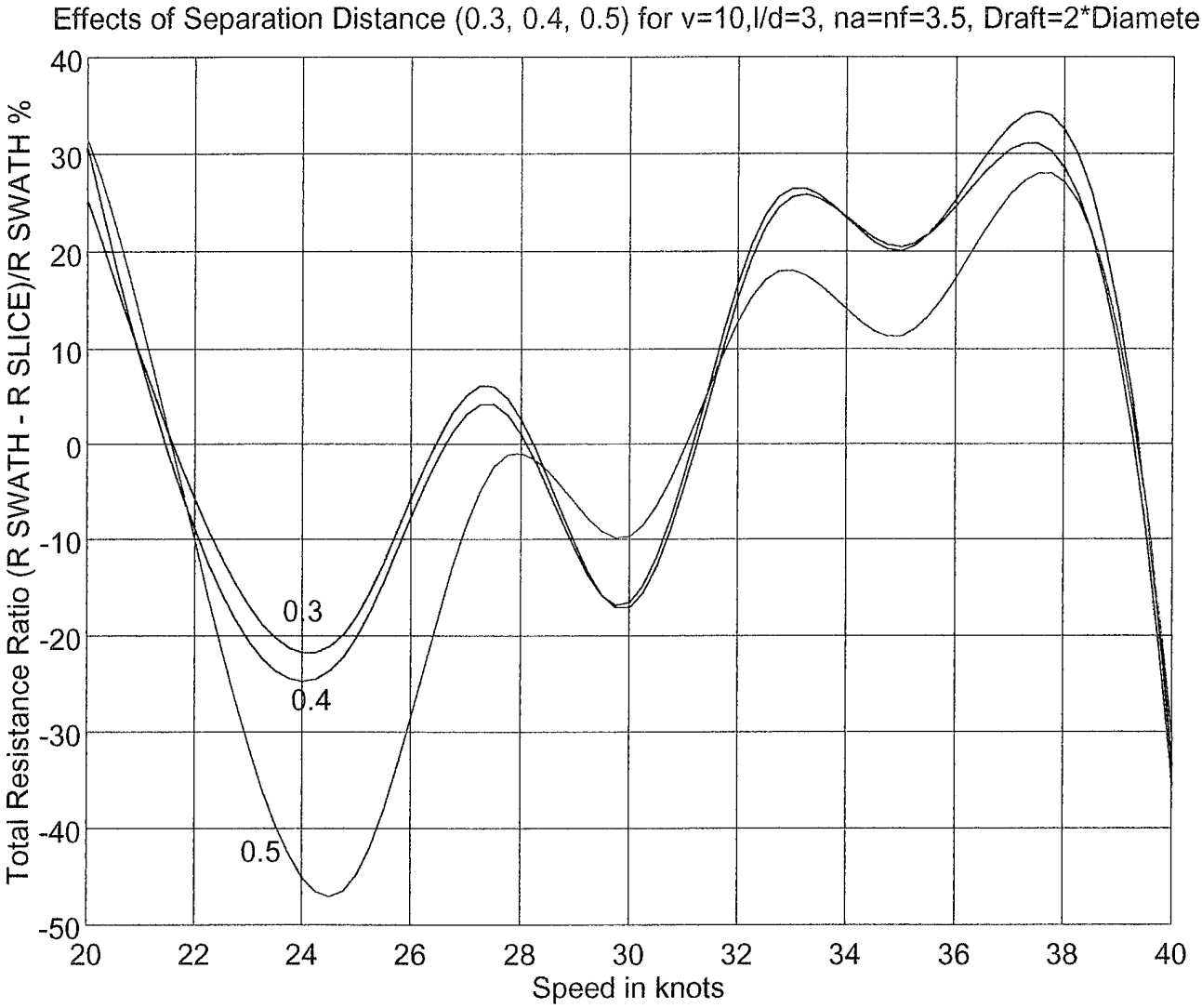


**Figure 3.16: Total resistance ratio vs. speed for limited diameter case for different separation distance alpha.**

Figure 3.8 for the shallower draft. The results are highly oscillatory, exhibiting peaks and troughs, mainly due to wave interaction effects between the two pods.

## E. DISCUSSION OF RESULTS

The previous results show that shallow drafts seem to favor a two-pod configuration versus one. From the three main components of the resistance, frictional, form drag, and wavemaking, the one component that is mostly related to draft is the wavemaking. The waves generated by a body in proximity to a free surface, and therefore its wavemaking resistance, decay exponentially with distance from the free surface. Therefore, it appears that a SLICE configuration will owe its success over a SWATH to a reduction in wavemaking resistance. For deeper drafts where wavemaking resistance is less of a problem, a SWATH configuration appears to be better. Therefore, a SWATH configuration offers less viscous resistance; i.e., frictional and form drag that a SLICE.

In order to test this hypothesis, we offer the results shown in the following figures. For the limited length case, Figure 3.17 shows that a SLICE configuration has always larger wetted surface that a SWATH. The remaining Figures 3.18 through 3.46 show that, in general, a SLICE configuration develops higher viscous resistance that a SWATH. This is predominantly due to a much higher form drag and less due to differences in skin friction. The wavemaking resistance of a SLICE can be made smaller that the corresponding wavemaking resistance of a SWATH, so that it develops less total resistance. This depends on a suitable selection of the parameters of the design as demonstrated in the previous section.

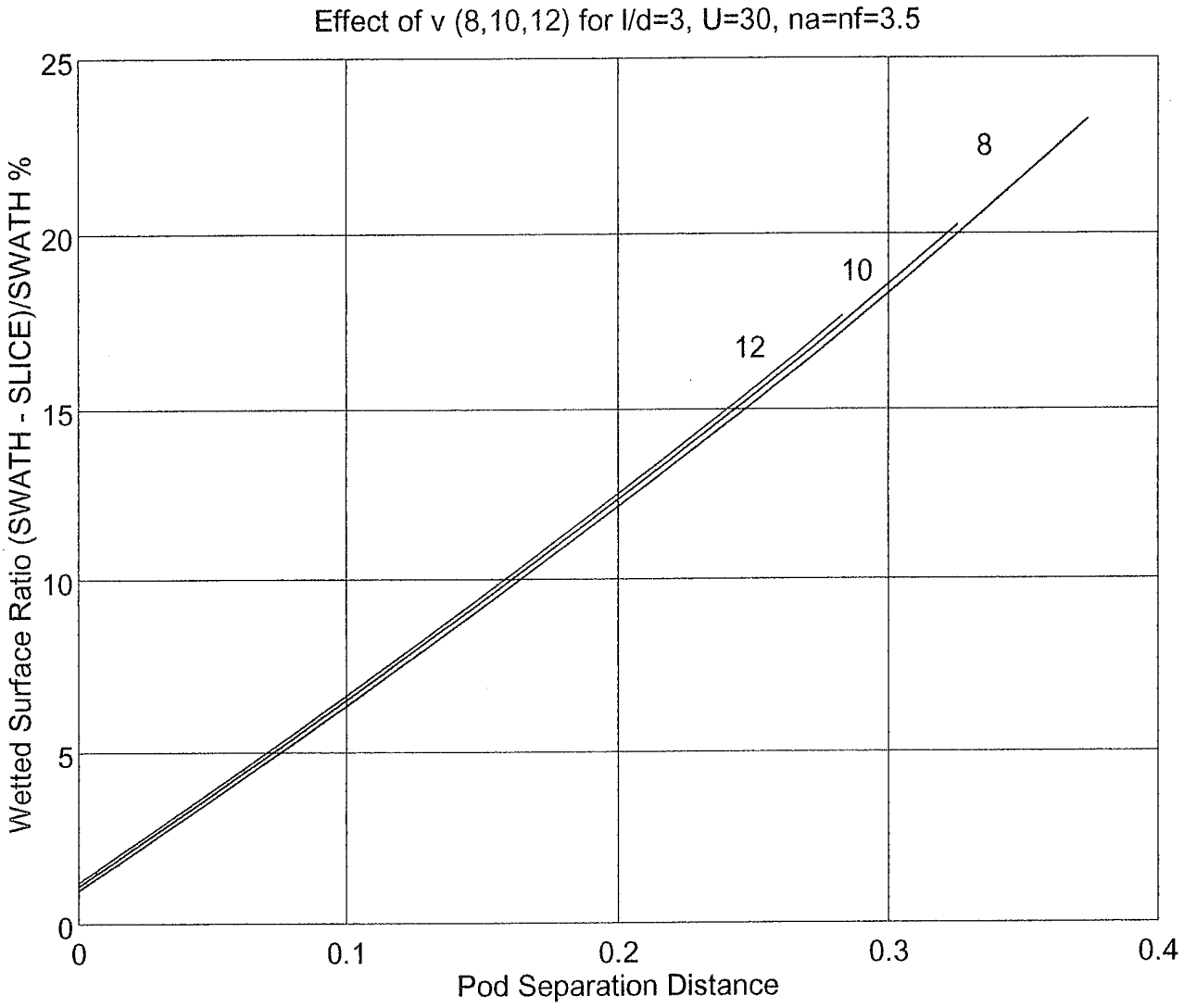


**Figure 3.17: Wetted surface ratio for viscous resistance only vs. pod separation distance for limited length case for different displacement to length ratios.**

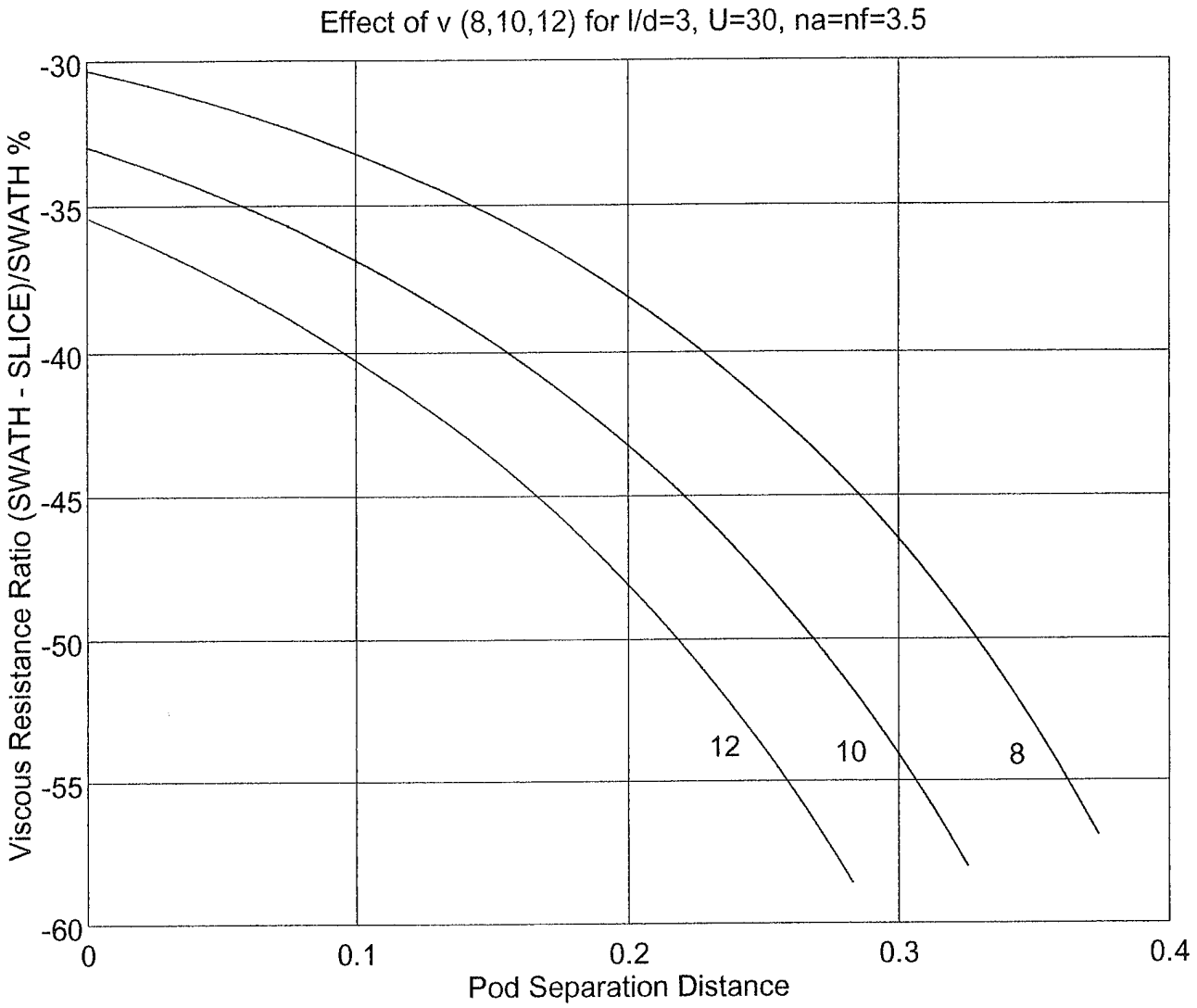


**Figure 3.18: Viscous resistance ratio vs. pod separation distance for limited length case for different displacement to length ratios.**

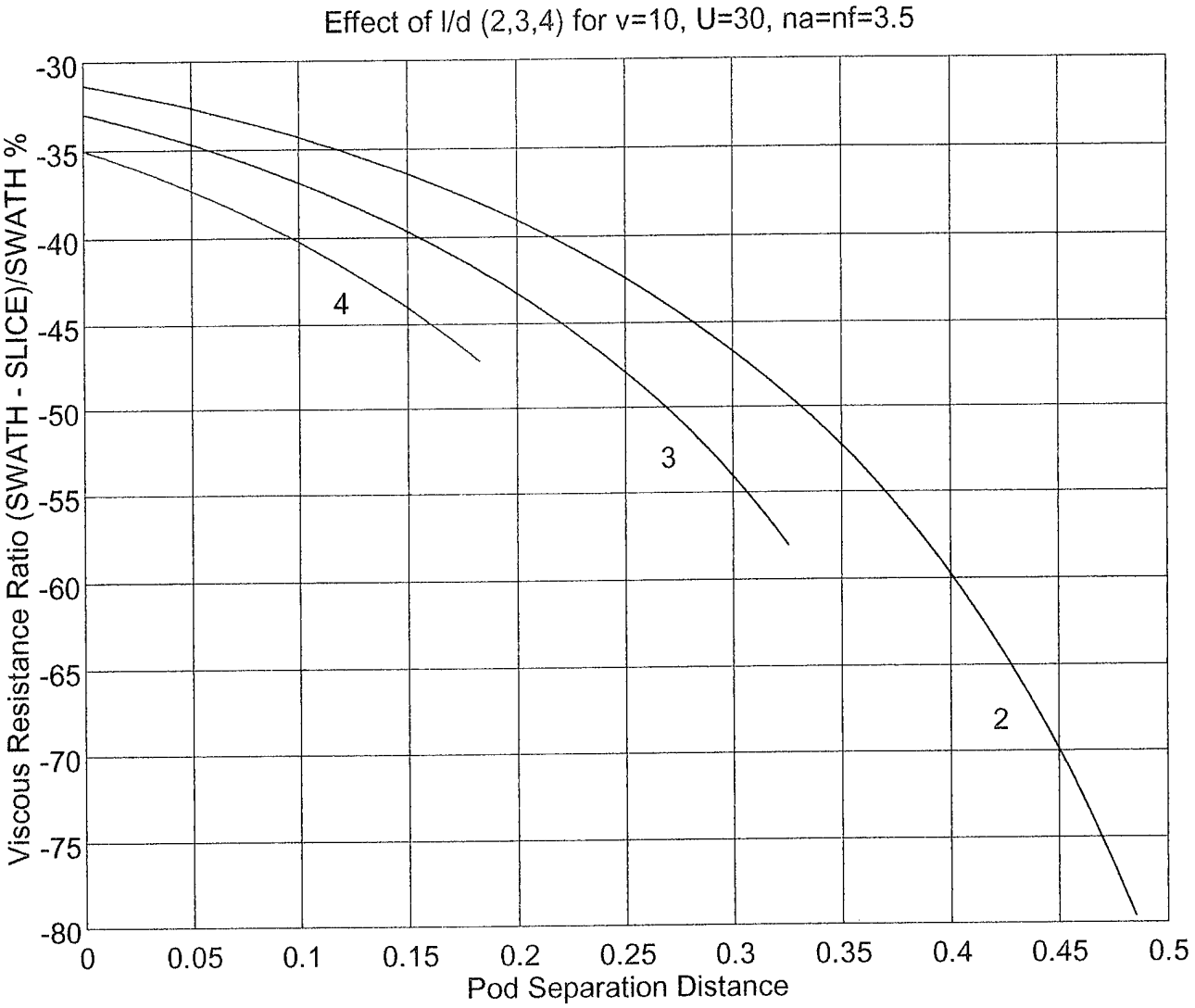


**Figure 3.19: Viscous resistance ratio vs. pod separation distance for limited length case for different length to diameter ratios.**

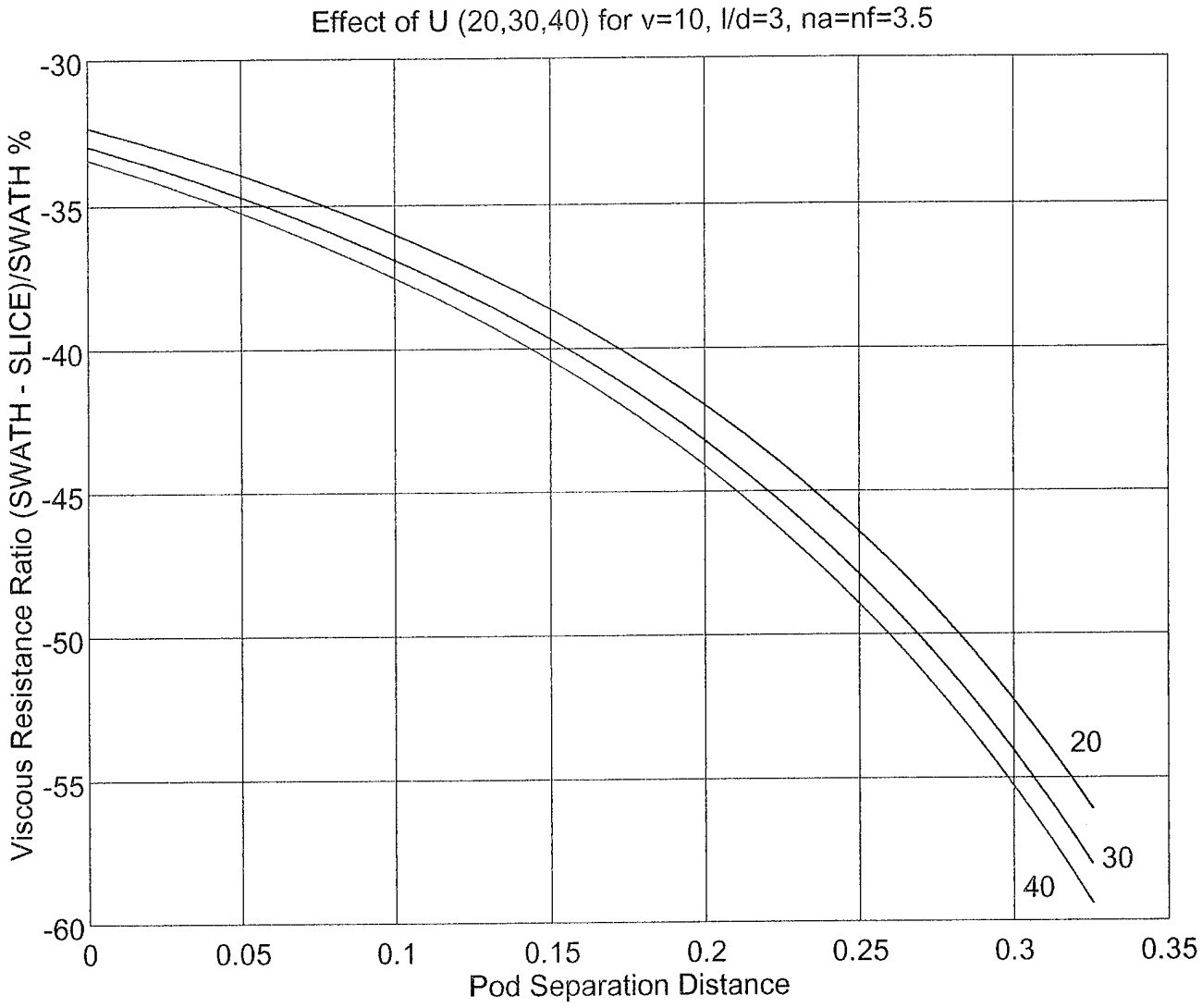


**Figure 3.20: Viscous resistance ratio vs. pod separation distance for limited length case for different speeds.**

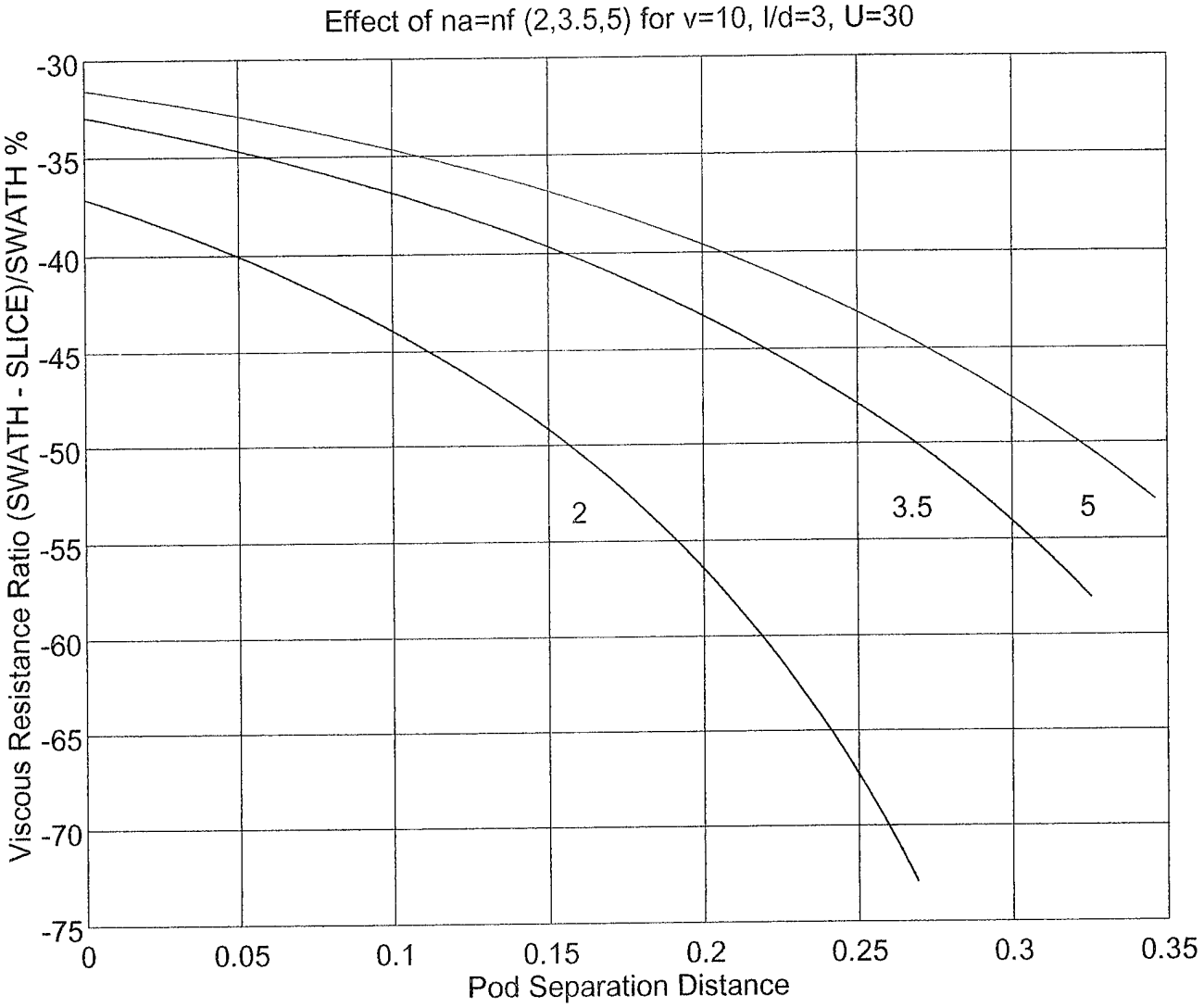


**Figure 3.21: Viscous resistance ratio vs. pod separation distance for limited length case for different shape factors.**

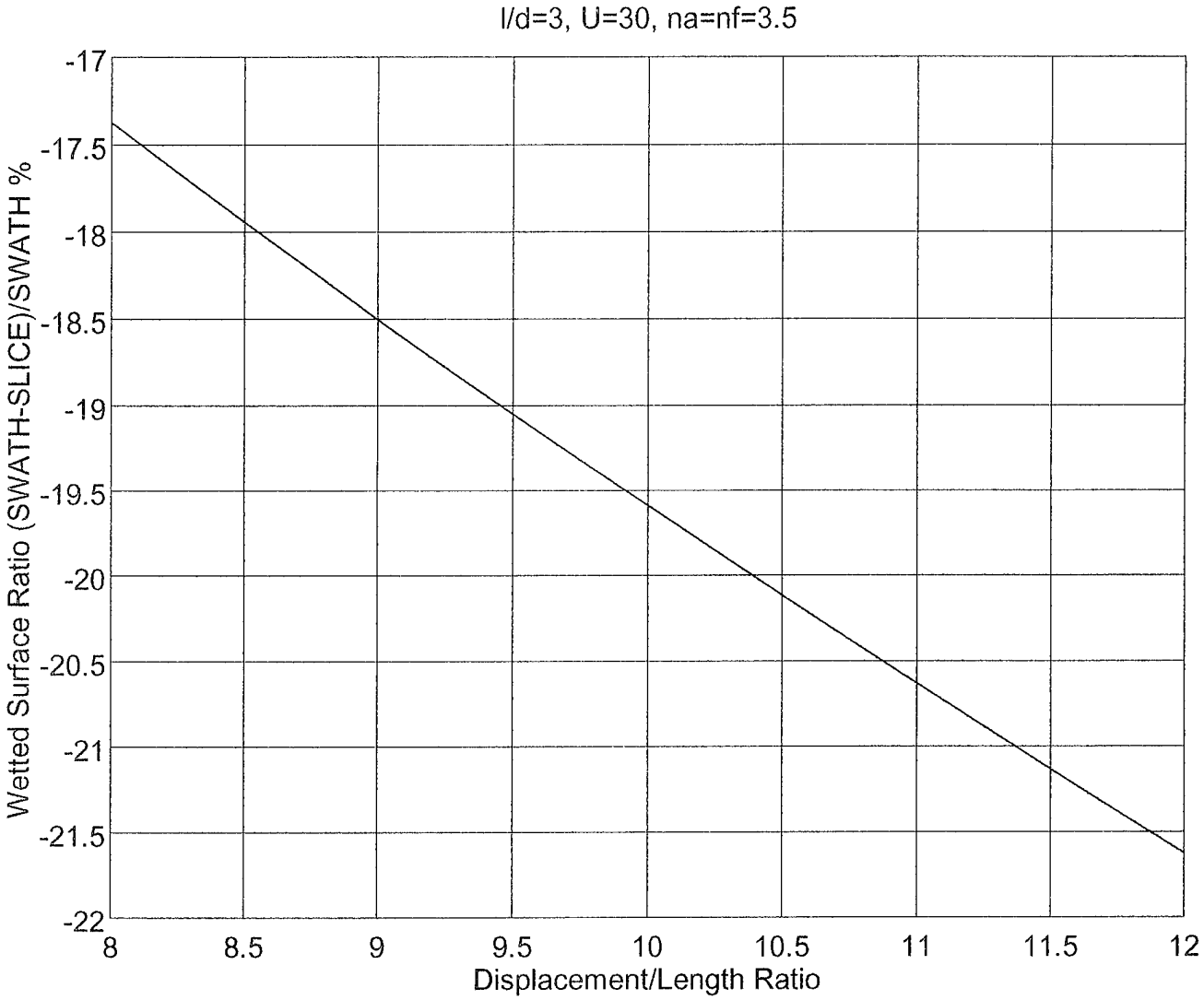


**Figure 3.22: Wetted surface ratio for viscous resistance only vs. displacement to length ratio for limited diameter case.**

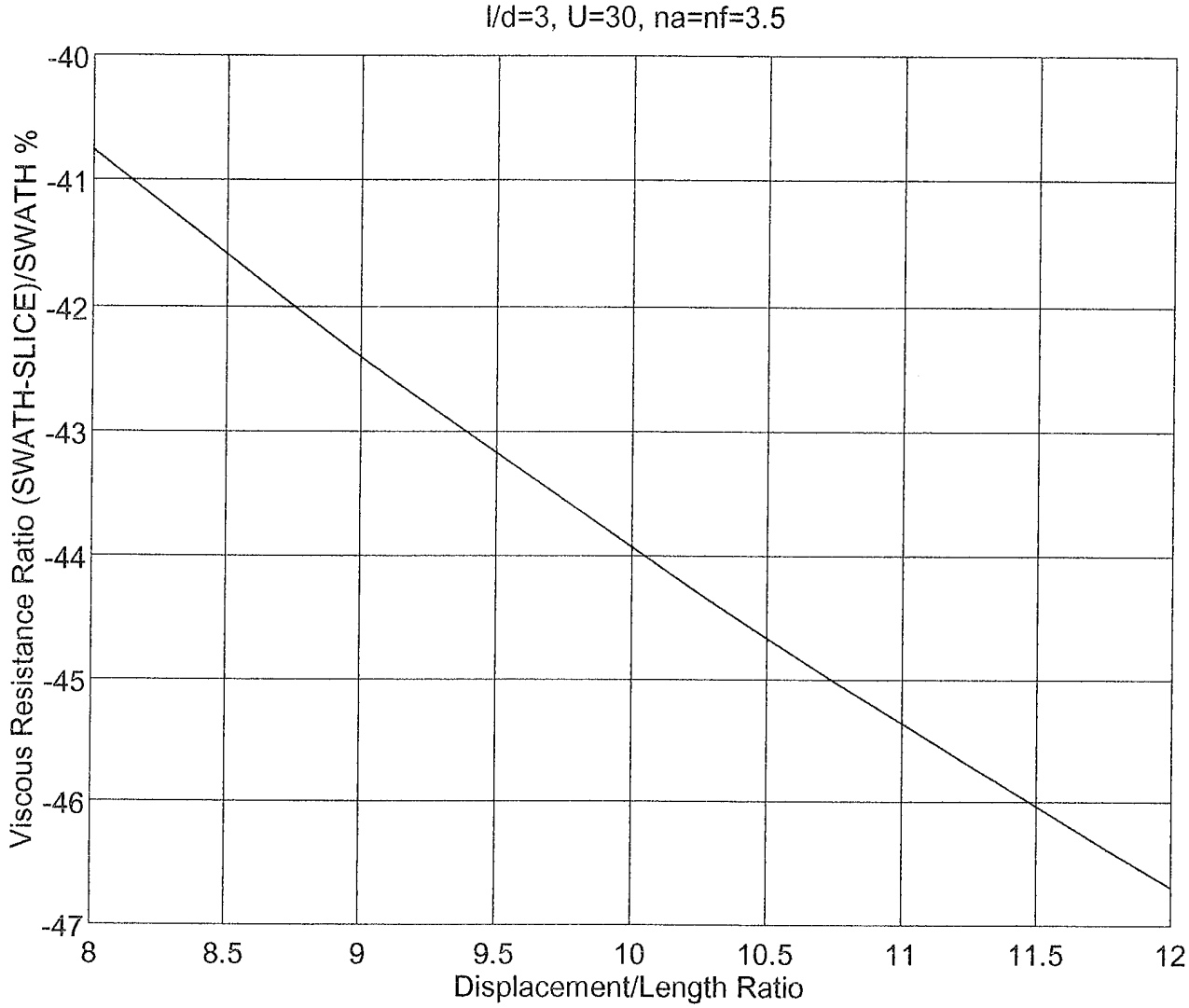


**Figure 3.23: Viscous resistance ratio vs. displacement to length ratio for limited diameter case.**

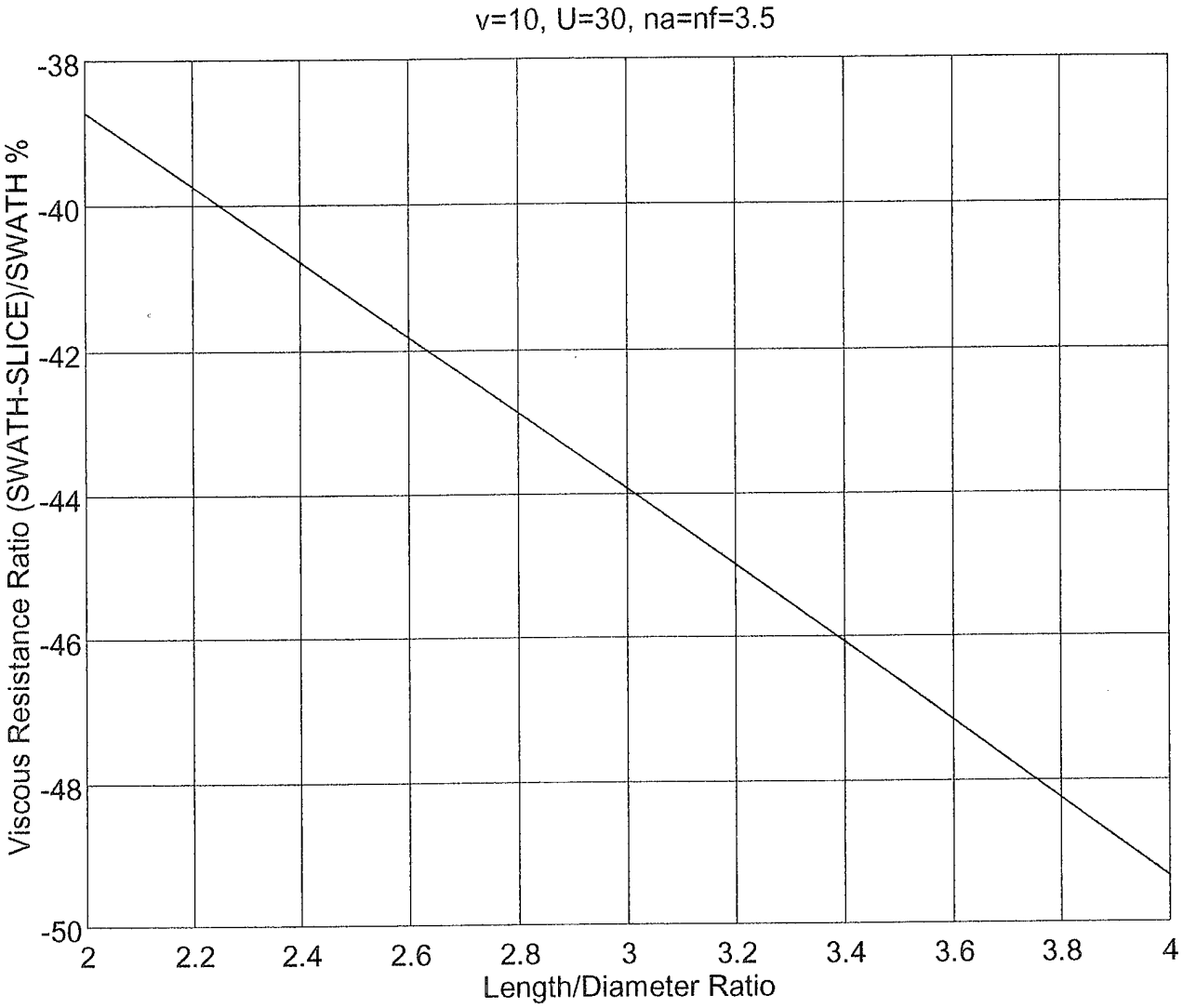


**Figure 3.24: Viscous resistance ratio vs. length to diameter ratio for limited diameter case.**

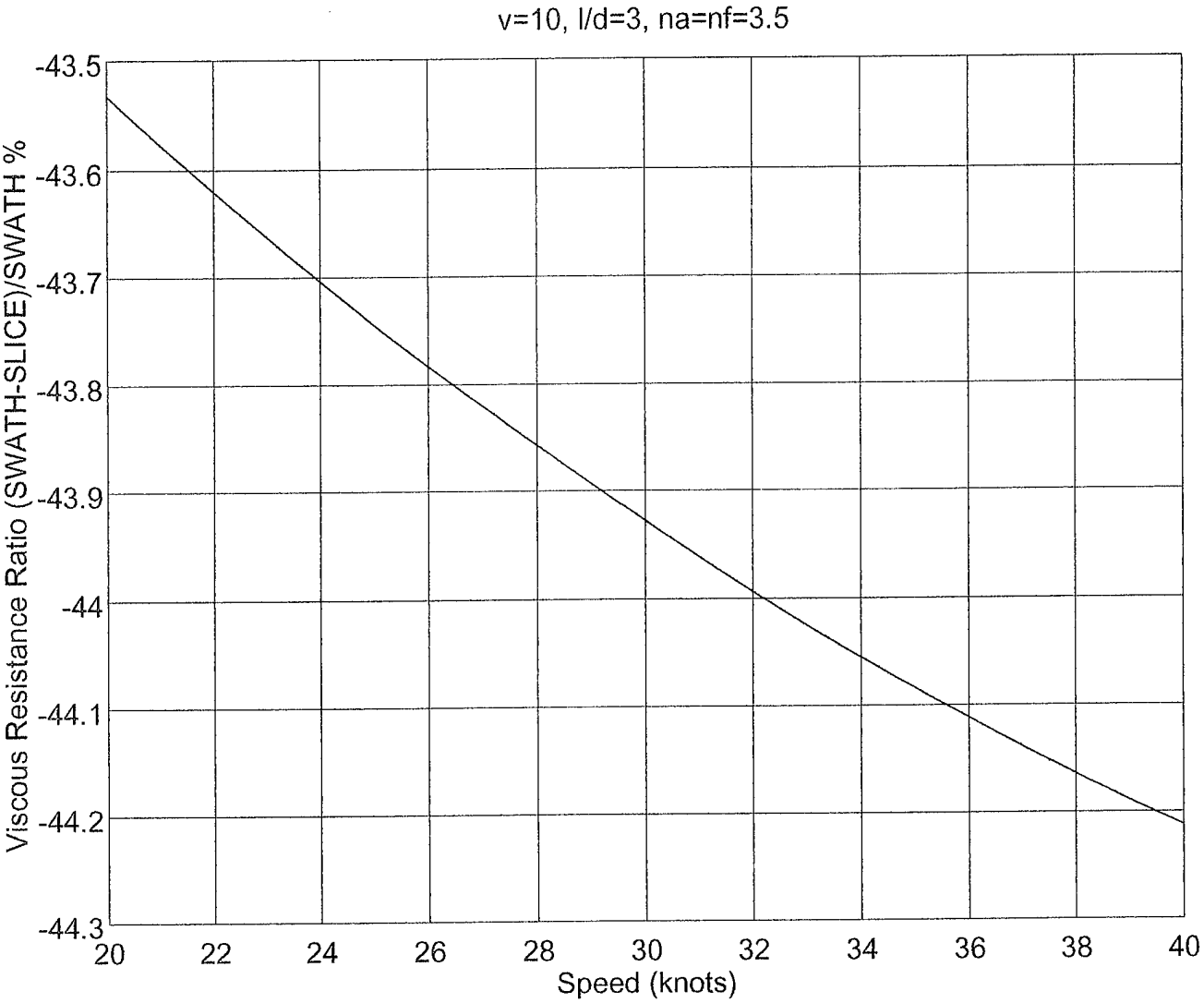


**Figure 3.25: Viscous resistance ratio vs. speed for limited diameter case.**

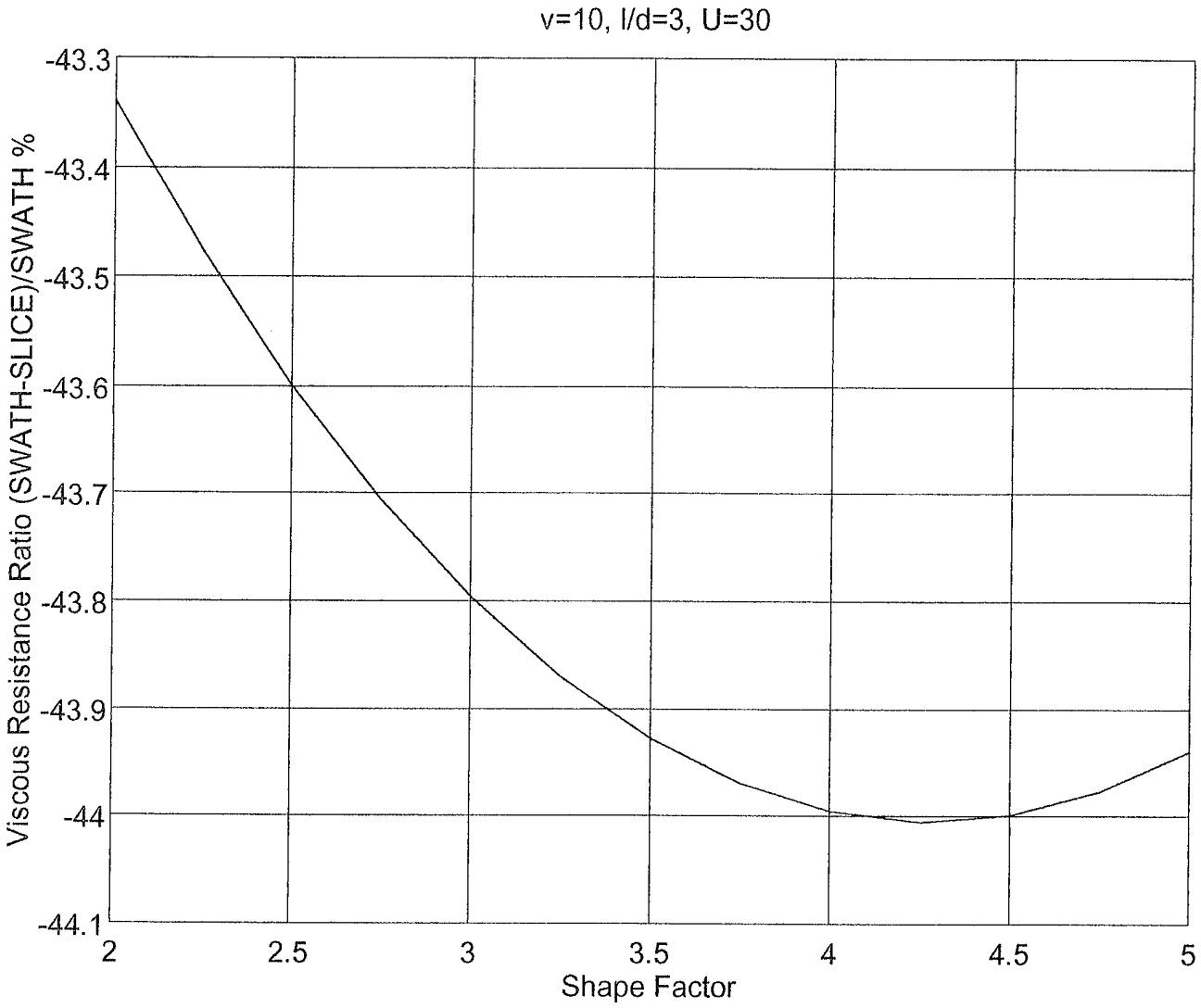


**Figure 3.26: Viscous resistance ratio vs. shape factor for limited diameter case.**

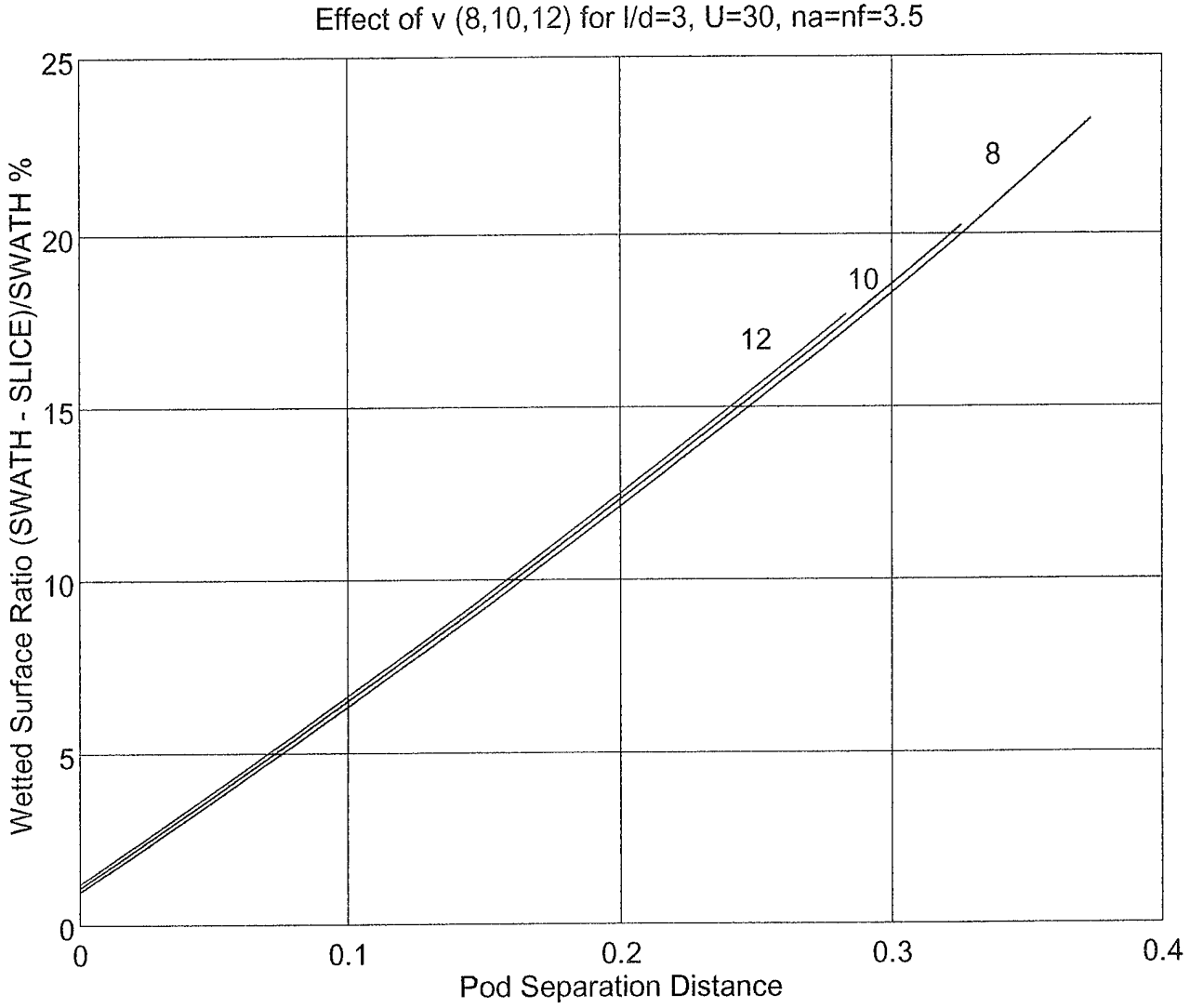


**Figure 3.27: Wetted surface ratio for skin friction only vs. pod separation distance for limited length case for different displacement to length ratios.**

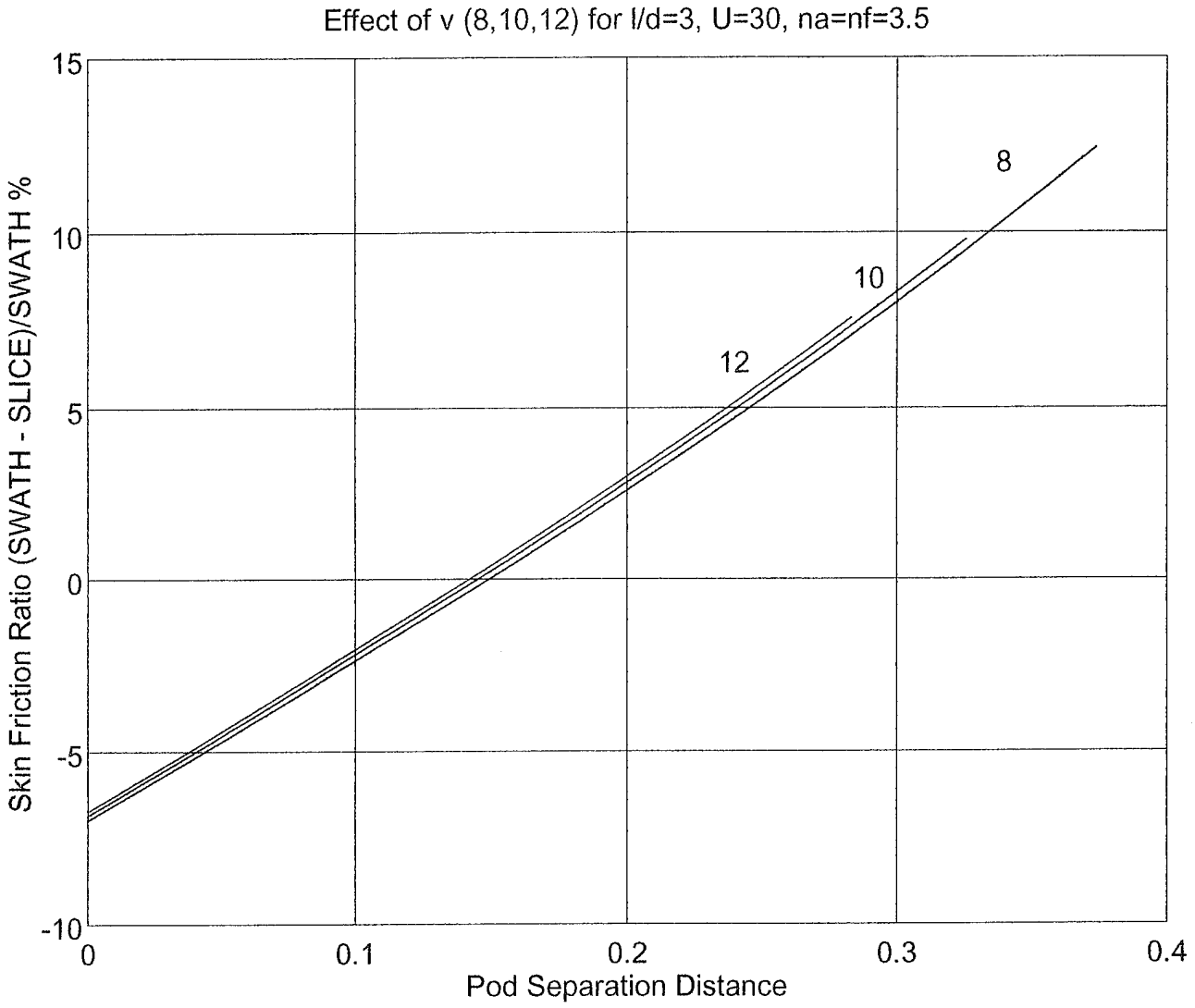


**Figure 3.28: Skin friction ratio vs. pod separtion distance for limited length case for different displacement to length ratios.**

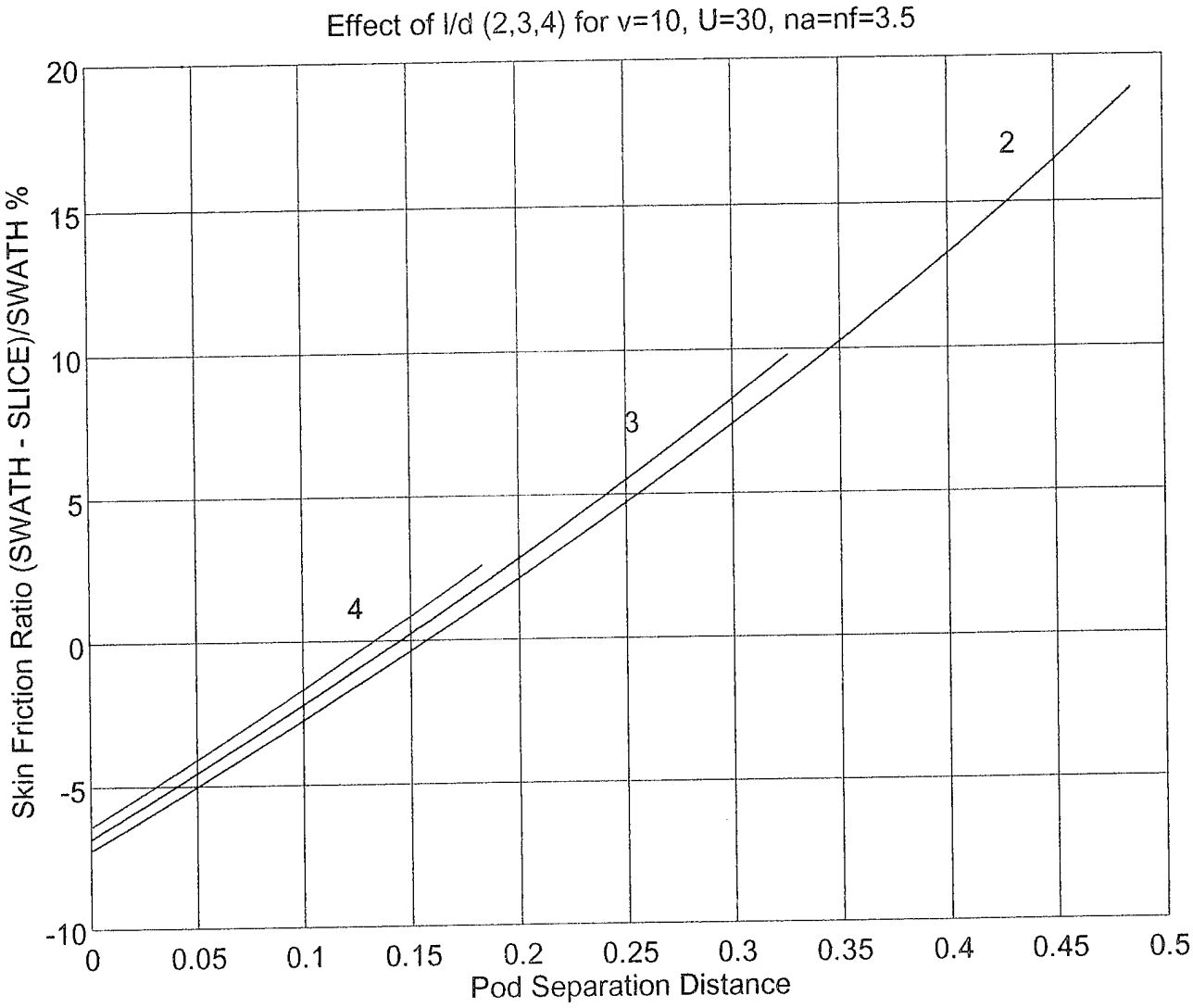


**Figure 3.29: Skin friction ratio vs. pod separation distance for limited length case for different length to diameter ratios.**

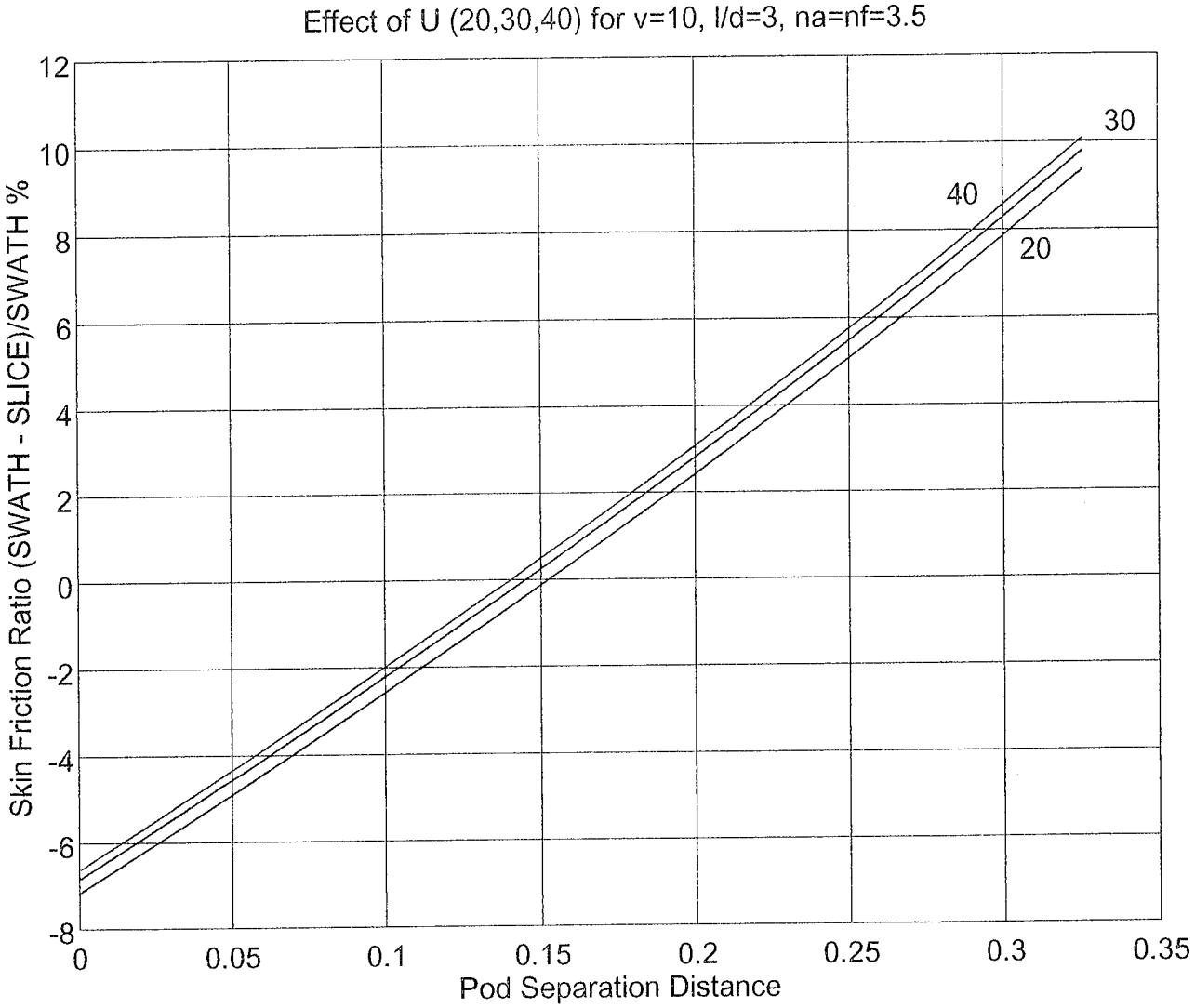


**Figure 3.30: Skin friction ratio vs. pod separation distance for limited length case for different speeds.**

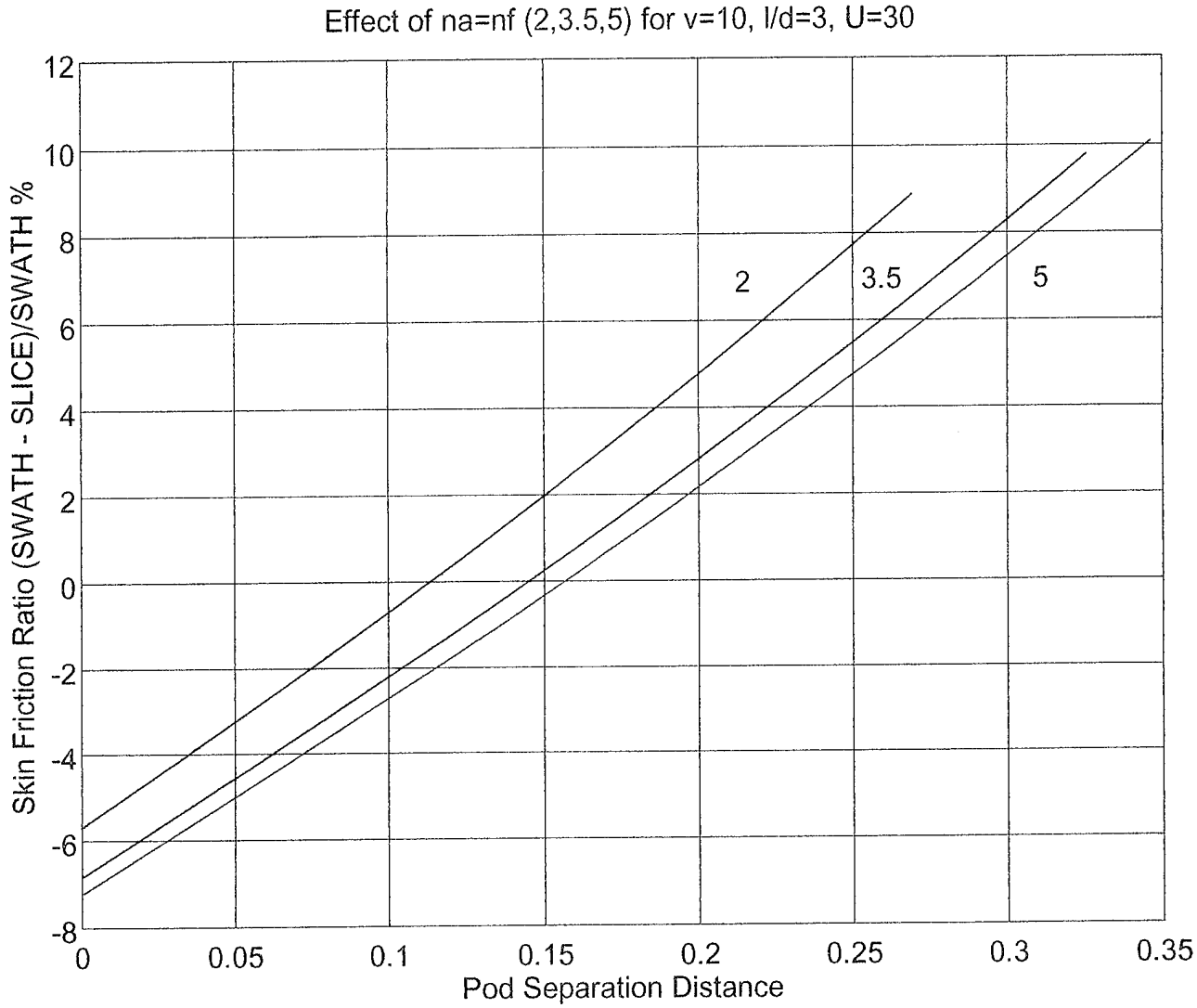


**Figure 3.31: Skin friction ratio vs. pod separation distance for limited length case for different shape factors.**

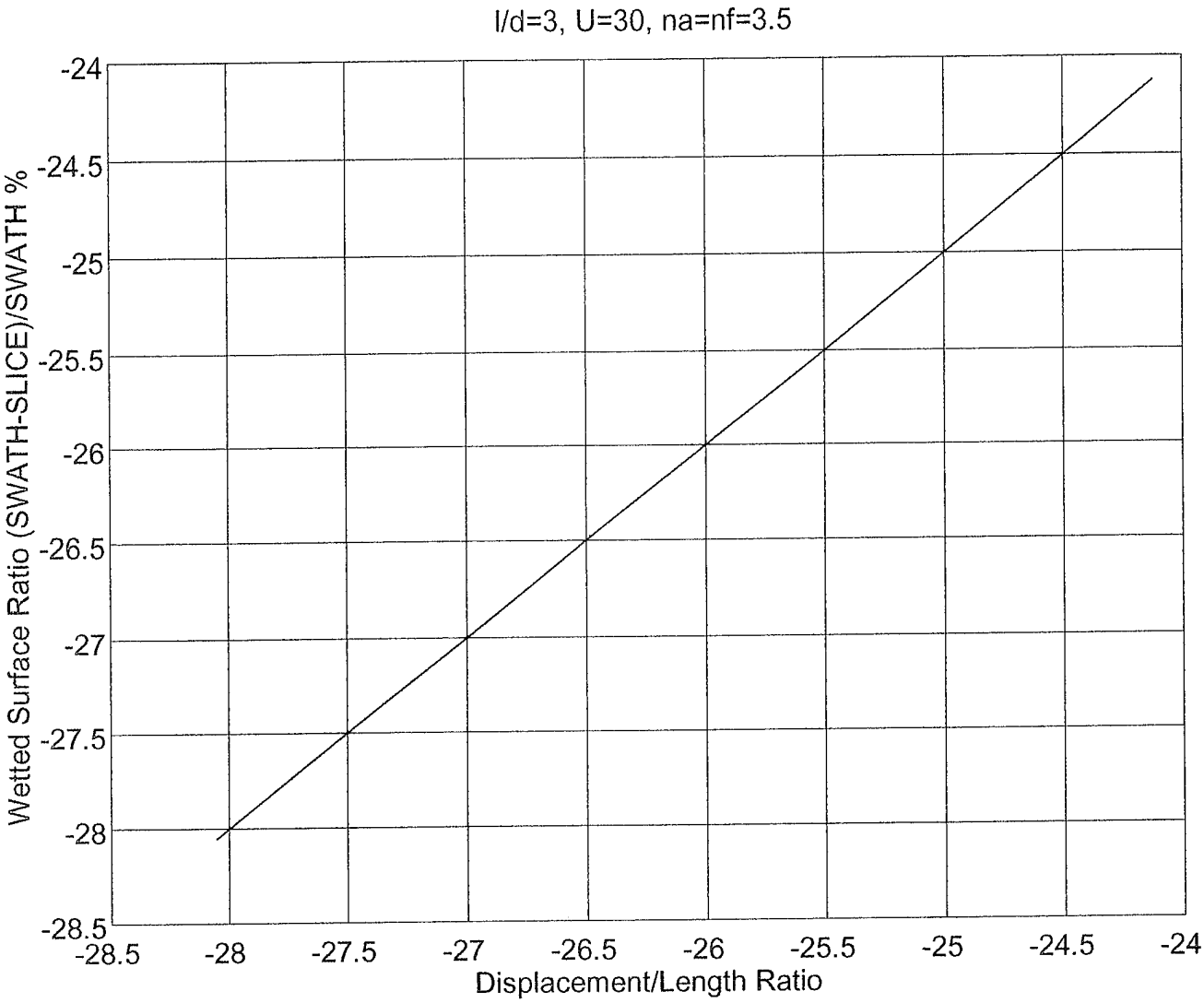


**Figure 3.32: Wetted surface ratio for skin friction only vs. displacement to length ratio for limited diameter case.**

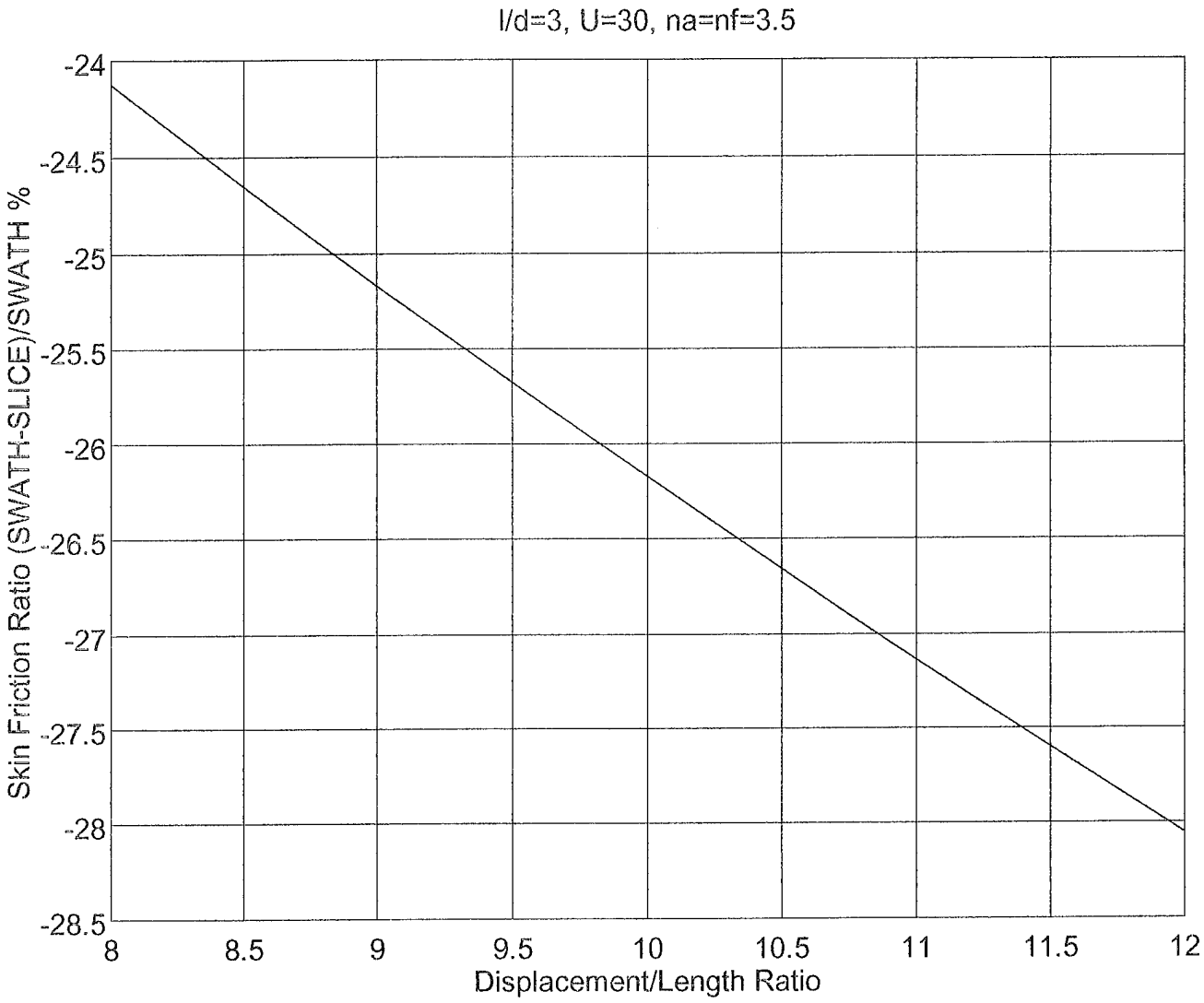


**Figure 3.33: Skin friction ratio vs. displacement to length ratio for limited diameter case.**

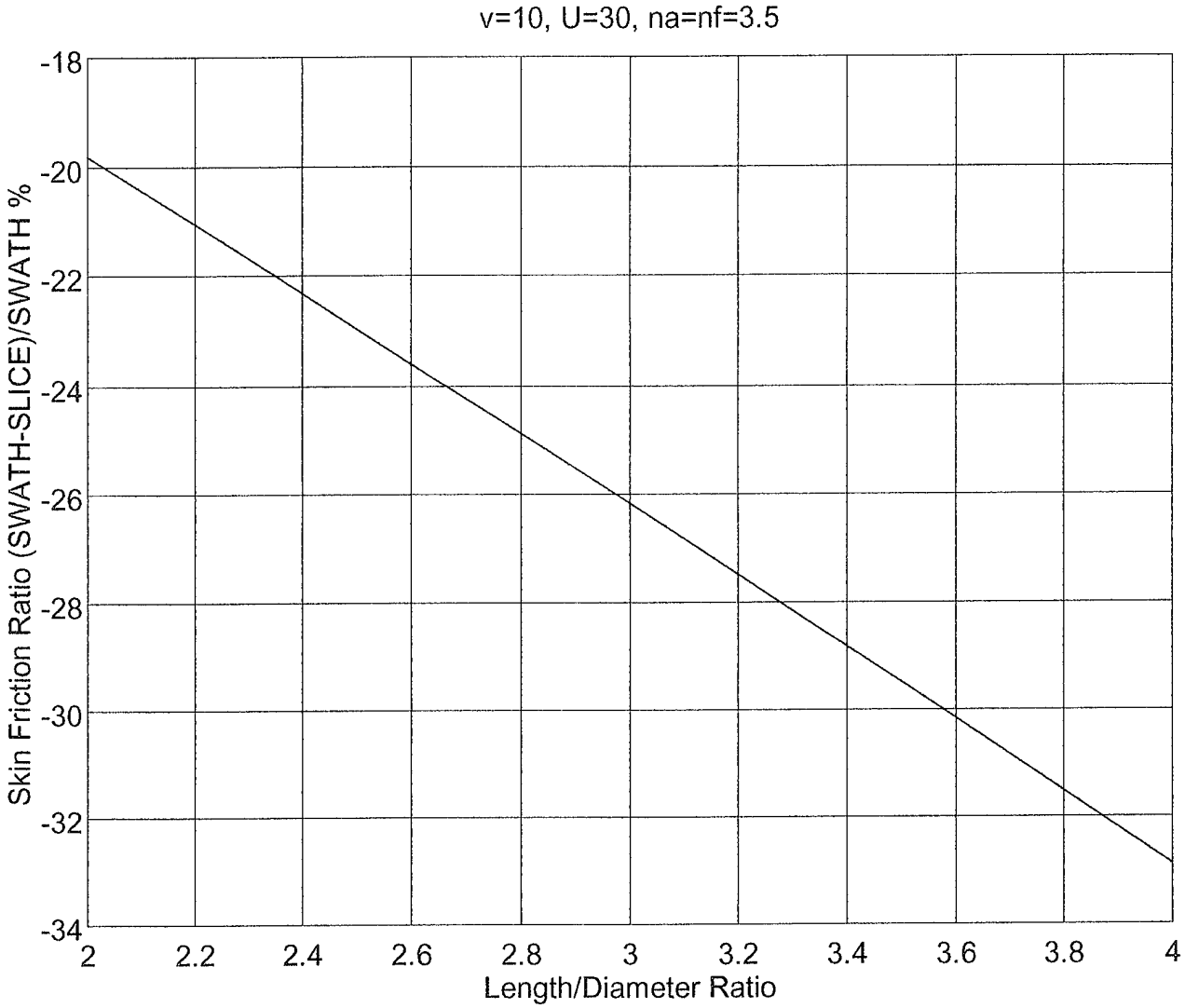


**Figure 3.34: Skin friction ratio vs. length to diameter ratio for limited diameter case.**

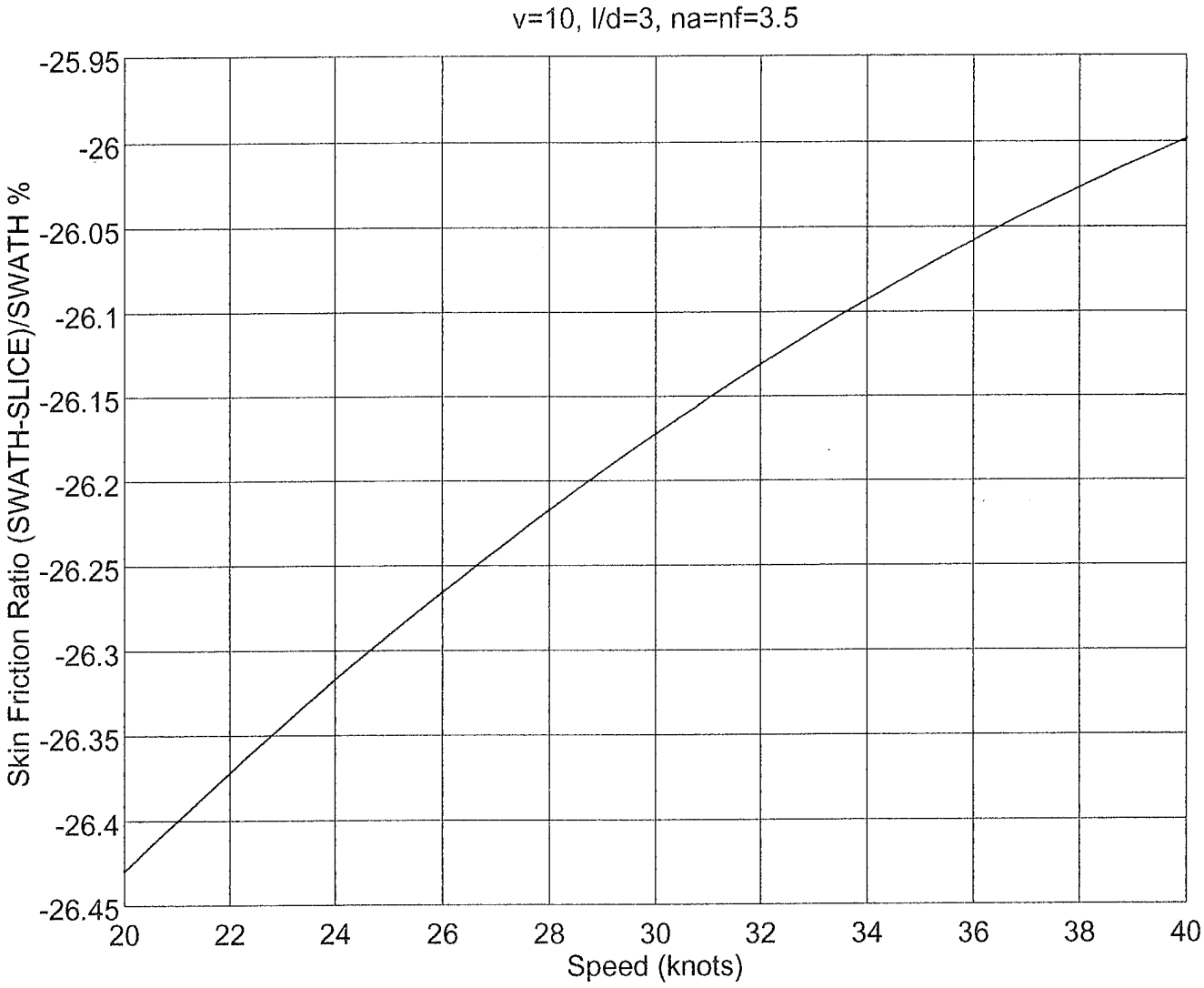


**Figure 3.35: Skin friction ratio vs. speed for limited diameter case.**

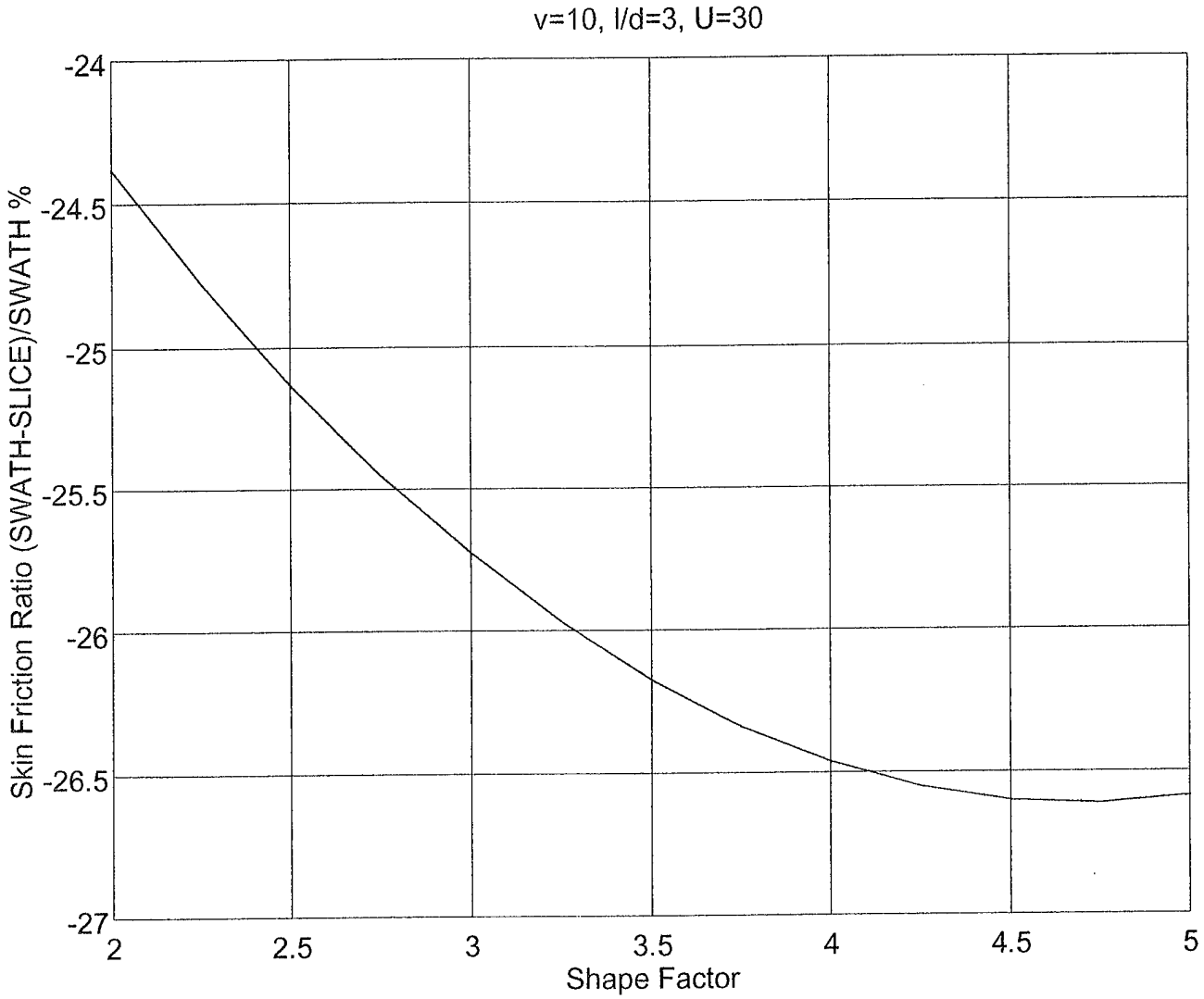


**Figure 3.36: Skin friction ratio vs. shape factor for limited diameter case.**

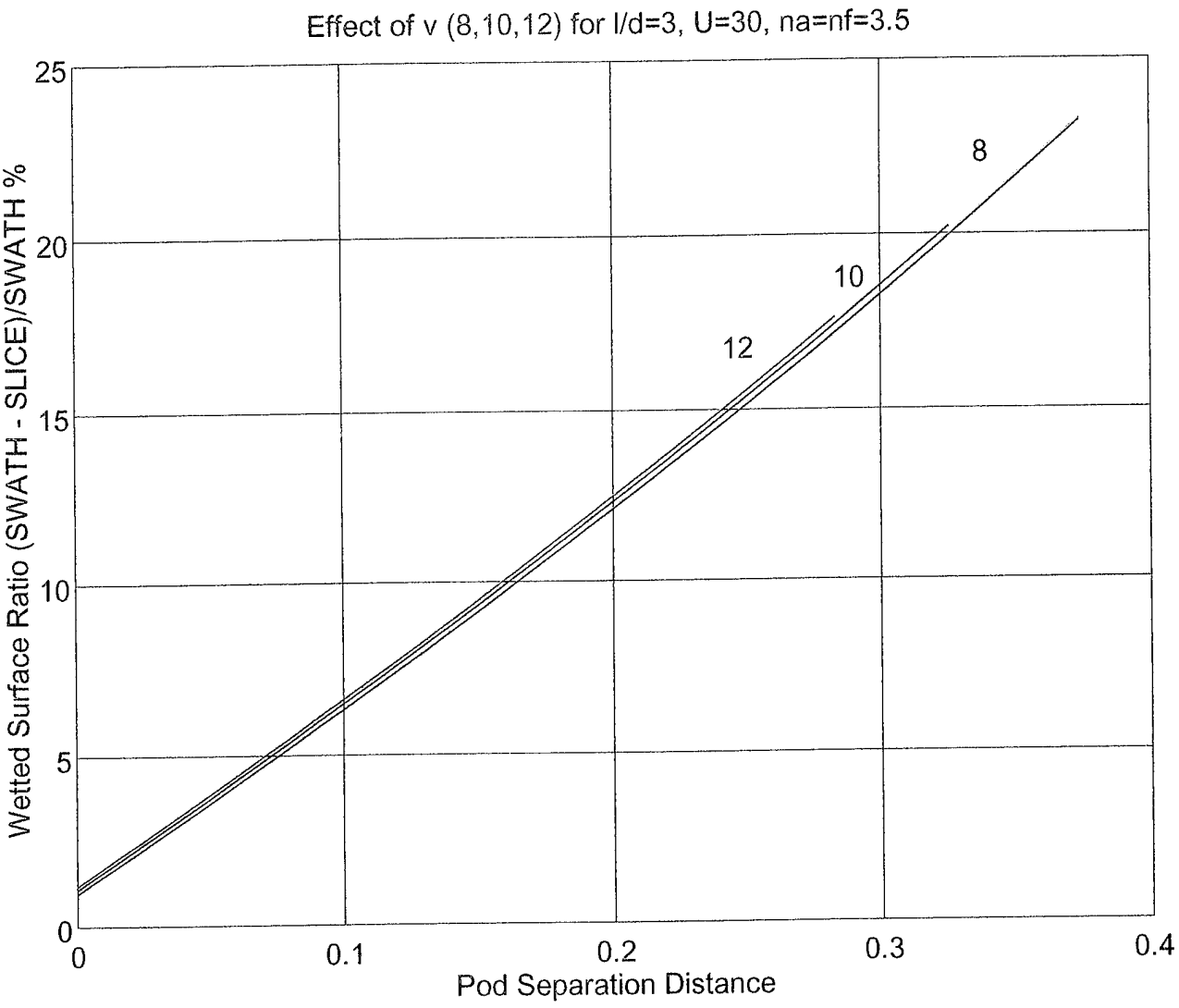


**Figure 3.37: Wetted surface ratio for form drag only vs. pod separation distance for limited length for different displacement to length ratios.**

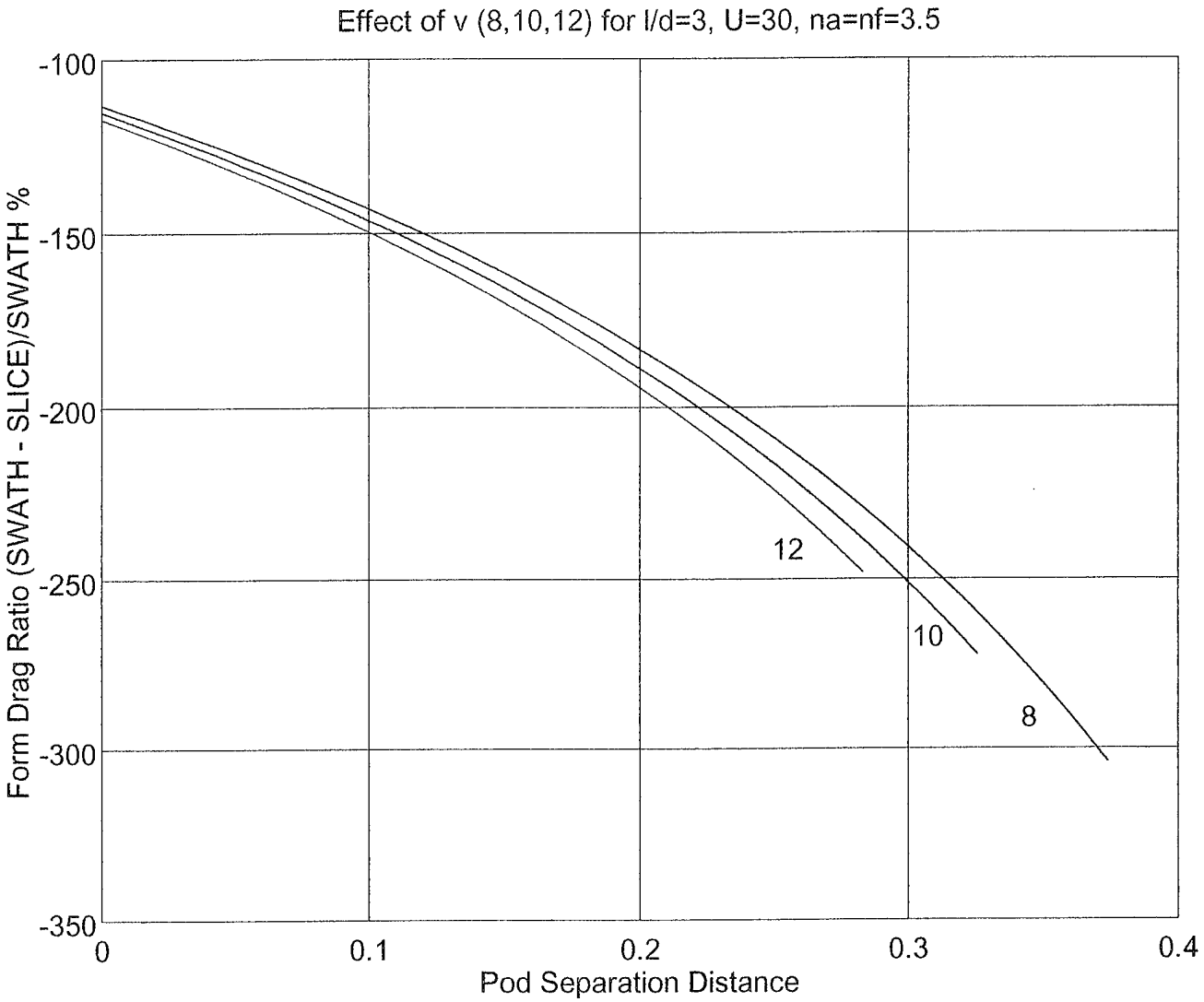


**Figure 3.38: Form drag vs. pod separation distance for limited length for different displacement to length ratios.**

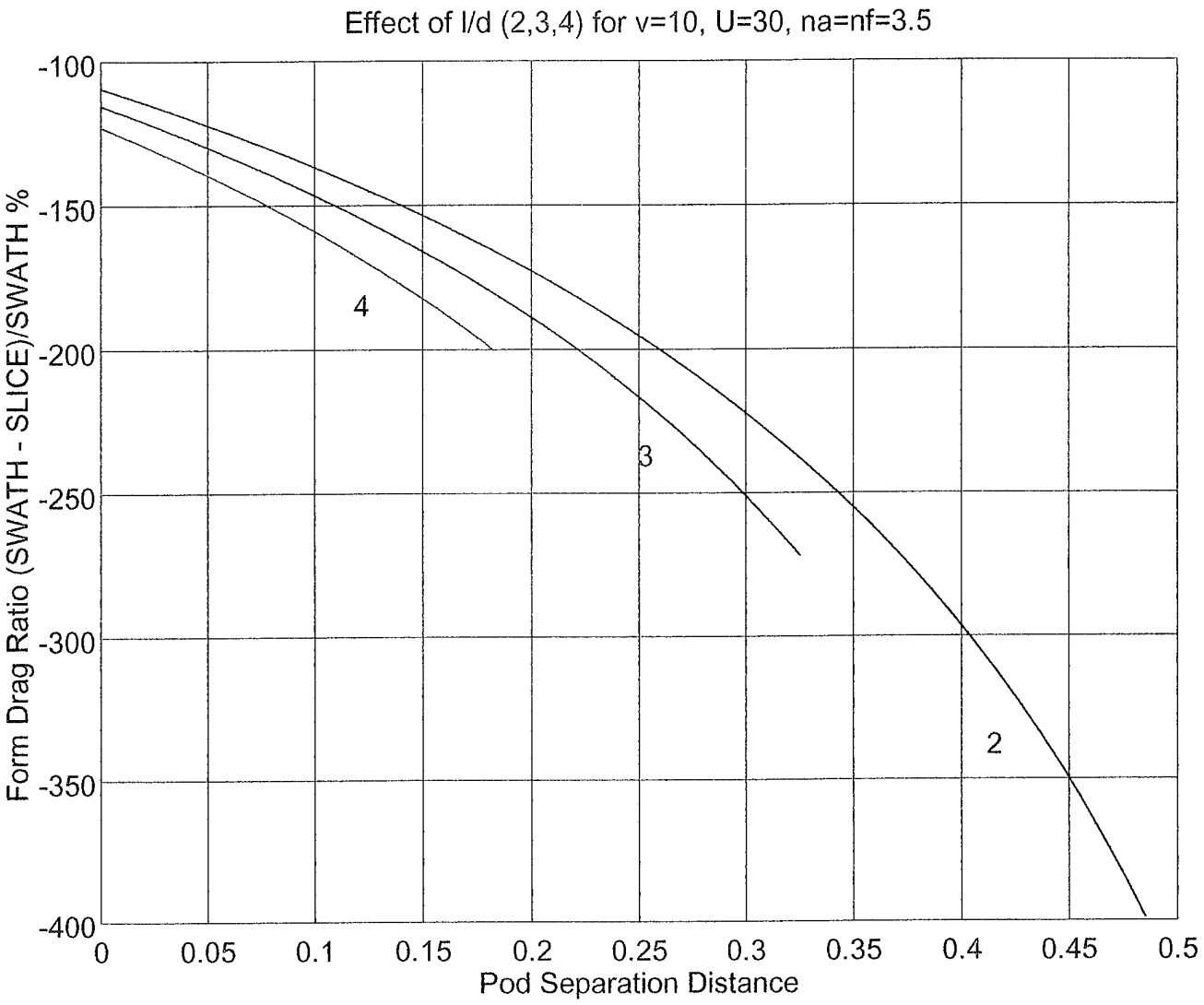


**Figure 3.39: Form drag ratio vs. pod separation distance for limited length for different length to diameter ratios.**

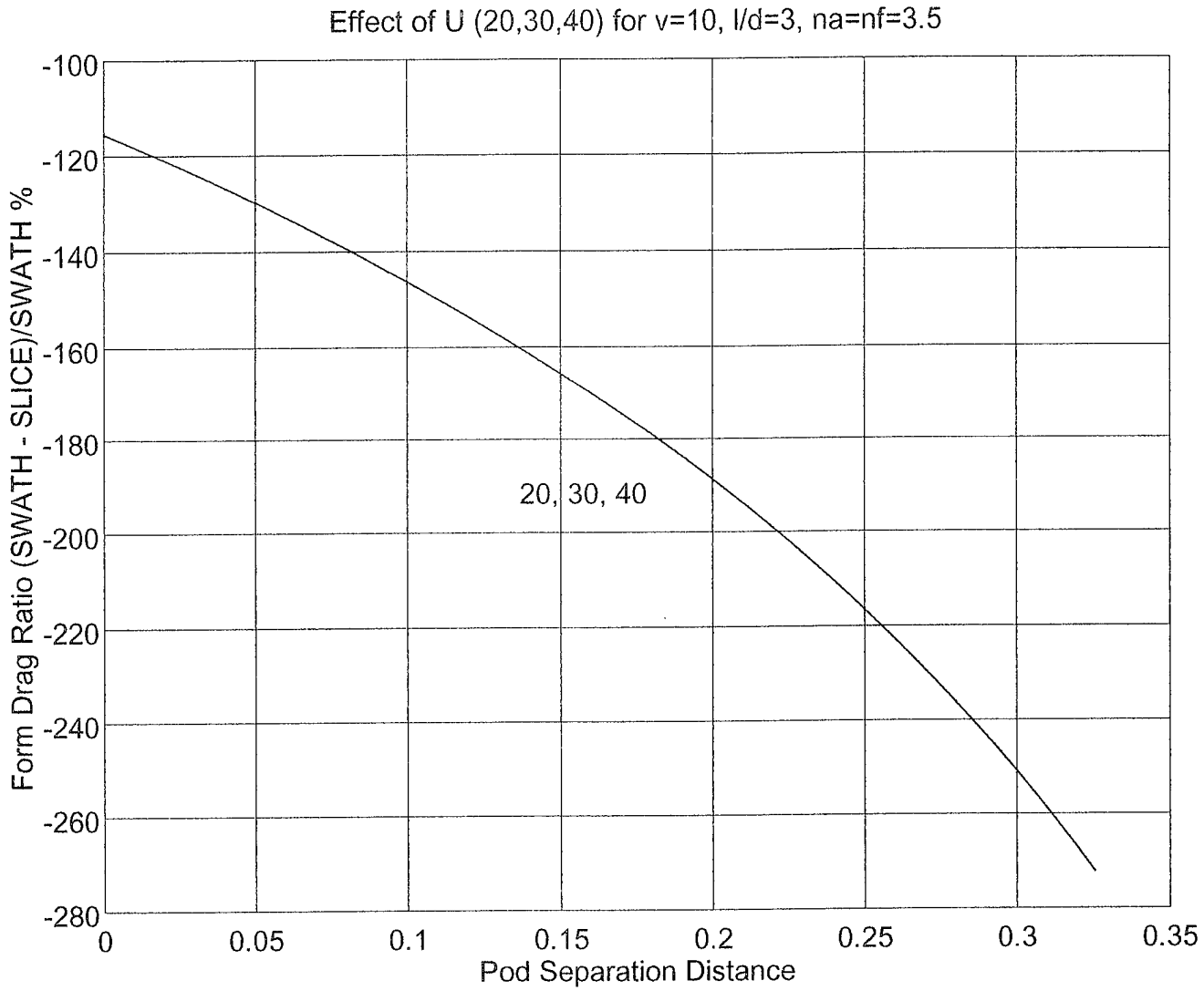


**Figure 3.40: Form drag ratio vs. pod separation distance for limited length for different speeds.**

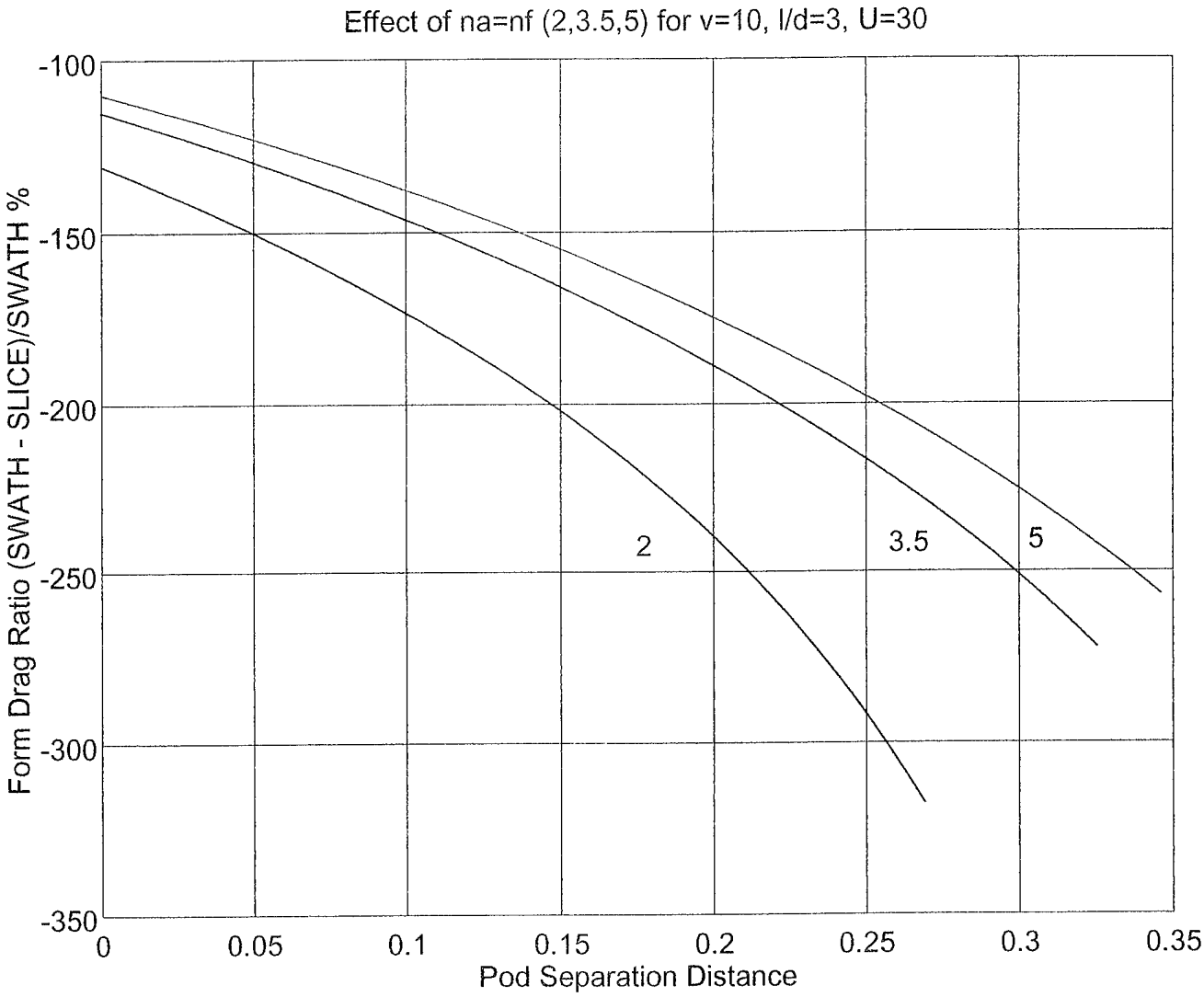


**Figure 3.41: Form drag ratio vs. pod separation distance for limited length for different shape factors.**

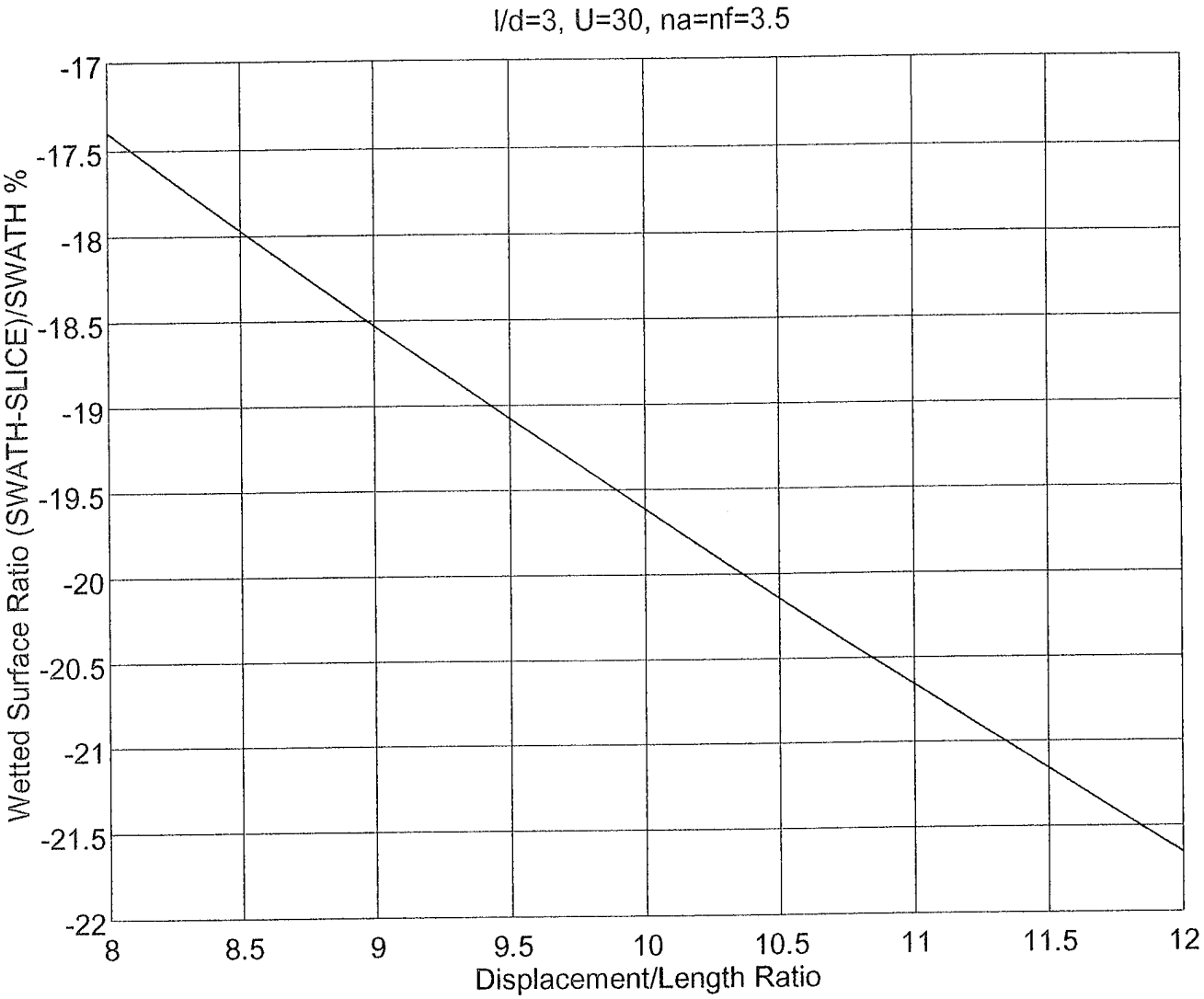


**Figure 3.42: Wetted surface ratio for form drag only vs. displacement to length for limited diameter.**

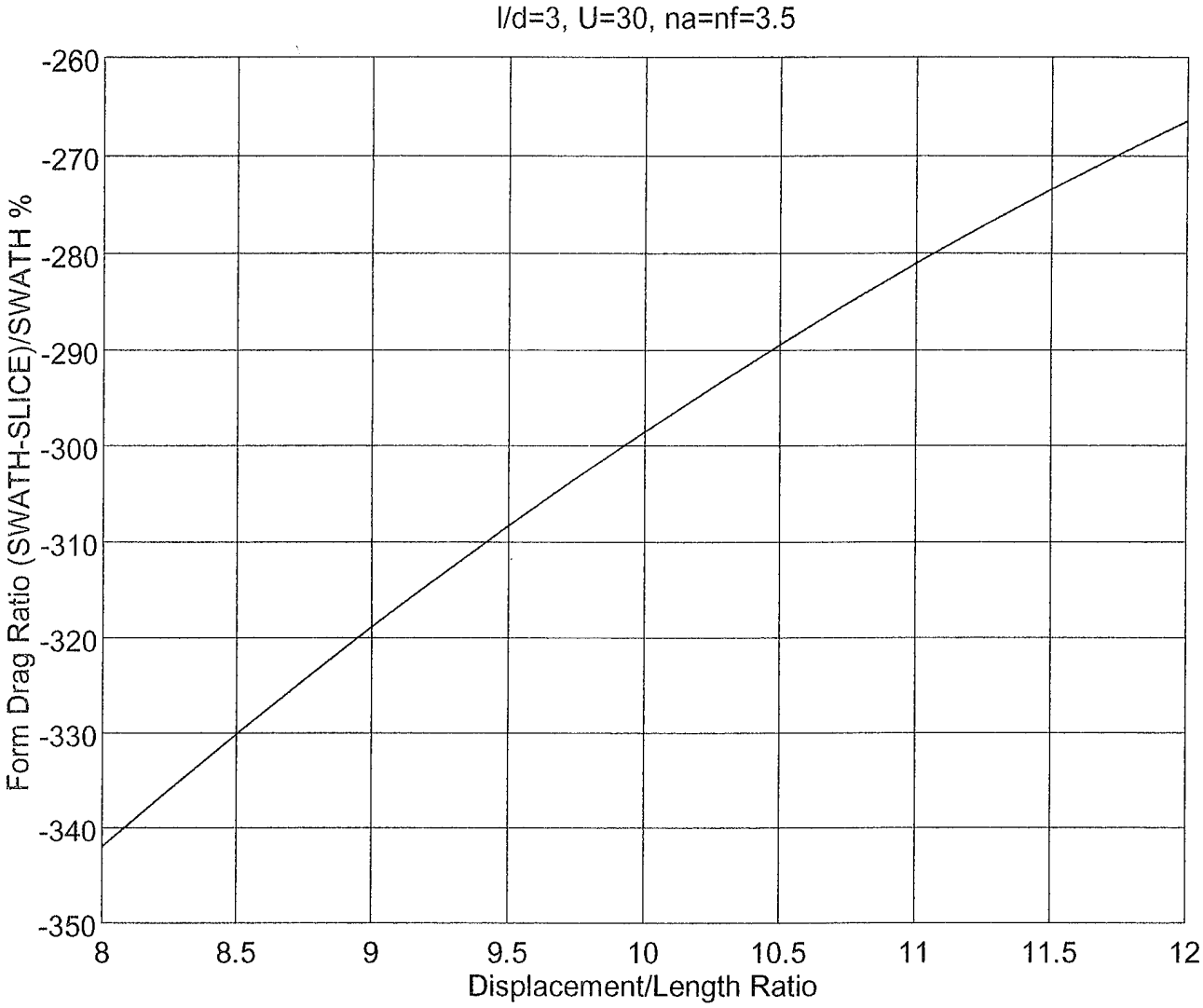


**Figure 3.43: Form drag ratio vs. displacement to length ratio for limited diameter.**

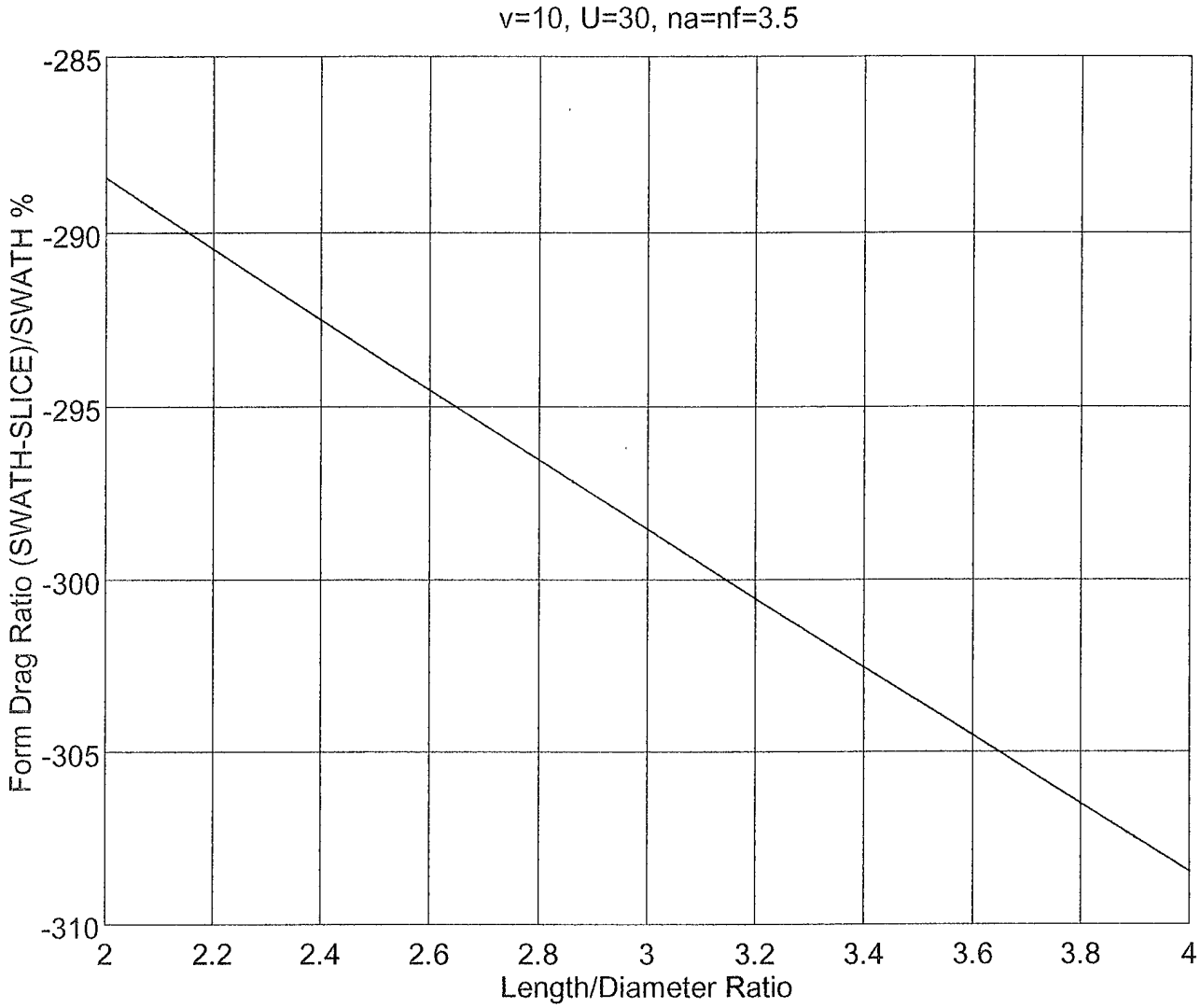


**Figure 3.44: Form drag ratio vs. length to diameter ratio for limited diameter.**

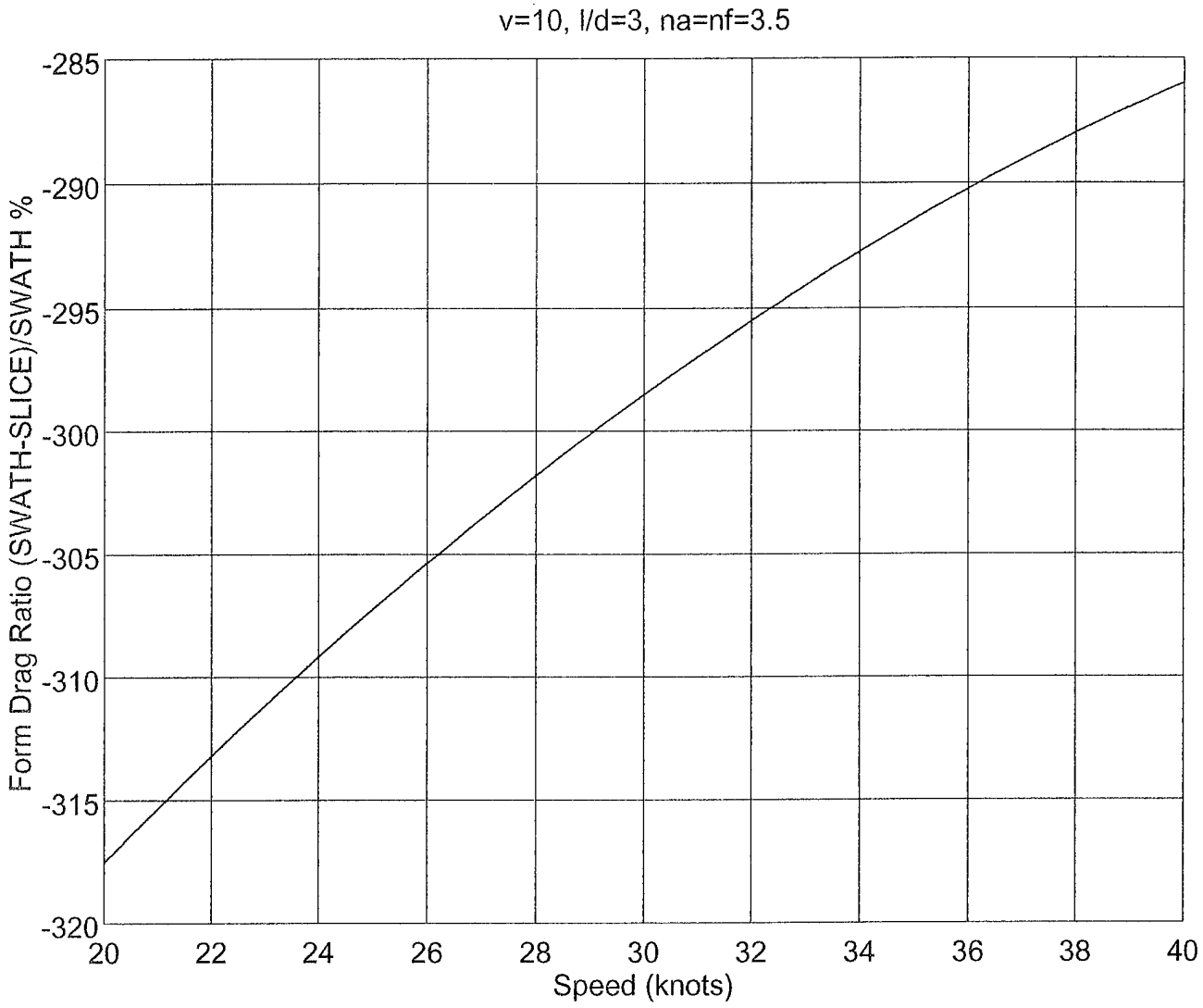


**Figure 3.45: Form drag ratio vs. speed for limited diameter.**

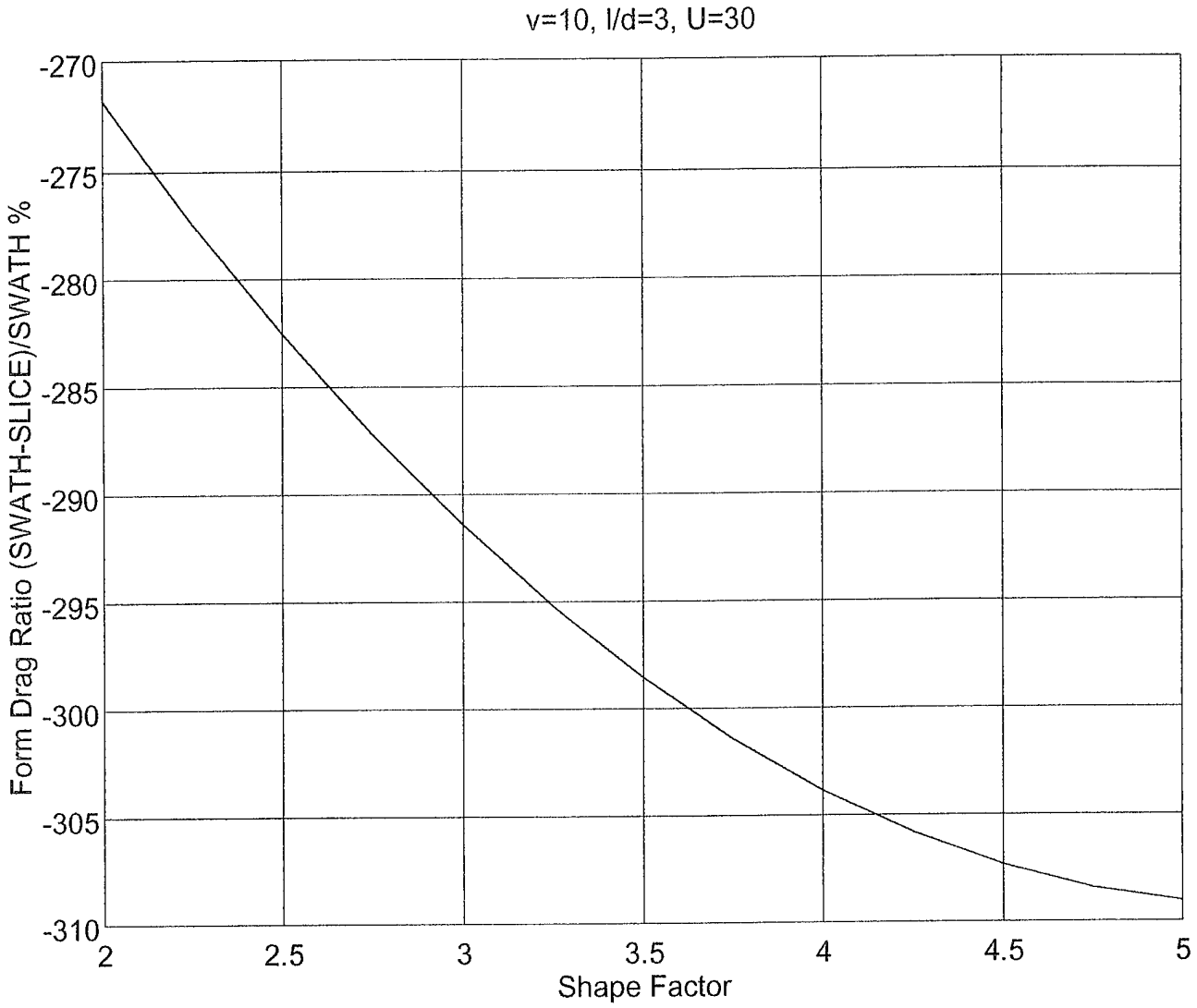


**Figure 3.46: Form drag ratio vs. shape factor for limited diameter.**

# IV. CONCLUSIONS AND RECOMMENDATIONS

This work focused on comparative resistance calculations for SWATH/SLICE hull forms for two different cases, limited length and limited diameter. For both cases the SWATH offers less viscous drag than the SLICE, but the wavemaking resistance plays the bigger role in the total resistance and the final results. Both viscous drag and wavemaking resistance depend upon the body shape, speed, draft, and the pod separation distance. From the different runs for each of the two cases, by changing one of the above parameters we reached a number of conclusions.

For the limited length case we conclude, that the total resistance ratio resulting from varying the body shape parameters $v$, $\ell/d$, $n_a$, and $n_f$ for draft of one diameter, is negative (in favor of SWATH) for pod separation distance starting from 0 to 0.15, then it changes to a positive value (in favor of SLICE) until the maximum range of the separation distance is reached. Second, once the draft increases to twice the diameter most of the results remain in favor of SWATH for the entire range of pod separation distance, except for some values of the parameters at the maximum separation distance. Third, the total resistance ratio versus speed has an oscillatory shape with higher amplitude as the separation distance increases. Finally, lower speeds produce higher positive total resistance ratio, with a very minor draft effect.

For the limited diameter case we conclude, that the higher the displacement to length ratio, the lower the length to diameter ratio, and the lower prismatic shape factor, the better the SLICE configuration over the SWATH for draft equal to the diameter. Second, as the draft increases to twice the diameter the results change and now the SWATH configuration produces less resistance than the SLICE. Third, the larger the pod separation distance the higher the positive value of the total resistance ratio. Fourth, as the speed increases it results in an oscillatory behavior of the total

resistance ratio. Depending on the draft, this may oscillate in the positive or negative region or oscillate back and forth between the two regions. Therefore to answer the basic question in the beginning of this study, whether SLICE hull offer less resistance than the SWATH hull, we need to consider the range of the design parameters. This means that by choosing the correct range value of the different body shape parameters, speed, and draft it is possible that the SLICE offers less resistance than the SWATH. Table 4.1 shows the speed range where the SLICE configuration is better in terms of resistance.

| **Approach Cases** | **Draft** | **Ship Speed** (in knots, at $v = 10$, $\ell/d = 3$, $n_a = n_f = 3.5$) | **Pod Separation Distance** |
|---|---|---|---|
| **Limited Length** | diameter | 30 | 0.09–0.4 |
| | | 30 | 0.1–0.4 |
| | | 40 | 0.4 |
| | 2* diameter | 20 | 0.09–0.4 |
| | | 30 | 0.38–0.4 |
| **Limited Diameter** | diameter | 20 to 22 | varies |
| | | 27 to 34 | |
| | 2* diameter | 31 to 39 | varies |

**Table 4.1: Speed Range Where SLICE Configuration Produces Less Resistance than the SWATH for Constant Body Shape Parameters**

For further improvement of the comparative resistance calculations presented in this study the following recommendations are proposed. First, for the two pods on each side of the SLICE configuration one of the assumptions must be modified so that they are not inline any more. We must perform the resistance calculations and compare with the results from this study. Second, study the speed ranges similar to the results from the above table but for different values for the body shape parameters.

These results would greatly assist in choosing the best pod geometry along with the speed. Finally, study the effect of the wave making resistance as the draft increases for more that twice the diameter, for the same pod shape parameters and speed. These recommendations with the results presented in this study would increase the accuracy of the values for the different parameters which allow the SLICE configuration to produce less resistance than what produced by the SWATH.

# APPENDIX A

## TABULATED RESULTS

The data for the figures presented in Chapter III were obtained by running the programs for calculating the viscous resistance and the wavemaking resistance. All data are arranged in different tables presented in this Appendix. These tables contain the following:

- The variable parameter.
- Pod separation distance $\alpha$, only for SLICE.
- Viscous resistance (lbs.).
- Wavemaking resistance (lbs.).
- Wave resistance coefficient.
- Froude number.
- Wetted surface area ($ft^2$).
- The total resistance (lbs.).

The total resistance percentage ratio for both limited diameter and limited length are presented in separate tables, computed using the information on the total resistance presented in above tables.

| Variable | Viscous Resistance (lbs) | Wave Resistance (lbs) | Wave Resistance Coefficient | Froude Number | Wetted Area (sq.ft) | SWATH Total Res. (lbs) |
|---|---|---|---|---|---|---|
| **v = 8** | 1992.5 | 3747.4 | 0.00052752 | 0.99839 | 2849.0 | 5739.9 |
| **v = 10** | 2287.4 | 5153.2 | 0.00064877 | 0.99839 | 3083.6 | 7440.6 |
| **v = 12** | 2565.7 | 6648.0 | 0.00076397 | 0.99839 | 3490.0 | 9213.7 |
| **U = 20** | 1051.7 | 6412.4 | 0.00181860 | 0.66556 | 1592.8 | 7464.1 |
| **U = 22.5** | 1317.8 | 6290.0 | 0.00140970 | 0.74870 | 1592.8 | 7607.8 |
| **U = 25** | 1612.6 | 5955.8 | 0.00108100 | 0.83195 | 1592.8 | 7568.4 |
| **U = 27.5** | 1935.8 | 5750.2 | 0.00094183 | 0.87579 | 1592.8 | 7686.0 |
| **U = 30** | 2287.4 | 5153.2 | 0.00064877 | 0.99839 | 1592.8 | 7440.6 |
| **U = 32.5** | 2667.1 | 4802.8 | 0.00052347 | 1.07360 | 1592.8 | 7469.9 |
| **U = 35** | 3074.7 | 4400.2 | 0.00040747 | 1.16470 | 1592.8 | 7474.9 |
| **U = 37.5** | 3510.2 | 4060.2 | 0.00032751 | 1.24797 | 1592.8 | 7570.4 |
| **U = 40** | 3973.4 | 3748.2 | 0.00026575 | 1.33110 | 1592.8 | 7721.6 |
| ***l/d* = 2** | 2281.3 | 5397.6 | 0.00067488 | 0.99839 | 3207.6 | 7678.9 |
| ***l/d* = 3** | 2287.4 | 5153.2 | 0.00064877 | 0.99839 | 3185.6 | 7440.6 |
| ***l/d* = 4** | 2294.3 | 5076.6 | 0.00064297 | 0.99839 | 6166.6 | 7370.9 |
| **na = 2** | 2297.0 | 5555.2 | 0.00070832 | 0.99839 | 3145.4 | 7852.2 |
| **na = 2.5** | 2293.0 | 5353.4 | 0.00067872 | 0.99839 | 3163.4 | 7646.4 |
| **na = 3** | 2289.8 | 5234.0 | 0.00066095 | 0.99839 | 3176.0 | 7523.8 |
| **na = 3.5** | 2287.4 | 5153.2 | 0.00064877 | 0.99839 | 3185.6 | 7440.6 |
| **na = 5** | 2282.6 | 5008.6 | 0.00062688 | 0.99839 | 3204.4 | 7291.2 |

**Table A.1 : SWATH Resistance at Draft = Diameter**

| Variable | Viscous Resistance (lbs) | Wave Resistance (lbs) | Wave Resistance Coefficient | Froude Number | Wetted Area (sq.ft) | SWATH Total Res. (lbs) |
|---|---|---|---|---|---|---|
| **v = 8** | 1992.5 | 1584.6 | 0.00052752 | 0.99839 | 2849.0 | 3577.1 |
| **v = 10** | 2287.4 | 2107.8 | 0.00064877 | 0.99839 | 3083.6 | 4395.2 |
| **v = 12** | 2565.7 | 2651.4 | 0.00076397 | 0.99839 | 3490.0 | 5217.1 |
| **U = 20** | 1051.7 | 3099.8 | 0.00181860 | 0.66556 | 1592.8 | 4151.5 |
| **U = 22.5** | 1317.8 | 2973.6 | 0.00140970 | 0.74870 | 1592.8 | 4291.4 |
| **U = 25** | 1612.6 | 1861.2 | 0.00108100 | 0.83195 | 1592.8 | 3473.8 |
| **U = 27.5** | 1935.8 | 2533.0 | 0.00094183 | 0.87579 | 1592.8 | 4468.8 |
| **U = 30** | 2287.4 | 2107.8 | 0.00064877 | 0.99839 | 1592.8 | 4395.2 |
| **U = 32.5** | 2667.1 | 1863.2 | 0.00052347 | 1.07360 | 1592.8 | 4530.3 |
| **U = 35** | 3074.7 | 4777.3 | 0.00040747 | 1.16470 | 1592.8 | 7852.0 |
| **U = 37.5** | 3510.2 | 1469.7 | 0.00032751 | 1.24797 | 1592.8 | 4979.9 |
| **U = 40** | 3973.4 | 1314.9 | 0.00026575 | 1.33110 | 1592.8 | 5288.3 |
| ***l/d* = 2** | 2281.3 | 2480.2 | 0.00067488 | 0.99839 | 3207.6 | 4761.6 |
| ***l/d* = 3** | 2287.4 | 2107.8 | 0.00064877 | 0.99839 | 3185.6 | 4395.2 |
| ***l/d* = 4** | 2294.3 | 2065.0 | 0.00064297 | 0.99839 | 6166.6 | 4359.3 |
| **na = 2** | 2297.0 | 2179.2 | 0.00070832 | 0.99839 | 3145.4 | 4476.2 |
| **na = 2.5** | 2293.0 | 2140.6 | 0.00067872 | 0.99839 | 3163.4 | 4433.6 |
| **na = 3** | 2289.8 | 2120.4 | 0.00066095 | 0.99839 | 3176.0 | 4410.2 |
| **na = 3.5** | 2287.4 | 2107.8 | 0.00064877 | 0.99839 | 3185.6 | 4395.2 |
| **na = 5** | 2282.6 | 2084.2 | 0.00062688 | 0.99839 | 3204.4 | 4366.8 |

**Table A.2 : SWATH Resistance at Draft = 2 × Diameter**

| Variable | Separation Distance Alpha | Pod Diameter (ft) | Viscous Resistance (lbs) | Wave Resistance (lbs) | Wave Resistance Coefficient | Froude Number | Wetted Area (sq.ft) | SLICE Total Res. (lbs) |
|---|---|---|---|---|---|---|---|---|
| | 0.3738 | 8.353 | 3127.3 | 2131.8 | 0.000379 | 0.99839 | 2252.8 | 5259.1 |
| | 0.2803 | 7.521 | 2878.5 | 2479.8 | 0.000413 | 0.99839 | 2408.8 | 5358.3 |
| $v = 8$ | 0.1869 | 6.918 | 2736 | 2884.8 | 0.000453 | 0.99839 | 2554.8 | 5620.8 |
| | 0.0934 | 6.450 | 2649.7 | 3342.2 | 0.000489 | 0.99839 | 2739.8 | 5991.9 |
| | 0.0 | 6.073 | 2596.6 | 3726.4 | 0.000529 | 0.99839 | 2821.2 | 6323.0 |
| | 0.3254 | 8.998 | 3615 | 3202.6 | 0.000493 | 0.99839 | 2603.8 | 6817.6 |
| | 0.2440 | 8.249 | 3368.6 | 3633.0 | 0.000529 | 0.99839 | 2751.6 | 7001.6 |
| $v = 10$ | 0.1627 | 7.679 | 3213.4 | 3325.2 | 0.000485 | 0.99839 | 2748.2 | 6538.6 |
| | 0.0813 | 7.224 | 3110.8 | 4609.4 | 0.000611 | 0.99839 | 3024.2 | 7720.2 |
| | 0.0 | 6.847 | 3041.6 | 5051.0 | 0.000643 | 0.99839 | 3150.8 | 8092.6 |
| | 0.2831 | 9.562 | 4069.4 | 4462.8 | 0.000611 | 0.99839 | 2931.8 | 8532.2 |
| | 0.2123 | 8.893 | 3831.8 | 4953.6 | 0.000647 | 0.99839 | 3069.4 | 8785.4 |
| $v = 12$ | 0.1416 | 8.364 | 3670.2 | 5468.0 | 0.000685 | 0.99839 | 3200.6 | 9138.2 |
| | 0.0708 | 7.928 | 3556.2 | 5993.8 | 0.000723 | 0.99839 | 3327.0 | 9550.0 |
| | 0.0 | 7.559 | 3474 | 6451.2 | 0.000750 | 0.99839 | 3448.2 | 9925.2 |
| | 0.3254 | 8.999 | 1641.8 | 3884.8 | 0.001348 | 0.66556 | 2603.8 | 5526.6 |
| | 0.2440 | 8.249 | 1533.7 | 4439.8 | 0.001458 | 0.66556 | 2751.6 | 5973.5 |
| $U = 20$ | 0.1627 | 7.679 | 1466 | 4055.4 | 0.001333 | 0.66556 | 2748.2 | 5521.4 |
| | 0.0813 | 7.224 | 1421.6 | 5842.4 | 0.001745 | 0.66556 | 3024.2 | 7264.0 |
| | 0.0 | 6.847 | 1391.9 | 6570.4 | 0.001884 | 0.66556 | 3150.8 | 7962.3 |
| | 0.3254 | 8.998 | 3615 | 3202.6 | 0.000493 | 0.99839 | 2603.8 | 6817.6 |
| | 0.2440 | 8.249 | 3368.6 | 3633.0 | 0.000529 | 0.99839 | 2751.6 | 7001.6 |
| $U = 30$ | 0.1627 | 7.679 | 3213.4 | 3325.2 | 0.000485 | 0.99839 | 2748.2 | 6538.6 |
| | 0.0813 | 7.224 | 3110.8 | 4609.4 | 0.000611 | 0.99839 | 3024.2 | 7720.2 |
| | 0.0 | 6.847 | 3041.6 | 5051.0 | 0.000643 | 0.99839 | 3150.8 | 8092.6 |
| | 0.3254 | 8.999 | 6333.9 | 2396.2 | 0.000208 | 1.33110 | 2603.8 | 8730.1 |
| | 0.2440 | 8.249 | 5892.3 | 2702.4 | 0.000222 | 1.33110 | 2751.6 | 8594.7 |
| $U = 40$ | 0.1627 | 7.679 | 5612.9 | 2464.2 | 0.000202 | 1.33110 | 2748.2 | 8077.1 |
| | 0.0813 | 7.224 | 5427.4 | 3361.6 | 0.000251 | 1.33110 | 3024.2 | 8789.0 |
| | 0.0 | 6.847 | 5301.4 | 3650.0 | 0.000262 | 1.33110 | 3150.8 | 8951.4 |

**Table A.3 : SLICE Resistance for Limited Length Case at Draft =Diameter.** $v$ (8, 10, 12) at $U = 30$ knots, $l/d = 3$, $n_a = n_f = 3.5$; $U$ (20, 30, 40 knots) at $v = 10$, $l/d = 3$, $n_a = n_f = 3.5$; $l/d$ (2, 3, 4) at $v = 10$, $U = 30$ knots, $n_a = n_f = 3.5$; $n_a = n_f$ (2, 3.5, 5) at $v = 10$, $l/d = 3$, $U = 30$ knots.

| Variable | Separation Distance Alpha | Pod Diameter (ft) | Viscous Resistance (lbs) | Wave Resistance (lbs) | Wave Resistance Coefficient | Froude Number | Wetted Area (sqft) | SLICE Total Res. (lbs) |
|---|---|---|---|---|---|---|---|---|
| | 0.4852 | 10.3 | 4097.8 | 2783.6 | 0.000462 | 0.99839 | 2414.4 | 6881.4 |
| | 0.3639 | 8.818 | 3516.5 | 3222.4 | 0.000492 | 0.99839 | 2628.6 | 6738.9 |
| *l/d* = 2 | 0.2426 | 7.784 | 3236 | 3954.8 | 0.000559 | 0.99839 | 2835.2 | 7190.8 |
| | 0.1216 | 7.196 | 3083 | 4669.0 | 0.000618 | 0.99839 | 3028.0 | 7752.0 |
| | 0.0 | 6.674 | 2996.3 | 5356.8 | 0.000669 | 0.99839 | 3211.2 | 8353.1 |
| | 0.3254 | 8.998 | 3615 | 3202.6 | 0.000493 | 0.99839 | 2603.8 | 6817.6 |
| | 0.2440 | 8.249 | 3368.6 | 3633.0 | 0.000529 | 0.99839 | 2751.6 | 7001.6 |
| *l/d* = 3 | 0.1627 | 7.679 | 3213.4 | 3325.2 | 0.000485 | 0.99839 | 2748.2 | 6538.6 |
| | 0.0813 | 7.224 | 3110.8 | 4609.4 | 0.000611 | 0.99839 | 3024.2 | 7720.2 |
| | 0.0 | 6.847 | 3041.6 | 5051.0 | 0.000643 | 0.99839 | 3150.8 | 8092.6 |
| | 0.1828 | 8.175 | 3376.7 | 3779.8 | 0.000544 | 0.99839 | 2784.8 | 7156.5 |
| | 0.1371 | 7.834 | 3279.6 | 4053.8 | 0.000567 | 0.99839 | 2866.0 | 7333.4 |
| *l/d* = 4 | 0.0914 | 7.538 | 3204.1 | 4333.6 | 0.000590 | 0.99839 | 2944.4 | 7537.7 |
| | 0.0457 | 7.278 | 3144.7 | 4610.6 | 0.000612 | 0.99839 | 3020.4 | 7755.3 |
| | 0.0 | 7.045 | 3097.5 | 4861.4 | 0.000630 | 0.99839 | 3094.2 | 7958.9 |
| | 0.2690 | 9.751 | 3972.6 | 2989.6 | 0.000457 | 0.99839 | 2622.0 | 6962.2 |
| | 0.2017 | 8.811 | 3600.4 | 3933.4 | 0.000496 | 0.99839 | 2743.6 | 6993.8 |
| *na* = 2 | 0.1345 | 8.158 | 3384.5 | 3842.2 | 0.000538 | 0.99839 | 2862.4 | 7226.7 |
| | 0.0672 | 7.657 | 3244.7 | 4311.4 | 0.000581 | 0.99839 | 2976.8 | 7556.1 |
| | 0.0 | 7.252 | 3149.2 | 4765.4 | 0.000619 | 0.99839 | 3085.8 | 7914.6 |
| | 0.3254 | 8.998 | 3615 | 3202.6 | 0.000493 | 0.99839 | 2603.8 | 6817.6 |
| | 0.2440 | 8.249 | 3368.6 | 3633.0 | 0.000529 | 0.99839 | 2751.6 | 7001.6 |
| *na* = 3.5 | 0.1627 | 7.679 | 3213.4 | 3325.2 | 0.000485 | 0.99839 | 2748.2 | 6538.6 |
| | 0.0813 | 7.224 | 3110.8 | 4609.4 | 0.000611 | 0.99839 | 3024.2 | 7720.2 |
| | 0.0 | 6.847 | 3041.6 | 5051.0 | 0.000643 | 0.99839 | 3150.8 | 8092.6 |
| | 0.3460 | 8.724 | 3491.9 | 3314.0 | 0.000512 | 0.99839 | 2595.6 | 6805.9 |
| | 0.2595 | 8.035 | 3284 | 3764.6 | 0.000549 | 0.99839 | 2752.2 | 7048.6 |
| *na* = 5 | 0.1730 | 7.497 | 3150.5 | 4251.2 | 0.000588 | 0.99839 | 2899.8 | 7401.7 |
| | 0.0865 | 7.061 | 3062.1 | 4771.0 | 0.000629 | 0.99839 | 3039.6 | 7833.1 |
| | 0.0 | 6.697 | 3003.1 | 5468.2 | 0.000679 | 0.99839 | 3230.0 | 8471.3 |

**Table A.3 : Continued**

| Variable | Separation Distance Alpha | Pod Diameter (ft) | Viscous Resistance (lbs) | Wave Resistance (lbs) | Wave Resistance Coefficient | Froude Number | Wetted Area (sq.ft) | SLICE Total Res. (lbs) |
|---|---|---|---|---|---|---|---|---|
| | 0.3738 | 8.353 | 3127.3 | 948.7 | 0.000169 | 0.99839 | 2254.4 | 4076.0 |
| | 0.2803 | 7.521 | 2878.5 | 1099.8 | 0.000183 | 0.99839 | 2408.8 | 3978.3 |
| $v = 8$ | 0.1869 | 6.918 | 2736 | 1266.7 | 0.000199 | 0.99839 | 2554.8 | 4002.7 |
| | 0.0934 | 6.450 | 2649.7 | 1461.2 | 0.000214 | 0.99839 | 2739.8 | 4110.9 |
| | 0.0 | 6.073 | 2596.6 | 1595.8 | 0.000227 | 0.99839 | 2821.2 | 4192.4 |
| | 0.3254 | 8.998 | 3615 | 1371.2 | 0.000211 | 0.99839 | 2603.8 | 4986.2 |
| | 0.2440 | 8.249 | 3368.6 | 1551.1 | 0.000226 | 0.99839 | 2751.6 | 4919.7 |
| $v = 10$ | 0.1627 | 7.679 | 3213.4 | 1403.8 | 0.000205 | 0.99839 | 2748.2 | 4617.2 |
| | 0.0813 | 7.224 | 3110.8 | 1937.9 | 0.000257 | 0.99839 | 3024.2 | 5048.4 |
| | 0.0 | 6.847 | 3041.6 | 2097.8 | 0.000267 | 0.99839 | 3150.8 | 5139.4 |
| | 0.2831 | 9.562 | 4069.4 | 1841.2 | 0.000252 | 0.99839 | 2933.0 | 5910.6 |
| | 0.2123 | 8.893 | 3831.8 | 2039.0 | 0.000266 | 0.99839 | 3069.4 | 5870.8 |
| $v = 12$ | 0.1416 | 8.364 | 3670.2 | 2249.0 | 0.000282 | 0.99839 | 3200.6 | 5919.2 |
| | 0.0708 | 7.928 | 3556.2 | 2417.8 | 0.000203 | 0.99839 | 3200.6 | 5974.0 |
| | 0.0 | 7.559 | 3474 | 2634.2 | 0.000306 | 0.99839 | 3448.2 | 6108.2 |
| | 0.3254 | 8.999 | 1641.8 | 1527.9 | 0.000529 | 0.66556 | 2605.0 | 3169.7 |
| | 0.2440 | 8.249 | 1533.7 | 1873.3 | 0.000615 | 0.66556 | 2751.6 | 3407.0 |
| $U = 20$ | 0.1627 | 7.679 | 1466 | 1802.6 | 0.000593 | 0.66556 | 2748.2 | 3268.6 |
| | 0.0813 | 7.224 | 1421.6 | 2712.0 | 0.000810 | 0.66556 | 3024.2 | 4132.6 |
| | 0.0 | 6.847 | 1391.9 | 2874.6 | 0.000824 | 0.66556 | 3150.8 | 4266.5 |
| | 0.3254 | 8.998 | 3615 | 1371.2 | 0.000211 | 0.99839 | 2603.8 | 4986.2 |
| | 0.2440 | 8.249 | 3368.6 | 1551.1 | 0.000226 | 0.99839 | 2751.6 | 4919.7 |
| $U = 30$ | 0.1627 | 7.679 | 3213.4 | 1403.8 | 0.000205 | 0.99839 | 2748.2 | 4617.2 |
| | 0.0813 | 7.224 | 3110.8 | 1937.9 | 0.000257 | 0.99839 | 3024.2 | 5048.4 |
| | 0.0 | 6.847 | 3041.6 | 2097.8 | 0.000267 | 0.99839 | 3150.8 | 5139.4 |
| | 0.3254 | 8.999 | 6333.9 | 1245.5 | 0.000089 | 1.33110 | 3150.8 | 7579.4 |
| | 0.2440 | 8.249 | 5892.3 | 993.5 | 0.000082 | 1.33110 | 2715.6 | 6885.8 |
| $U = 40$ | 0.1627 | 7.679 | 5612.9 | 893.8 | 0.000074 | 1.33110 | 2748.2 | 6506.7 |
| | 0.0813 | 7.224 | 5427.4 | 1214.4 | 0.000091 | 1.33110 | 3024.2 | 6641.8 |
| | 0.0 | 6.847 | 5301.4 | 1324.8 | 0.000095 | 1.33110 | 3150.8 | 6626.2 |

**Table A.4 : SLICE Resistance for Limited Length Case at Draft = 2 × Diameter.** $v$ (8, 10, 12) at $U = 30$ knots, $l/d = 3$, $n_a = n_f = 3.5$; $U$ (20, 30, 40 knots) at $v = 10$, $l/d = 3$, $n_a = n_f = 3.5$; $l/d$ (2, 3, 4) at $v = 10$, $U = 30$ knots, $n_a = n_f = 3.5$; $n_a = n_f$ (2, 3.5, 5) at $v = 10$, $l/d = 3$, $U = 30$ knots.

| Variable | Separation Distance Alpha | Pod Diameter (ft) | Viscous Resistance (lbs) | Wave Resistance (lbs) | Wave Resistance Coefficient | Froude Number | Wetted Area (sq.ft) | SLICE Total Res. (lbs) |
|---|---|---|---|---|---|---|---|---|
| | 0.4852 | 10.3 | 4097.8 | 1210.0 | 0.000205 | 0.99839 | 2367.8 | 5307.8 |
| | 0.3639 | 8.818 | 3516.5 | 1428.2 | 0.000218 | 0.99839 | 2628.6 | 4944.7 |
| ***l/d* = 2** | 0.2426 | 7.784 | 3236.0 | 1709.3 | 0.000242 | 0.99839 | 2835.2 | 4945.3 |
| | 0.1216 | 7.196 | 3083.0 | 1979.4 | 0.000262 | 0.99839 | 3028.0 | 5062.4 |
| | 0.0 | 6.674 | 2996.3 | 2238.4 | 0.000279 | 0.99839 | 3211.2 | 5234.7 |
| | 0.3254 | 8.998 | 3615.0 | 1371.2 | 0.000211 | 0.99839 | 2603.8 | 4986.2 |
| | 0.2440 | 8.249 | 3368.6 | 1551.1 | 0.000226 | 0.99839 | 2751.6 | 4919.7 |
| ***l/d* = 3** | 0.1627 | 7.679 | 3213.4 | 1403.8 | 0.000205 | 0.99839 | 2748.2 | 4617.2 |
| | 0.0813 | 7.224 | 3110.8 | 1937.9 | 0.000257 | 0.99839 | 3024.2 | 5048.4 |
| | 0.0 | 6.847 | 3041.6 | 2097.8 | 0.000267 | 0.99839 | 3150.8 | 5139.4 |
| | 0.1828 | 8.175 | 3376.7 | 1596.1 | 0.000231 | 0.99839 | 2766.8 | 4954.8 |
| | 0.1371 | 7.834 | 3279.6 | 1695.0 | 0.000237 | 0.99839 | 2866.0 | 4974.6 |
| ***l/d* = 4** | 0.0914 | 7.538 | 3204.1 | 1803.8 | 0.000246 | 0.99839 | 2944.4 | 5007.9 |
| | 0.0457 | 7.278 | 3144.7 | 1914.0 | 0.000254 | 0.99839 | 3020.4 | 5058.7 |
| | 0.0 | 7.045 | 3097.5 | 1921.1 | 0.000249 | 0.99839 | 3094.2 | 5018.6 |
| | 0.2690 | 9.751 | 3972.6 | 1212.7 | 0.000185 | 0.99839 | 2622.0 | 5185.3 |
| | 0.2017 | 8.811 | 3600.4 | 1392.3 | 0.000203 | 0.99839 | 2743.6 | 4992.7 |
| ***na* = 2** | 0.1345 | 8.158 | 3384.5 | 1574.7 | 0.000221 | 0.99839 | 2862.4 | 4959.2 |
| | 0.0672 | 7.657 | 3244.7 | 1755.0 | 0.000236 | 0.99839 | 2976.8 | 4999.7 |
| | 0.0 | 7.252 | 3149.2 | 1935.1 | 0.000251 | 0.99839 | 3085.8 | 5084.3 |
| | 0.3254 | 8.998 | 3615 | 1371.2 | 0.000211 | 0.99839 | 2603.8 | 4986.2 |
| | 0.2440 | 8.249 | 3368.6 | 1551.1 | 0.000226 | 0.99839 | 2751.6 | 4919.7 |
| ***na* = 3.5** | 0.1627 | 7.679 | 3213.4 | 1403.8 | 0.000205 | 0.99839 | 2748.2 | 4617.2 |
| | 0.0813 | 7.224 | 3110.8 | 1937.9 | 0.000257 | 0.99839 | 3024.2 | 5048.4 |
| | 0.0 | 6.847 | 3041.6 | 2097.8 | 0.000267 | 0.99839 | 3150.8 | 5139.4 |
| | 0.3460 | 8.724 | 3491.9 | 1473.8 | 0.000228 | 0.99839 | 2595.6 | 4965.7 |
| | 0.2595 | 8.035 | 3284 | 1642.7 | 0.000239 | 0.99839 | 2752.2 | 4926.7 |
| ***na* = 5** | 0.1730 | 7.497 | 3150.5 | 1831.6 | 0.000253 | 0.99839 | 2899.8 | 4982.1 |
| | 0.0865 | 7.061 | 3062.1 | 2028.2 | 0.000268 | 0.99839 | 3039.6 | 5090.3 |
| | 0.0 | 6.697 | 3003.1 | 2310.4 | 0.000287 | 0.99839 | 3230.0 | 5313.5 |

**Table A.4 : Continued**

| Variable | Separation Distance Alpha | Pod Diameter (ft) | Viscous Resistance (lbs) | Wave Resistance (lbs) | Wave Resistance Coefficient | Froude Number | Wetted Area (sq.ft) | SLICE Total Res. (lbs) |
|---|---|---|---|---|---|---|---|---|
| | 0.3 | | | 4538.6 | 0.00107 | 0.55951 | 3799.8 | 6048.2 |
| $U = 20$ | 0.4 | 6.596 | 1509.6 | 4877.6 | 0.00116 | 0.54778 | 3800.4 | 6387.2 |
| | 0.5 | | | 5517.2 | 0.00131 | 0.53676 | 3801.0 | 7026.8 |
| | 0.3 | | | 4317.2 | 0.00081 | 0.62941 | 3799.8 | 6210.2 |
| $U = 22.5$ | 0.4 | 6.596 | 1893.0 | 4320.0 | 0.00081 | 0.61621 | 3800.4 | 6213.0 |
| | 0.5 | | | 4566.4 | 0.00085 | 0.60381 | 3801.0 | 6459.4 |
| | 0.3 | | | 4071.8 | 0.00062 | 0.69939 | 3799.8 | 6389.9 |
| $U = 25$ | 0.4 | 6.596 | 2318.1 | 3875.4 | 0.00059 | 0.68473 | 3800.4 | 6193.5 |
| | 0.5 | | | 3871.6 | 0.00059 | 0.67095 | 3801.0 | 6189.7 |
| | 0.3 | | | 3964.0 | 0.00054 | 0.73624 | 3799.8 | 6748.5 |
| $U = 27.5$ | 0.4 | 6.596 | 2784.5 | 3694.8 | 0.00051 | 0.72081 | 3800.4 | 6479.3 |
| | 0.5 | | | 3602.0 | 0.00049 | 0.70630 | 3801.0 | 6386.5 |
| | 0.3 | | | 3724.6 | 0.00039 | 0.83976 | 3799.8 | 7016.8 |
| $U = 30$ | 0.4 | 6.596 | 3292.2 | 3354.4 | 0.00035 | 0.82216 | 3800.4 | 6646.6 |
| | 0.5 | | | 3101.4 | 0.00033 | 0.80561 | 3801.0 | 6393.6 |
| | 0.3 | | | 3605.4 | 0.00033 | 0.90254 | 3799.8 | 7446.1 |
| $U = 32.5$ | 0.4 | 6.596 | 3840.7 | 3226.2 | 0.00029 | 0.88362 | 3800.4 | 7066.9 |
| | 0.5 | | | 2927.0 | 0.00026 | 0.86584 | 3801.0 | 6767.7 |
| | 0.3 | | | 3471.4 | 0.00027 | 0.97914 | 3799.8 | 7901.4 |
| $U = 35$ | 0.4 | 6.596 | 4430.0 | 3111.0 | 0.00024 | 0.95862 | 3800.4 | 7541.0 |
| | 0.5 | | | 2780.0 | 0.00022 | 0.93933 | 3801.0 | 7210.0 |
| | 0.3 | | | 3362.4 | 0.00023 | 1.11330 | 3799.8 | 8422.3 |
| $U = 37.5$ | 0.4 | 6.596 | 5059.9 | 3019.6 | 0.00020 | 1.11280 | 3800.4 | 8079.5 |
| | 0.5 | | | 2706.6 | 0.00018 | 1.11210 | 3801.0 | 7766.5 |
| | 0.3 | | | 3238.8 | 0.00019 | 1.11900 | 3799.8 | 8968.9 |
| $U = 40$ | 0.4 | 6.596 | 5730.1 | 2932.6 | 0.00017 | 1.11850 | 3800.4 | 8662.7 |
| | 0.5 | | | 2621.6 | 0.00016 | 1.11780 | 3801.0 | 8351.7 |

**Table A.5 : SLICE Resistance for Limited Diameter Case at Draft = Diameter.** $U$(20, 2.5, 25, 27.5, 30, 32.5, 35, 37.5, 40 knots) at $v = 10$, $l/d = 3$, $n_a = n_f = 3.5$; $v$ (8, 10, 12) at $U = 30$ knots, $l/d = 3$, $n_a = n_f = 3.5$; $l/d$ (2, 3, 4) at $v = 10$, $U = 30$ knots, $n_a = n_f = 3.5$; $n_a = n_f$ (2, 2.5, 3, 3.5) at $v = 10$, $l/d = 3$, $U = 30$ knots.

| Variable | Separation Distance Alpha | Pod Diameter (ft) | Viscous Resistance (lbs) | Wave Resistance (lbs) | Wave Resistance Coefficient | Froude Number | Wetted Area (sq.ft) | SLICE Total Res. (lbs) |
|---|---|---|---|---|---|---|---|---|
| | 0.3 | | | 2705.2 | 0.00032 | 0.84843 | 3337.2 | 5509.9 |
| $v = 8$ | 0.4 | 5.878 | 2804.7 | 2403.8 | 0.00029 | 0.83064 | 3337.8 | 5208.5 |
| | 0.5 | | | 2222.8 | 0.00027 | 0.81393 | 3338.4 | 5027.5 |
| | 0.3 | | | 3724.6 | 0.00039 | 0.83976 | 3799.8 | 7016.8 |
| $v = 10$ | 0.4 | 6.596 | 3292.2 | 3354.4 | 0.00035 | 0.82216 | 3800.4 | 6646.6 |
| | 0.5 | | | 3101.4 | 0.00033 | 0.80561 | 3801.0 | 6393.6 |
| | 0.3 | | | 4899.0 | 0.00046 | 0.83208 | 4231.6 | 8662.6 |
| $v = 12$ | 0.4 | 7.249 | 3763.6 | 4397.0 | 0.00042 | 0.81461 | 4238.6 | 8160.6 |
| | 0.5 | | | 3981.6 | 0.00038 | 0.79819 | 4232.8 | 7745.2 |
| | 0.3 | | | 4133.8 | 0.00046 | 0.86781 | 3633.0 | 7298.3 |
| $l/d = 2$ | 0.4 | 6.522 | 3164.5 | 3541.6 | 0.00039 | 0.84958 | 3633.6 | 6706.1 |
| | 0.5 | | | 3196.0 | 0.00035 | 0.83244 | 3634.2 | 6360.5 |
| | 0.3 | | | 3724.6 | 0.00039 | 0.83976 | 3799.8 | 7016.8 |
| $l/d = 3$ | 0.4 | 6.596 | 3092.2 | 3354.4 | 0.00035 | 0.82216 | 3800.4 | 6646.6 |
| | 0.5 | | | 3101.4 | 0.00033 | 0.80561 | 3801.0 | 6393.6 |
| | 0.3 | | | 3606.6 | 0.00036 | 0.81359 | 3982.4 | 7033.4 |
| $l/d = 4$ | 0.4 | 6.674 | 3426.8 | 3332.2 | 0.00033 | 0.79660 | 3983.2 | 6759.0 |
| | 0.5 | | | 3101.2 | 0.00031 | 0.78063 | 3983.8 | 6528.0 |
| | 0.3 | | | 3972.0 | 0.00041 | 0.83644 | 3914.2 | 7264.5 |
| $na = 2$ | 0.4 | 6.748 | 3292.5 | 3570.4 | 0.00037 | 0.81904 | 3914.8 | 6862.9 |
| | 0.5 | | | 3259.6 | 0.00033 | 0.80236 | 3915.4 | 6552.1 |
| | 0.3 | | | 3868.0 | 0.00040 | 0.83791 | 3865.0 | 7162.7 |
| $na = 2.5$ | 0.4 | 6.679 | 3294.7 | 3516.4 | 0.00036 | 0.82008 | 3865.6 | 6811.1 |
| | 0.5 | | | 3200.4 | 0.00033 | 0.80366 | 3866.2 | 6495.1 |
| | 0.3 | | | 3784.8 | 0.00040 | 0.83902 | 3828.1 | 7076.8 |
| $na = 3$ | 0.4 | 6.631 | 3292.0 | 3416.6 | 0.00036 | 0.82112 | 3828.8 | 6708.6 |
| | 0.5 | | | 3150.2 | 0.00033 | 0.80463 | 3829.6 | 6442.2 |
| | 0.3 | | | 3724.6 | 0.00039 | 0.83976 | 3799.8 | 7016.6 |
| $na = 3.5$ | 0.4 | 6.596 | 3292.2 | 3354.4 | 0.00035 | 0.82216 | 3800.4 | 6646.6 |
| | 0.5 | | | 3101.4 | 0.00033 | 0.80561 | 3801.0 | 6393.6 |

**Table A.5 : Continued**

| Variable | Separation Distance Alpha | Pod Diameter (ft) | Viscous Resistance (lbs) | Wave Resistance (lbs) | Wave Resistance Coefficient | Froude Number | Wetted Area (sq.ft) | SLICE Total Res. (lbs) |
|---|---|---|---|---|---|---|---|---|
| | 0.3 | | | 1597.1 | 0.00038 | 0.55951 | 3799.8 | 3106.7 |
| $U = 20$ | 0.4 | 6.596 | 1509.6 | 1370.9 | 0.00033 | 0.54778 | 3800.4 | 2880.5 |
| | 0.5 | | | 1333.8 | 0.00032 | 0.53676 | 3801.0 | 2843.4 |
| | 0.3 | | | 1885.8 | 0.00035 | 0.62941 | 3799.8 | 3778.8 |
| $U = 22.5$ | 0.4 | 6.596 | 1893.0 | 1729.1 | 0.00032 | 0.61621 | 3800.4 | 3622.1 |
| | 0.5 | | | 1478.5 | 0.00027 | 0.60381 | 3801.0 | 3371.5 |
| | 0.3 | | | 1969.9 | 0.00030 | 0.69939 | 3799.8 | 4287.9 |
| $U = 25$ | 0.4 | 6.596 | 2318.1 | 1856.0 | 0.00028 | 0.68473 | 3800.4 | 4174.1 |
| | 0.5 | | | 1566.9 | 0.00024 | 0.67095 | 3801.0 | 3884.9 |
| | 0.3 | | | 1957.5 | 0.00027 | 0.73624 | 3799.8 | 4742.0 |
| $U = 27.5$ | 0.4 | 6.596 | 2784.5 | 1872.9 | 0.00026 | 0.72081 | 3800.4 | 4657.4 |
| | 0.5 | | | 1576.8 | 0.00021 | 0.70630 | 3801.0 | 4361.3 |
| | 0.3 | | | 1852.8 | 0.00020 | 0.83976 | 3799.8 | 5144.9 |
| $U = 30$ | 0.4 | 6.596 | 3292.2 | 1831.2 | 0.00019 | 0.82216 | 3800.4 | 5119.4 |
| | 0.5 | | | 1528.7 | 0.00016 | 0.80561 | 3801.0 | 1820.9 |
| | 0.3 | | | 1708.4 | 0.00015 | 0.90254 | 3799.8 | 5549.1 |
| $U = 32.5$ | 0.4 | 6.596 | 3840.7 | 1763.9 | 0.00016 | 0.88362 | 3800.4 | 5604.7 |
| | 0.5 | | | 1465.2 | 0.00013 | 0.86584 | 3801.0 | 5305.9 |
| | 0.3 | | | 1867.9 | 0.00021 | 0.97914 | 3799.8 | 6297.9 |
| $U = 35$ | 0.4 | 6.596 | 4430.0 | 1846.9 | 0.00021 | 0.95862 | 3800.4 | 6276.9 |
| | 0.5 | | | 1392.0 | 0.00011 | 0.93933 | 3801.0 | 5822.0 |
| | 0.3 | | | 1467.3 | 0.00009 | 1.11330 | 3799.8 | 6527.2 |
| $U = 37.5$ | 0.4 | 6.596 | 5059.9 | 1634.8 | 0.00011 | 1.11280 | 3800.4 | 6694.7 |
| | 0.5 | | | 1315.9 | 0.00009 | 1.11210 | 3801.0 | 6375.9 |
| | 0.3 | | | 1437.8 | 0.00008 | 1.11900 | 3799.8 | 7167.9 |
| $U = 40$ | 0.4 | 6.596 | 5730.1 | 1332.5 | 0.00008 | 1.11850 | 3800.4 | 7062.6 |
| | 0.5 | | | 1196.3 | 0.00007 | 1.11780 | 3801.0 | 6926.4 |

**Table A.6 : SLICE Resistance for Limited Diameter Case at Draft = 2 × Diameter.** $U$ (20, 22.5, 25, 27.5, 30, 32.5, 35, 37.5, 40 knots) at $v = 10$, $l/d = 3$, $n_a = n_f = 3.5$; $v$(8, 10, 12) at $U = 30$ knots, $l/d = 3$, $n_a = n_f = 3.5$; $l/d$(2, 3, 4) at $v = 10$, $U = 30$ knots, $n_a = n_f = 3.5$; $n_a = n_f$(2, 2.5, 3, 3.5) at $v = 10$, $l/d = 3$, $U = 30$ knots.

| Variable | Separation Distance Alpha | Pod Diameter (ft) | Viscous Resistance (lbs) | Wave Resistance (lbs) | Wave Resistance Coefficient | Froude Number | Wetted Area (sq.ft) | SLICE Total Res. (lbs) |
|---|---|---|---|---|---|---|---|---|
| $v = 8$ | 0.3 | 5.878 | 2804.7 | 1406.2 | 0.00017 | 0.84843 | 3337.2 | 4210.9 |
| | 0.4 | | | 1231.4 | 0.00015 | 0.83064 | 3337.8 | 4036.1 |
| | 0.5 | | | 1141.3 | 0.00014 | 0.81393 | 3338.4 | 3946.0 |
| $v = 10$ | 0.3 | 6.596 | 3292.2 | 1852.8 | 0.00020 | 0.83976 | 3799.8 | 5144.9 |
| | 0.4 | | | 1827.2 | 0.00019 | 0.82216 | 3800.4 | 5119.4 |
| | 0.5 | | | 1528.7 | 0.00016 | 0.80561 | 3801.0 | 4820.9 |
| $v = 12$ | 0.3 | 7.249 | 3763.6 | 2430.4 | 0.00023 | 0.83208 | 4231.6 | 6194.1 |
| | 0.4 | | | 2206.0 | 0.00021 | 0.81461 | 4238.6 | 5969.6 |
| | 0.5 | | | 2009.5 | 0.00019 | 0.79819 | 4232.8 | 5773.1 |
| $l/d = 2$ | 0.3 | 6.522 | 3164.5 | 2346.6 | 0.00026 | 0.86781 | 3633.0 | 5511.1 |
| | 0.4 | | | 2078.8 | 0.00023 | 0.84958 | 3633.6 | 5243.3 |
| | 0.5 | | | 1787.5 | 0.00020 | 0.83244 | 3634.2 | 4952.0 |
| $l/d = 3$ | 0.3 | 6.596 | 3092.2 | 1852.8 | 0.00020 | 0.83976 | 3799.8 | 5144.9 |
| | 0.4 | | | 1831.2 | 0.00019 | 0.82216 | 3800.4 | 5119.4 |
| | 0.5 | | | 1528.7 | 0.00016 | 0.80561 | 3801.0 | 4820.9 |
| $l/d = 4$ | 0.3 | 6.674 | 3426.8 | 1843.9 | 0.00019 | 0.81359 | 3982.4 | 5270.7 |
| | 0.4 | | | 1672.2 | 0.00017 | 0.79660 | 3983.2 | 5098.9 |
| | 0.5 | | | 1487.2 | 0.00015 | 0.78063 | 3983.8 | 4913.9 |
| $na = 2$ | 0.3 | 6.748 | 3292.5 | 2011.8 | 0.00021 | 0.83644 | 3914.2 | 5304.3 |
| | 0.4 | | | 1827.1 | 0.00019 | 0.81904 | 3914.8 | 5119.6 |
| | 0.5 | | | 1638.7 | 0.00017 | 0.80236 | 3915.4 | 4931.2 |
| $na = 2.5$ | 0.3 | 6.679 | 3294.7 | 1992.1 | 0.00021 | 0.83791 | 3865.0 | 5286.8 |
| | 0.4 | | | 1694.9 | 0.00018 | 0.82008 | 3865.6 | 4989.7 |
| | 0.5 | | | 1564.5 | 0.00016 | 0.80366 | 3866.2 | 4859.2 |
| $na = 3$ | 0.3 | 6.631 | 3292.0 | 1720.9 | 0.00018 | 0.83902 | 3828.1 | 5014.9 |
| | 0.4 | | | 1720.9 | 0.00018 | 0.82112 | 3828.8 | 5014.9 |
| | 0.5 | | | 1549.1 | 0.00016 | 0.80463 | 3829.6 | 4843.1 |
| $na = 3.5$ | 0.3 | 6.596 | 3292.2 | 1852.8 | 0.00020 | 0.83976 | 3799.8 | 5144.9 |
| | 0.4 | | | 1831.2 | 0.00019 | 0.82216 | 3800.4 | 5119.4 |
| | 0.5 | | | 1528.7 | 0.00016 | 0.80561 | 3801.0 | 4820.9 |

**Table A.6 : Continued**

| Variable | Separation Distance Alpha | Resistance Ratio (Draft = Dia) | Resistance Ratio (Draft = 2*Dia) |
|---|---|---|---|
| | 0.4852 | 10.4 | -11.5 |
| | 0.3639 | 12.2 | -3.84 |
| ***l/d* = 2** | 0.2426 | 6.36 | -3.86 |
| | 0.1216 | -0.95 | -6.32 |
| | 0.0 | -8.78 | -9.94 |
| | 0.3254 | 8.37 | -13.4 |
| | 0.2440 | 5.9 | -11.9 |
| ***l/d* = 3** | 0.1627 | 12.1 | -5.05 |
| | 0.0813 | -3.76 | -14.9 |
| | 0.0 | -8.76 | -16.9 |
| | 0.1828 | 2.91 | -13.7 |
| | 0.1371 | 0.51 | -14.1 |
| ***l/d* = 4** | 0.0914 | -2.26 | -14.9 |
| | 0.0457 | -5.21 | -16.0 |
| | 0.0 | -7.98 | -15.1 |
| | 0.2690 | 11.3 | -15.8 |
| | 0.2017 | 10.9 | -11.5 |
| ***na* = 2** | 0.1345 | 7.96 | -10.8 |
| | 0.0672 | 3.77 | -11.7 |
| | 0.0 | -0.79 | -13.6 |
| | 0.3254 | 8.37 | -13.4 |
| | 0.2440 | 5.90 | -11.9 |
| ***na* = 3.5** | 0.1627 | 12.1 | -5.05 |
| | 0.0813 | -3.76 | -14.9 |
| | 0.0 | -8.76 | -16.9 |
| | 0.3460 | 6.66 | -13.7 |
| | 0.2595 | 3.33 | -12.8 |
| ***na* = 5** | 0.1730 | -1.52 | -14.1 |
| | 0.0865 | -7.43 | -16.6 |
| | 0.0 | -16.2 | -21.7 |

**Table A.7 : Total Resistance Ratio for Limited Length Case**

| Variable | Separation Distance Alpha | Resistance Ratio (Draft =Dia) | Resistance Ratio (Draft =2*Dia) |
|---|---|---|---|
| | 0.3738 | 8.38 | -13.9 |
| | 0.2803 | 6.65 | -11.2 |
| $v = 8$ | 0.1869 | 2.07 | -11.9 |
| | 0.0934 | -4.39 | -14.9 |
| | 0.0 | -10.2 | -17.2 |
| | 0.3254 | 8.37 | -13.4 |
| | 0.2440 | 5.90 | -11.9 |
| $v = 10$ | 0.1627 | 12.1 | -5.05 |
| | 0.0813 | -3.76 | -14.9 |
| | 0.0 | -8.76 | -16.9 |
| | 0.2831 | 7.40 | -13.3 |
| | 0.2123 | 4.65 | -12.1 |
| $v = 12$ | 0.1416 | 0.82 | -13.1 |
| | 0.0708 | -3.65 | -14.5 |
| | 0.0 | -7.72 | -17.1 |
| | 0.3254 | 25.9 | 23.6 |
| | 0.2440 | 19.9 | 17.9 |
| $U = 20$ | 0.1627 | 26.0 | 21.3 |
| | 0.0813 | 2.68 | 0.004 |
| | 0.0 | -6.67 | -2.77 |
| | 0.3254 | 8.37 | -13.4 |
| | 0.2440 | 5.90 | -11.9 |
| $U = 30$ | 0.1627 | 12.1 | -5.05 |
| | 0.0813 | -3.76 | -14.9 |
| | 0.0 | -8.76 | -16.9 |
| | 0.3254 | -13.1 | -43.3 |
| | 0.2440 | -11.31 | -30.2 |
| $U = 40$ | 0.1627 | -4.6 | -23.0 |
| | 0.0813 | -13.8 | -25.6 |
| | 0.0 | -15.9 | -25.3 |

**Table A.7 : Continued**

| Variable | Separation Distance Alpha | Resistance Ratio (Draft = Dia) | Resistance Ratio (Draft= 2*Dia) |
|---|---|---|---|
| $v = 8$ | 0.3 $l$ | 4.01 | -17.7 |
| | 0.4 $l$ | 9.26 | -12.8 |
| | 0.5 $l$ | 12.4 | -10.3 |
| $v = 10$ | 0.3 $l$ | 5.69 | -17.1 |
| | 0.4 $l$ | 10.7 | -16.5 |
| | 0.5 $l$ | 14.1 | -9.69 |
| $v = 12$ | 0.3 $l$ | 5.98 | -18.7 |
| | 0.4 $l$ | 11.4 | -14.4 |
| | 0.5 $l$ | 15.9 | -10.7 |
| $l/d = 2$ | 0.3 $l$ | 4.96 | -15.7 |
| | 0.4 $l$ | 12.7 | -10.1 |
| | 0.5 $l$ | 17.2 | -4.00 |
| $l/d = 3$ | 0.3 $l$ | 5.69 | -17.1 |
| | 0.4 $l$ | 10.7 | -16.6 |
| | 0.5 $l$ | 14.1 | -9.69 |
| $l/d = 4$ | 0.3 $l$ | 4.58 | -20.9 |
| | 0.4 $l$ | 8.30 | -16.9 |
| | 0.5 $l$ | 11.4 | -12.7 |
| $na = 2$ | 0.3 $l$ | 7.48 | -18.5 |
| | 0.4 $l$ | 12.6 | -14.4 |
| | 0.5 $l$ | 16.6 | -10.2 |
| $na = 2.5$ | 0.3 $l$ | 6.33 | -19.2 |
| | 0.4 $l$ | 10.9 | -12.5 |
| | 0.5 $l$ | 15.1 | -9.60 |
| $na = 3$ | 0.3 $l$ | 5.94 | -13.7 |
| | 0.4 $l$ | 10.8 | -13.7 |
| | 0.5 $l$ | 14.4 | -9.77 |
| $na = 3.5$ | 0.3 $l$ | 5.69 | -17.1 |
| | 0.4 $l$ | 10.7 | -16.6 |
| | 0.5 $l$ | 14.1 | -9.69 |

**Table A.8 : Total Resistance Ratio for Limited Diameter**

| Variable | Separation Distance Alpha | Resistance Ratio (Draft = Dia) | Resistance Ratio (Draft= 2*Dia) |
|---|---|---|---|
| $U = 20$ | 0.3 $l$ | 18.9 | 25.2 |
| | 0.4 $l$ | 14.4 | 30.6 |
| | 0.5 $l$ | 5.86 | 31.5 |
| $U = 22.5$ | 0.3 $l$ | 18.4 | -11.9 |
| | 0.4 $l$ | 18.3 | -15.6 |
| | 0.5 $l$ | 15.1 | -21.4 |
| $U = 25$ | 0.3 $l$ | -15.6 | -17.9 |
| | 0.4 $l$ | -18.2 | -20.2 |
| | 0.5 $l$ | -18.2 | -44.82 |
| $U = 27.5$ | 0.3 $l$ | 12.2 | 6.11 |
| | 0.4 $l$ | 15.7 | 4.22 |
| | 0.5 $l$ | 15.9 | -2.41 |
| $U = 30$ | 0.3 $l$ | 5.69 | -17.1 |
| | 0.4 $l$ | 10.7 | -16.6 |
| | 0.5 $l$ | 14.1 | -9.68 |
| $U = 32.5$ | 0.3 $l$ | 0.32 | 22.5 |
| | 0.4 $l$ | 5.24 | 23.7 |
| | 0.5 $l$ | 9.40 | 17.1 |
| $U = 35$ | 0.3 $l$ | 5.71 | 20.5 |
| | 0.4 $l$ | 0.88 | 20.1 |
| | 0.5 $l$ | -3.54 | 11.4 |
| $U = 37.5$ | 0.3 $l$ | -11.3 | 31.1 |
| | 0.4 $l$ | -6.72 | 34.4 |
| | 0.5 $l$ | -2.59 | 28.0 |
| $U = 40$ | 0.3 $l$ | 4.82 | -35.5 |
| | 0.4 $l$ | -12.2 | -33.5 |
| | 0.5 $l$ | -8.16 | -30.9 |

**Table A.8 : Continued**

# APPENDIX B

## MATLAB PROGRAMS

In this Appendix, two Matlab programs are presented, one for each case, the limited diameter and the limited length. The purpose of these programs, as was explained in Chapter II, is to compute the viscous resistance (skin friction as well as form drag). Once the program is executed, it asks for the values for the different parameters, $v$, $\ell/d$, $U$, $n_a$, and $n_f$ so that it can continue performing the calculations. Both programs calculate the pod wetted surface area.

```
% Limited diameter.
global na nf
v=input('Enter displacement/length ratio : ');
l_d=input('Enter length/diameter ratio : ');
U=input('Enter ship speed in knots : ');
lf=0.4*l_d;
la=0.6*l_d;
nf=input('Enter nf : ');              % fore body shape factor
na=input('Enter na : ');              % aft body shape factor
cpf=quad('funcpf',0,1);               % fore prismatic coefficient
cpa=quad('funcpa',0,1);               % aft prismatic coefficient
cwsf=quad('funcwsf',0,1);             % fore wetted area coefficient
cwsa=quad('funcwsa',0,1);             % aft wetted area coefficient
L=24.4;                                     % length overall (m)
V=v*(0.1*L)^3;                        % displacement volume m^3)
U=U*0.51444;                          % ship speed (m/sec)
nu=1.04*10^(-6);                      % kinematic viscosity of seawater
rho=1025;                                   % water density (kg/m^3)
c(1)=lf*cpf+la*cpa-l_d;
c(2)=L;
c(3)=0;
c(4)=-2*V/pi;
Droots=roots(c);
D=Droots(2,1)
WS=2*pi*D^2*(L/D-l_d+lf*cwsf+la*cwsa)
Re=U*L/nu;
CF=0.075/(log10(Re)-2)^2;
DCF=0.0004;
CR=0.00789/(L/D-l_d+lf*cwsf+la*cwsa);
F_R=0.5*rho*(CF+DCF+CR)*U^2*WS*0.022481;   %SWATH viscous drag in lbs.
d=D;
l=((V/pi)-((CF*cpf+la*cpa-l_d)*D^3))/D^2

  ws=4*pi*d^2*(l/d-l_d+lf*cwsf+la*cwsa);
  Re=U*l/nu;
  cf=0.075/(log10(Re)-2)^2;
  dcf=0.0004;
  cr=0.00789/(l/d-l_d+lf*cwsf+la*cwsa);
  f_r=0.5*rho*(cf+dcf+cr)*U^2*ws*0.022481;  %SLICE viscous drag in lbs.

ratio=100*(f_r-F_R)/F_R
end
```

```
%Limited length.
global na nf
v=input('Enter displacement/length ratio : ');
l_d=input('Enter length/diameter ratio : ');
U=input('Enter ship speed in knots : ');
lf=0.4*l_d;
la=0.6*l_d;
nf=input('Enter nf : ');              % fore body shape factor
na=input('Enter na : ');             % aft body shape factor
cpf=quad('funcpf',0,1);            % fore prismatic coefficient
cpa=quad('funcpa',0,1);           % aft prismatic coefficient
cwsf=quad('funcwsf',0,1);       % fore wetted area coefficient
cwsa=quad('funcwsa',0,1);       % aft wetted area coefficient
L=24.4;                                  % length overall (m)
V=v*(0.1*L)^3;                       % displacement volume (m^3)
U=U*0.51444;                         % ship speed (m/sec)
nu=1.04*10^(-6);                     % kinematic viscosity of seawater
rho=1025;                                % water density
c(1)=lf*cpf+la*cpa-l_d;
c(2)=L;
c(3)=0;
c(4)=-2*V/pi;
Droots=roots(c)
D=Droots(2,1)
WS=2*pi*D^2*(L/D-l_d+lf*cwsf+la*cwsa);
Re=U*L/nu;
CF=0.075/(log10(Re)-2)^2;
DCF=0.0004;
CR=0.00789/(L/D-l_d+lf*cwsf+la*cwsa);
F_R=0.5*rho*(CF+DCF+CR)*U^2*WS*0.022481;    %SWATH viscous drag in lbs.
dmax=(V/(pi*(lf*cpf+la*cpa)))^(1/3);
lmin=l_d*dmax;
lmax=0.5*L;
incr=50;
c(1)=lf*cpf+la*cpa-l_d;
c(3)=0;
c(4)=-V/pi;
for i=1:incr;i;
  l(i)=lmin+(lmax-lmin)*(i-1)/(incr-1);
  c(2)=l(i);
  droots=roots(c);
  d(i)=droots(2,1);
  alpha(i)=1-2*l(i)/L;
  ws(i)=4*pi*d(i)^2*(l(i)/d(i)-l_d+lf*cwsf+la*cwsa);
  Re=U*l(i)/nu;

  cf(i)=0.075/(log10(Re)-2)^2;
  dcf=0.0004;
  cr(i)=0.00789/(l(i)/d(i)-l_d+lf*cwsf+la*cwsa);
  f_r(i)=0.5*rho*(cf(i)+dcf+cr(i))*U^2*ws(i)*0.022481; %SLICE viscous drag in lbs.
end
ratio=100*(f_r-F_R)/F_R
```

# APPENDIX C

## DATA FILES SAMPLES

This Appendix contains sample data files used for calculating the wavemaking resistance. These files are the typical files for SUB.DAT as explained in Chapter II. The first column is the offset from the pod maximum diameter for the SWATH, or the offset from the middle of the pod separation distance in case of SLICE. The second column is the corresponding radii for these offset points. We show here one sample file for each hull form.

| Offset Points | Radii |
|---|---|
| -40.0160 | 0.0000 |
| -39.1465 | 1.1016 |
| -38.2769 | 1.9077 |
| -37.4074 | 2.4719 |
| -36.5378 | 2.8441 |
| -35.6683 | 3.0700 |
| -34.7987 | 3.1911 |
| -33.9292 | 3.2439 |
| -33.0596 | 3.2539 |
| -32.1901 | 3.2608 |
| 34.7987 | 3.2608 |
| 35.1714 | 3.2607 |
| 35.5440 | 3.2598 |
| 35.9167 | 3.2566 |
| 36.2894 | 3.2491 |
| 36.6620 | 3.2352 |
| 37.0347 | 3.2119 |
| 37.4074 | 3.1757 |
| 37.7800 | 3.1222 |
| 38.1527 | 3.0451 |
| 38.5253 | 2.9352 |
| 38.8980 | 2.7771 |
| 39.2707 | 2.5397 |
| 39.6433 | 2.1386 |
| 40.0160 | 0.0000 |

**Table C.1 : SWATH Sample Data File**

| Offset Points | Radii |
|---|---|
| -52.9808 | 0.0000 |
| -50.3721 | 2.4719 |
| -47.7635 | 3.1911 |
| -45.1548 | 3.2608 |
| -12.1278 | 3.2608 |
| -11.3825 | 3.2598 |
| -10.6372 | 3.2491 |
| -9.8918 | 3.2119 |
| -9.1465 | 3.1222 |
| -8.4012 | 2.9352 |
| -7.6559 | 2.5397 |
| -6.9105 | 0.0100 |
| 0.0000 | 0.0100 |
| 6.9105 | 0.0100 |
| 9.5192 | 2.4719 |
| 12.1278 | 3.1911 |
| 14.7365 | 3.2608 |
| 47.7635 | 3.2608 |
| 48.5088 | 3.2598 |
| 49.2541 | 3.2491 |
| 49.9994 | 3.2119 |
| 50.7448 | 3.1222 |
| 51.4901 | 2.9352 |
| 52.2354 | 2.5397 |
| 52.9808 | 0.0000 |

**Table C.2 : SLICE Sample Data File**

# LIST OF REFERENCES


1. Rodriguez, M., "Structural Analysis of SLICE," Master's Thesis, Naval Postgraduate School, Monterey, CA, Winter 1995.

2. Jackson, H., "Fundamental of Submarine Concepts Design," SNAME paper, pp. 15-4–15-5, October 1992.

3. Abramowitz, M., and Stegun, I. A., *Handbook of Mathematical Functions*, Dover Publications, New York, 1970.

4. Harvald, SV. AA., *Resistance of Propulsion of Ships*, John Wiley & Sons, Inc., 1983.

5. Aretzen, E. S., and Mandel, P., "Naval Architecture Aspects of Submarine Design," *Transactions of the Society of Naval Architecture and Marine Engineering*, 1960.

6. Doctors, L., Beck, R., "Convergence Properties of the Neumann-Kelvin Problem for a Submerged Body," *Journal of Ship Research*, pp. 227–228, December 1987.

7. Papoulias, F., "Dynamics of Marine Vehicles," informal lecture notes for ME 4823, Naval Postgraduate School, Monterey, CA, Summer 1993.

8. Papoulias, F., and Beck, R., "WAVEAMP: A Program for Computation of Wave Elevations Created by a Ship Travelling at a Constant Speed," Technical Report No. 88-03, University of Michigan, Ann Arbor, MI, pp. 2–3, July 1988.

9. Hess, J., and Smith, A., "Calculation of Nonlifting Potential Flow About Arbitrary Three-Dimensional Bodies, *Journal of Ship Research*, pp. 22–44, September 1964.

# INITIAL DISTRIBUTION LIST

| | | No. Copies |
|---|---|---|
| 1. | Defense Information Center<br>Cameron Station<br>Alexandria, VA 22304-6145 | 2 |
| 2. | Library Code 52<br>Naval Postgraduate School<br>Monterey, CA 93943-5101 | 2 |
| 3. | Chairman, Code ME<br>Department of Mechanical Engineering<br>Naval Postgraduate School<br>Monterey, CA 93943-5000 | 1 |
| 4. | Professor F. A. Papoulias, Code ME/Pa<br>Department of Mechanical Engineering<br>Naval Postgraduate School<br>Monterey, CA 93943-5000 | 5 |
| 5. | LTCOL Abdullatif Al-zayani<br>HQ, Organization and Planning Department<br>BDF, P.O. Box 245<br>State of Bahrain | 1 |
| 6. | LTCOL Yousif Ahmed Malalla<br>Commander, Bahrain Amiry Navy<br>BDF, P.O. Box 245<br>Naval Base<br>State of Bahrain | 2 |
| 7. | Major Jassim Abdulla Aljowder<br>Bahrain Naval Amiri Force<br>P.O. Box 245<br>State of Bahrain | 2 |